PENICILLIN V ACYLASES FROM GRAM-NEGATIVE BACTERIA: BIOCHEMICAL AND STRUCTURAL ASPECTS

THESIS SUBMITTED TO
SAVITRIBAI PHULE PUNE UNIVERSITY

FOR THE DEGREE OF
DOCTOR OF PHILOSOPHY IN

BIOTECHNOLOGY

V. S. AVINASH

Dr. ARCHANA PUNDLE (RESEARCH GUIDE)

Dr. SURESHKUMAR RAMASAMY (RESEARCH CO-GUIDE)

BIOCHEMICAL SCIENCES DIVISION
CSIR- NATIONAL CHEMICAL LABORATORY
PUNE - 411008, INDIA

DECEMBER 2015

सीएसआयआर–राष्ट्रीय रासायनिक प्रयोगशाला
(वैज्ञानिक तथा औद्योगिक अनुसंधान परिषद)
डॉ. होमी भाभा मार्ग, पुणे – 411 008. भारत
CSIR-NATIONAL CHEMICAL LABORATORY
(Council of Scientific & Industrial Research)
Dr. Homi Bhabha Road, Pune - 411008. India

CERTIFICATE

Certified that the work incorporated in the thesis entitled **"Penicillin V acylases from Gram-negative bacteria: Biochemical and structural aspects"** submitted by Mr. V.S. Avinash, for the Degree of ***Doctor of Philosophy***, was carried out by the candidate under our supervision/guidance at Biochemical sciences Division, CSIR-National Chemical Laboratory, Pune – 411008, India. Material obtained from other sources has been duly acknowledged in the thesis.

Dr. Archana V. Pundle
(Research Supervisor)

Dr. Sureshkumar Ramasamy
(Research co-guide)

Date: 3.12.15

Place: Pune

Communications Channels
NCL Level DID : 2590
NCL Board No. : +91-20-25902000
Four PRI Lines : +91-20-25902000
FAX
Director's Office : +91-20-25902601
COA's Office : +91-20-25902660
SPO's Office : +91 20 25902664
WEBSITE
www.ncl-india.org

DECLARATION BY RESEARCH SCHOLAR

I hereby declare that the thesis entitled "**Penicillin V acylases from Gram-negative bacteria: Biochemical and structural aspects"** submitted by me for the Degree of Doctor of Philosophy to Savitribai Phule Pune University is the record of work carried out by me at Biochemical Sciences Division, CSIR- National Chemical Laboratory, Pune - 411008, India, under the supervision of Dr. Archana V. Pundle (research guide) and Dr. Sureshkumar Ramasamy (research co-guide). The work is original and has not formed the basis for the award of any degree, diploma, associateship, and fellowship titles in this or any other university or other institute of higher learning. I further declare that the material obtained from other resources has been duly acknowledged in the thesis.

V.S. Avinash

Biochemical Sciences Division
CSIR-National Chemical Laboratory
Pune - 411008

Dedicated to my late grandfather Dr. V. Nagarajan

whose genes gave me the gift of science...

Table of Contents

Chapter 3: Crystallization and structural analysis of *Pa*PVA

Chapter 4: Analysis of substrate binding in *Pa*PVA using docking, mutagenesis and molecular dynamics simulations

Chapter 6: Application of immobilized PVA system for 6-APA production

Acknowledgement

This thesis is the culmination of a long journey towards a Ph. D. Reaching this destination was made possible by the help, support and encouragement from many people. It gives me great pleasure to acknowledge everyone whose contributions have made this thesis possible and travelled with me through the highs and lows on this roller coaster expedition of research.

I am extremely thankful to Dr. Archana Pundle, my research supervisor, for providing rock-solid support and believing in me whenever I was lacking motivation to go on. Her insightful guidance and reassuring nature have provided me with the knowledge and creative freedom to pursue my research with full confidence. I am also grateful to Dr. Asmita Prabhune for her constant backing and encouragement. I have immensely enjoyed working in their lab, the whole spectrum from rigorous scientific discussions on enzymes to impromptu parties.

I will always have a deep sense of gratitude to Dr. Sureshkumar Ramasamy, my research co-guide for infusing new life to my research work. His effortless transitions from industrious scientist to endearing mentor have helped me a great deal in gaining confidence and momentum to cross the finish line. I also have an everlasting gratitude for Dr. C.G. Suresh, who has followed my progress from the first day I stepped foot in NCL and always provided me with unlimited access and support. His coursework lectures and discussions have helped me gain a firm foundation in protein structure research. His meticulous attention to detail has significantly helped me improve my experimental and manuscript writing skills.

Research work is by nature hugely collaborative, and many people have helped make my Ph. D. journey easier by sharing their lab facilities and allowing me to pick their brains. I would like to acknowledge Dr. C.G. Suresh, Dr. Saikrishnan (IISER), Dr. Radha Chauhan (NCCS) for providing lab facilities for protein crystallization and X-ray diffraction; and Dr. Moneesha Fernandes (NCL) for fluorescence and CD measurements. I extend my sincere thanks to Dr. Wim Quax and Putri (Groningen University, Netherlands) for helping with the AHL degradation experiments. I would also like to thank Dr. W.D. Fessner (Darmstadt TU, Germany) for hosting me in his lab for a month as part of the DST-DAAD exchange program.

I am eternally grateful to all my labmates (long list) from AVP/AAP and CGS/SKR labs, who have taught me a lot in science and in life and have always encouraged me to reach for the stars. I would like to thank the lab seniors (Dr. Atul, Dr. Ambrish, Dr. Sridevi, Dr. Nishant) for introducing me to the world of Ntn hydrolases and patiently teaching me many techniques related to protein science. I extend my sincere thanks to Pushpa, Pradeep, Mihir, Priti, Parul, Hrishi, Pooja, Palna, Shraddha, Amruta, Kasturi, Vrushali, Ruchira, Dr. Snehal More, Siddharth, Aparna, Aditi, Uma, Reetika, Dr. Madhura, Sonali for creating a very cordial atmosphere in the

lab and generously helping me in times of need. Our scientific debates, mealtime banter, TT/badminton games and group excursions have kept me greatly invigorated during my time here. Pushpa deserves a special mention just for being there for me as one of my best friends, from motivating me when I was down all the way to participating in my joy discussing lines from *Friends*. I am also grateful to Pooja, Palna and Shraddha for helping me with the immobilization experiments. I would also like to thank all the trainees who have worked with me for their M.Sc. projects.

A big shout-out to Deepak, Manu, Priyabrata (PP), Aditi, Sridhar, Ameya, Deepanjan, Yashpal, Shiva et al. for such an accommodating and wonderful group. I have always depended on their lab for help with experiments and also the lively discussions that were such stress busters. Much of what I know about protein crystallization and structure determination I owe to Deepak, while Priyabrata has generously sacrificed many of his weekends computationally explaining my experimental results. The endless discussions with them on the structural and functional intricacies of Ntn hydrolases have been truly delightful. Time spent with the Sunday dinner gang (Manu, Rupa, Deepak, Pushpa, Prasaenjit) has also given me many enjoyable memories. I should also mention my roommates and friends from GJ hostel for their support and wonderful experiences we have shared.

I take this opportunity to thank Dr. Sourav Pal (former Director), Director NCL, Dr. Vidya Gupta (former Chair, Biochemical Sciences Division) and Dr. C.G. Suresh for giving me an opportunity to work in CSIR-NCL and providing the infrastructure and advanced facilities to carry out my research work. I would also like to acknowledge CSIR, Govt. of India for the research fellowship. I wish to express my thanks to Dr. J.K. Pal (Pune University) and Dr. S.R. Thengane for periodically evaluating my research work and providing valuable suggestions. The support provided by Mrs. Indira Mohanadasan and others in Biochemical Division office, and Mrs. Kolhe from SAO for official and administrative work is highly appreciated.

At this time, I would also like to remember the contributions of my teachers and mentors from DAV BHEL School and Bharathiar University, who played a crucial role in moulding my character and fostering scientific temper. Finally, this thesis has been made possible by the limitless support from my family; especially my parents and relatives who have encouraged my passion for scientific research and stood by me even when the journey took longer than expected. My younger brother and sister have been the backbone of my life, supporting me in every endeavour even when they are miles away. Special thanks to my cousins in Pune, in whose home I've spent many enjoyable weekends. I wish to express my sincere thanks to everyone who has helped me in any small way towards the successful completion of my doctoral research.

Avinash V.S.

List of abbreviations

6-APA	6-amino penicillanic acid
7-ACA	7-amino cephalosporanic acid
*Af*PGA	*Alcaligenes faecalis* penicillin G acylase
AHL	Acylhomoserine lactone
AIM	Auto induction medium
ATCC	American Type culture collection
*At*PVA	*Agrobacterium tumefaciens* penicillin V acylase
*Bl*BSH	*Bifidobacterium longum* bile salt hydrolase
βME	β-mercapto ethanol
BrMmC	4-bromomethyl-7-methoxycoumarin
BSH	Bile salt hydrolase
*Bsp*PVA	*Bacillus sphaericus* penicillin V acylase
*Bsu*PVA	*Bacillus subtilis* penicillin V acylase
*Bt*BSH	*Bacteroides thetaiotamicron* bile salt hydrolase
CBAH	Conjugated bile acid hydrolase
CCD	Charge coupled device
CGH	Cholylglycine hydrolase
CPB	Citrate phosphate buffer
*Cp*BSH	*Clostridium perfringens* bile salt hydrolase
DMSO	Dimethyl sulfoxide
DTT	Dithiothreitol
*Ec*PGA	*Escherichia coli* penicillin G acylase
EDTA	Ethylene diamine tetra-acetic acid
F(hkl)	Structure factor
GCA	Glycocholic acid
GDCA	Glycocholic acid
HEPES	N-(2-hydroxyethyl)-piperazine-N'-2-ethanesulfonic acid
HPLC	High pressure liquid chromatography
HSL	Homoserine lactone
IPTG	Isopropyl-β-D-thiogalactoside

IU	International Unit
$K_{0.5}$	Substrate concentration at half-maximal velocity
*Kc*PGA	*Kluyvera citrophila* penicillin G acylase
K_i	Inhibition constant
k_{cat}	Turnover number
MALDI	Matrix-associated Laser Desorption and Ionization
MDS	Molecular dynamics simulation
NCS	Non-crystallographic symmetry
NIPOAB	2-nitro 5-(phenoxyacetamido)-benzoic acid
Ntn	N-terminal nucleophile
*Pa*PVA	*Pectobacterium atrosepticum* penicillin V acylase
PCR	Polymerase chain reaction
PDB	Protein Data Bank
pDAB	para-dimethyl amino benzaldehyde
PEG	Polyethylene glycol
Pen G	Penicillin G
Pen V	Penicillin V
PGA	Penicillin G acylase
PVA	Penicillin V acylase
RMSD	Root mean square deviation
rpm	Revolutions per minute
SDS	Sodium dodecyl sulphate
*Sl*PVA	*Streptomyces lavendulae* penicillin V acylase
*Sm*PVA	*Streptomyces mobarensis* penicillin V acylase
TDCA	Taurodeoxycholic acid
TCA	Taurocholic acid
Tris	Tris-hydroxymethyl amino methane
V_m	Matthew's number
V_{max}	Maximum velocity

Abstract

Penicillin acylases (E.C. 3.5.1.11) are pharmaceutically important enzymes that cleave the acyl side chains of β-lactam antibiotics. They are widely used in the industrial production of the intermediate 6-amino penicillanic acid (6-APA), which can then be converted to a range of semi-synthetic antibiotics. Penicillin acylases are classified based on their substrate preference for benzyl penicillin (Pen G; PGA) or phenoxymethyl penicillin (Pen V; PVA).

Penicillin acylases are members of the protein superfamily of (Ntn) hydrolases, which contain an N-terminal nucleophile residue critical for catalysis housed in a common αββα structural fold. PGAs and PVAs share critical catalytic residues, although they exhibit low sequence homology and different subunit constitutions. PGAs are heterodimers with serine as the N-terminal catalytic nucleophile, while PVAs are homotetramers with cysteine as the nucleophile. PVAs are also evolutionarily related to and occasionally show substrate cross-reactivity with BSH, which are involved in the deconjugation of bile salts in gut microbiota. The biophysical and structural analysis of choloylglycine hydrolases has so far been restricted to a few species of Gram-positive bacteria. It is imperative to study such enzymes from Gram-negative bacteria, which might show unique biochemical and structural characteristics.

Further, the PGA enzyme from *E. coli* is the mostly preferred for industrial use for 6-APA production, though some reports have mentioned the advantages of a pen V–PVA system like stability at low pH and better conversion at higher substrate concentrations. In this regard, there is an unmet need for the development of highly active PVA preparations for industrial applications.

Although they enjoy immense industrial importance, the in vivo role of penicillin acylases is not known to date. Some hypotheses have been made regarding their possible role in scavenging for alternative carbon sources, while other reports indicate the possible involvement of penicillin acylases and homologous enzymes in bacterial cell signalling and pathogenesis networks. Exploration of activity of these

enzymes on related natural substrates could enhance our understanding of the importance of enzymes in microbial physiology.

The work described in the thesis lays emphasis on the structural and biochemical characterization of penicillin V acylases from Gram-negative bacteria. The characteristics of PVAs from two plant pathogens, *Pectobacterium atrosepticum* and *Agrobacterium tumefaciens*, have been detailed. The unique structural characteristics, substrate specificity and highly active nature of the PVAs from Gram-negative bacteria hold great potential for future studies as well as industrial applications.

The thesis is organized into six chapters:

The ***first chapter*** serves as a general introduction to the thesis and it gives a brief review on literature on penicillin acylases and penicillin acylase producing microorganisms. Characteristics of penicillin V acylases produced by various microorganisms and their application in industries are described. The chapter also deals with the Ntn hydrolase super family members, their structural similarities, catalysis behaviour and mechanism. Evolutionary relatedness of penicillin acylases with enzymes involved in other metabolic pathways is discussed in an effort to understand their probable roles in microbial physiology.

The ***second chapter*** deals with the cloning of penicillin V acylase genes from the Gram-negative plant pathogen *P. atrosepticum* (*Pa*PVA). Expression of the enzyme in *E. coli*, purification and biochemical characterization has been discussed. The activity and stability of the enzyme under different conditions of pH, temperature, guanidine hydrochloride and organic solvents are elaborated. *Pa*PVA was identified as a highly active enzyme that exhibits unique kinetic behaviour, with cooperative nature and substrate inhibition.

The ***third chapter*** deals with the crystallization of *Pa*PVA enzyme and elucidation of its structural characteristics. The methodology used for crystallization and X-ray diffraction, and refinement of the structural parameters has been discussed. The structure of *Pa*PVA was compared with different penicillin acylases, bile salt

hydrolases and other Ntn hydrolase enzymes to study the differences in oligomeric interactions and active site organization.

Using the structural information for PaPVA enzyme elucidated in Chapter 3, efforts were made to understand the unique biochemical characteristics of the enzyme. The ***fourth chapter*** deals with the study of substrate binding to the *Pa*PVA enzyme through different computational techniques and site-directed mutagenesis. The binding modes of Pen V and bile salt glycodeoxy cholic acid (GDCA) to the enzyme active site were studied by ligand docking analysis. The importance of two tryptophan residues for enhanced PVA activity has been established through mutation of active site residues. Molecular dynamics simulation of substrate binding to the native and mutant forms of the enzyme was explored to study the aromatic stacking and other interactions involved that contribute to favourable Pen V binding.

The ***fifth chapter*** describes the cloning and characterization of penicillin V acylase from another Gram-negative pathogen *A. tumefaciens* (*At*PVA), which exhibits sequence homology with *Pa*PVA. The biochemical and structural characteristics of *At*PVA and *Pa*PVA have been compared. The ability of PVAs to hydrolyze long chain acyl homoserine lactones (AHLs) involved in bacterial quorum sensing, and its significance in microbial physiology has also been explored.

The ***sixth chapter*** deals with the development of PVA enzyme preparations for probable industrial applications. Recombinant *E. coli* cells producing *Pa*PVA were permeabilized using detergents to improve cell-bound activity, and were encapsulated in calcium alginate beads. Optimization of process parameters was carried out to ensure maximum conversion of pen V to 6-APA and enhance the stability and recyclability of the immobilized system.

A brief ***summary*** of the thesis work and scope for possible further research in these areas is presented at the end of the thesis.

Chapter 1

Introduction

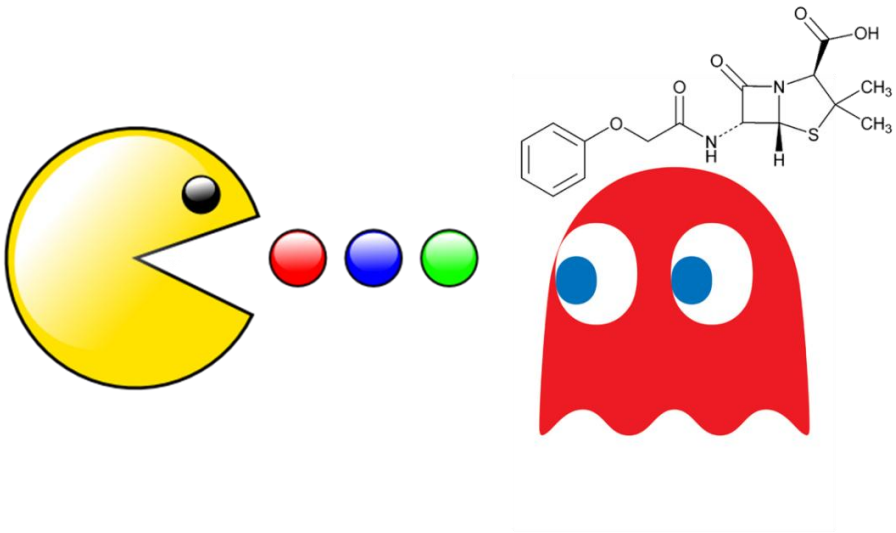

1.1. Enzymes – characteristics, structure and significance:

"Life ... is a relationship between molecules" - *Linus Pauling*

It is imperative that the existence and sustenance of life on earth requires a functioning diversity of chemical tools that have evolved over millions of years. Biological molecules play vital roles in the transfer of genetic information, response to environmental stimuli and maintenance of metabolic homeostasis. Enzymes form a variegated array of biological macromolecules (mostly proteins), which facilitate the progress of chemical reactions in living systems through catalysis. It is fitting to say that proteins and catalytic enzymes in particular, form the cornerstones of the subsistence of life on the planet. The study of action of enzymes would hence provide an insight into the crucial notes in the melody of life.

In technical terms, with the exception of ribozymes, most enzymes are proteins that catalyze reactions in biological metabolism. In vitro, these enzymes operate at optimum conditions including temperature, pH and ionic strength. The catalytic reaction proceeds as a result of rearrangement of chemical bonds and weak bonding interactions between the enzyme and substrate at the active site, first suggested by Haldane in 1930s. The formation of an intermediate transition complex of the enzyme with the substrate reduces the activation energy, thus facilitating the reaction at physiologically relevant conditions. In some cases, small molecules (co-enzymes and metal ion cofactors) are also involved in facilitating the reaction.

Over the last half-century, intensive research has been done on enzymes to purify them and study their characteristics and mechanism of action, and also elucidate their structure. The kinetics and thermodynamic parameters of enzyme-catalyzed reactions, including binding of substrate and inhibition, have helped understand their mechanism. Regulation of enzyme synthesis in living systems coordinates the action of enzyme networks in maintaining a proper metabolism and adaptation to environmental stimuli. Their convenience and efficacy have facilitated the exploitation and use of enzymes in industrial catalysis. Enzymes have now been purified, stabilized and applied in a multitude of industrial and commercial processes, from the production of active pharmaceutical intermediates and medical treatment to bioremediation to clean up toxic environmental waste **(Fig. 1.1)**.

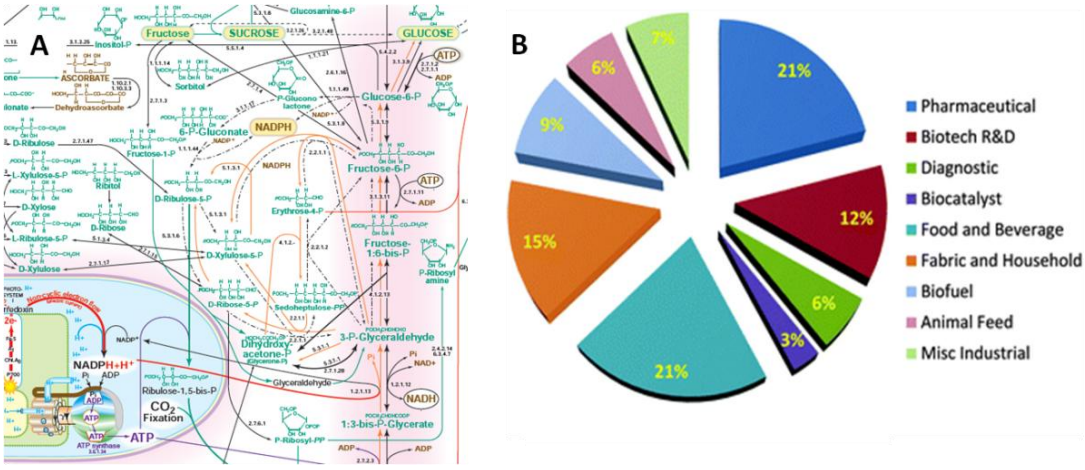

Fig. 1.1. Significance of enzymes: (A) Enzymes control the metabolism of the cell. [http://www.sigmaaldrich.com/life-science/metabolomics/learning-center/metabolic-pathways.html] (B) Applications of enzyme formulations in the industry.

Enzymes, like all proteins, undergo folding of polypeptide to form secondary structures (helices, sheets, loops and turns) which assemble to generate a functional and active tertiary or quarternary structure. Three-dimensional structure of enzymes is mainly determined by X-ray diffraction of protein crystals, although NMR and spectroscopic methods have also been employed recently to study the conformational variations and dynamics of protein molecules. Enzymes were first crystallized in 1920-30s (urease by Sumner and trypsin by Kunitz); since then, an explosion in the accumulation of knowledge and advancement of technology in the crystallization and structure determination of enzymes took place.

Since the advent of recombinant DNA technology, the preparation of pure enzyme in large quantities has become easier. The gene for a particular enzyme of interest can be expressed in a heterologous host, and the catalytic characteristics can be modified using targeted mutagenesis of residues in the sequence. This facilitates a faster strain improvement and production of commercially useful enzymes efficiently.

Rapid progress on the molecular biology front has also helped unravel the complete genome sequences of various organisms, especially bacteria. Using a suite of bioinformatics tools, different hypothetical protein-coding sequences have been annotated based on their sequence homology and placed in various families. However, such proteins require biochemical and structural analysis to study their functional uniqueness among other homologues, and their evolutionary paths. Enzymes are known for their relaxed substrate specificity and promiscuity towards

hydrolysis of unnatural substrates. It is therefore, imperative to study the catalytic characteristics, regulation and physiological roles of different enzymes to fully appreciate their place in the puzzle of life.

1.2. Enzymes for modifying antibiotics:

Antibiotics are small molecules produced by bacteria or fungi that adversely act on other microorganisms. β-lactams (penicillins and cephalosporins) are the first antibiotics to be discovered, which still has a major share of the antibiotic market (~65%) (Elander 2003). Produced by fungi such as *Penicillium chrysogenum* and *Acremonium chrysogenum*, their basic component is a β-lactam nucleus formed by the fusion of a 4-member β-lactam ring (Ala-cys-val cyclic tripetide) fused to a thiazolidine ring or a 6-carbon ring to give 6-amino penicillanic acid (6-APA) or 7-amino cephalosporanic acid (7-ACA). The side chain attached to the nucleus by an amide bond can be modified to produce different penicillins that vary in a range of antibacterial range and pharmacological properties. β-lactam antibiotics usually act as inhibitors of transpeptidase enzyme involved in bacterial peptidoglycan (cell wall) synthesis causing bacterial cell death (Demain and Elander 1999).

Over the years, the indiscriminate use of antibiotics has led to the development of resistance in bacteria. Bacteria acquire resistance by spontaneous mutations and gene transfer, or through modifications in the penicllin-binding proteins. Most bacteria use efflux pumps to eject the antibiotic or cleave the antibiotic molecules using β-lactamase enzyme, rendering them ineffective (Dever and Dermody 1991). Although antibiotic resistance is a natural phenomenon, its progress is aided by certain factors like inappropriate use of broad-spectrum antibiotics. One way to approach this problem is by developing a strict regimen for the use of antibiotics and the other is by the production of newer and more effective antibiotics targeted at a narrow range of pathogens.

The continuous evolutionary tug-of-war between pathogenic microbes and humans has kept alive the sustained need for newer antibiotics. In the case of β-lactam antibiotics, the custom addition of different chemical groups to the β-lactam nucleus in the place of natural acyl chain has been shown to improve the efficacy of the antibiotics. Semi-synthetic antibiotics, like ampicillin, amoxicillin, cephachlor and

so on, possess increased efficacy, diminished human toxicity and improved pharmacological properties including stability and absorption. Chemical synthesis of semi-synthetic β-lactams is cumbersome and will generate a lot of waste; in addition, during synthesis the β-lactam ring gets hydrolyzed (Matsumato 1983; Vandamme 1988). A greener process involves the use of enzymes that modify the antibiotic by specific hydrolysis of the acyl side chain under mild conditions. This approach has multiple advantages, including less chemical load on the environment, higher efficiency and faster downstream processing without compromising product quality. A number of enzymes (detailed below) have now been discovered and characterized which can hydrolyze or acylate the side chain (Arroyo et al. 2003), enabling applications in synthesis of newer semi-synthetic antibiotics **(Fig. 1.2)**. Immobilization techniques have facilitated greater enzyme stability and easy recovery of the product, making the whole process more environment-friendly and cost-effective. The production of 6-APA exceeds well over 10,000 tonnes annually, with a major chunk of it achieved using penicillin acylases and other enzymes (van de Sandt and de Vroom 2000). This caters to the substantial demand for b-lactam antibiotics, which represent one of the major biotechnology markets today (Chandel et al. 2008).

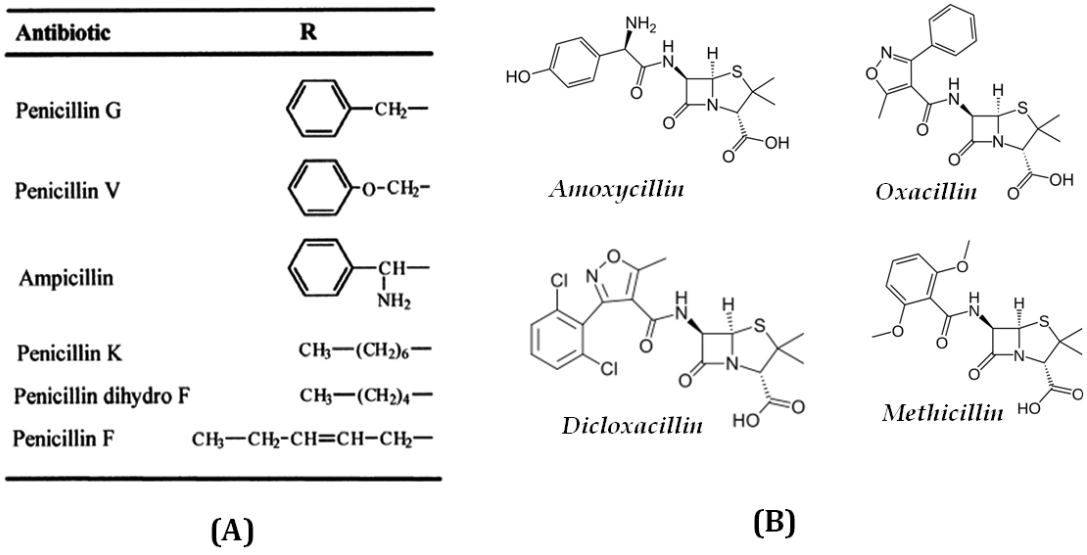

Fig. 1.2. (A) Acyl side chains of different natural penicillins (Arroyo et al. 2003). (B) Some commercially available semi-synthetic antibiotic molecules.

The original discovery of an enzyme that could hydrolyze the acyl side chain of a β-lactam antibiotic leaving the β-lactam nucleus intact was made by Japanese workers (Sakaguchi and Murao 1950; Murao 1955), who reported the hydrolysis of penicillin. Subsequently, Batchelor et al. (1959) confirmed that the reaction product of the acylase was in fact 6-amino penicillanic acid. The ability of the enzyme to catalyze the reverse (condensation) reaction was also reported (Vandamme and Voets 1974), allowing synthesis of newer antibiotics with modified side chain chemical groups. Since then, a number of bacteria and fungi have been identified that produce enzymes possessing acylase activity on natural penicillins (Arroyo et al. 2003). β-lactam acylases are conventionally classified based on their industrial substrate preference (Deshpande et al. 1994) – benzylpenicillin (pen G acylases), phenoxymethyl penicillin (pen V acylases), ampicillin and cephalosporin acylases. Recently, a few acylases that act on aliphatic penicillins such as octanoyl penicillin (pen K) have also been characterized (Torres-Guzman et al. 2002; Zhang et al. 2007; Torres et al. 2012). Another class of enzymes, α-amino ester hydrolases (AEH) have also been used in the synthesis of semi-synthetic antibiotics; they prefer esters with α-amino group over amides (ampicillin, cephalexin, amoxicillin) and capable of catalyzing both acyl transfer and hydrolysis (Takahashi et al. 1974, Polderman-Tijmes et al. 2002). However, penicillin acylases **(Fig. 1.3)** have been the enzyme of choice for many decades now in the pharmaceutical industry. Penicillin acylases belong to the Ntn hydrolase superfamily of proteins.

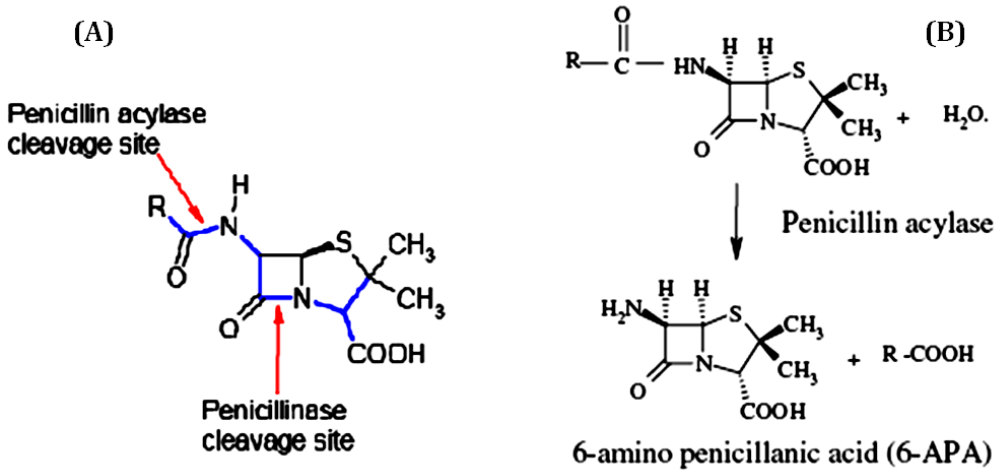

Fig. 1.3. (a) Penam ring structure of penicillins, showing site of action of penicillinase and penicillin acylase. (b) Reaction catalyzed by penicllin acylases.

1.3. Ntn hydrolases:

The N-terminal nucleophile (Ntn) hydrolases belong to a diverse superfamily of enzymes that has recently been characterized on the basis of presence of a nucleophilic residue at the N-terminal, involved in catalysis (Oinonen and Rouvinen 2000). They contain a distinct αββα structural fold, resulting in the N-terminal nucleophile exhibiting a similar spatial position in the active site. Both penicillin G acylases and penicillin V acylases, and other evolutionarily related enzymes, come under the Ntn hydrolase superfamily. A list of Ntn hydrolases for which structures are available, is presented in **Table 1.1**.

In all the structures of Ntn hydrolases elucidated so far, the N-terminal residue is housed in one of the β-strands of the characteristic αββα-fold, comprising two central anti-parallel β-sheets sandwiched between two layers of α-helices. The packing angle of the β-sheets varies from 5° in aspartyl glucosaminidase to 35° in proteasome (Oinonen and Rouvinen 2000). Eight conserved secondary structure elements are found, indicating a common ancestor (Brannigan et al. 1995). However, the composition of the core and the oligomeric states vary across Ntn hydrolases (Brannigan et al. 1995; Oinonen and Rouvinen 2000).

Table 1.1. List of important structurally characterized Ntn hydrolases.

Enzyme	**Catalytic nucelophile**	**Source organism**	**PDB code**	**References**
Penicillin G acylase	Serine	*Escherichia coli* *Alcaligenes faecalis*	1PNK 3K3W	Duggleby et al. 1995 Varshney et al. 2012
Penicillin V acylase	Cysteine	*Bacillus sphaericus* *B. subtilis*	2PVA 2OQC	Suresh et al. 1999 Rathinaswamy et al. 2005
Bile salt hydrolase	Cysteine	*Clostridium perfringens* *Bifidobacterium longum*	2BJF 2HF0	Rossocha et al. 2005 Kumar et al. 2006

Cephalosporin acylase	Serine	*Brevudimonas dimunuta*	1FM2	Kim et al. 2000
N-acyl homoserine lactone (AHL) acylase	Serine	*P. aeruginosa*	2WYE	Bokhove et al. 2010a
Glutamine-phosphoribosyl pyrophosphate (PRPP) transferase	Cysteine	*B. subtilis* *E. coli*	1GPH 1ECG	Smith et al. 1994 Kim et al. 1996
20 S proteasome	Threonine	*Thermoplasma acidophilum* *Saccharomyces cerivisiae*	1PMA 1RYP	Lowe et al. 1995 Groll et al. 1997
Glycosyl asparaginase	Threonine	*Flavobacterium meningsepticum*	1AYY	Xuan et al. 1998
Human aspartyl glucosaminidase	Threonine	*Homo sapiens*	1APY	Oinonen et al. 1995
L-asparaginase	Threonine	*Lupinus luteus*	2GEZ	Michalska et al. 2006
Ornithine acetyl transferase	Threonine	*Streptomyces clavuligerus*	1VZ8	Elkins et al. 2005
γ-glutamyl transpeptidase	Threonine	*E. coli*	2DBU	Okada et al. 2006
L-aminopeptidase – D-ala-esterase/amidase	Serine	*Ochrobactrum anthropi*	1B65	Bompard-Gilles et al. 2000
N-carbamyl D-amino acid amidohydrolase	Cysteine	*Agrobacterium sp.*	1ERZ	Nakai et al. 2000
acyl coenzyme A:isopenicillin N acyltransferase (acyl-coenzyme A:6-APA-transferase)	Cysteine	*Penicillium chrysogenum*	2X1C	Bokhove et al. 2010b
Carbepenam synthase (*carA*)	Serine	*Pectobacterium carotovorum*	1Q15	Miller et al. 2003
Lysosomal 66.3 kDa protein	Cysteine	*Mus musculus*	3FGR	Lakomek et al. 2009

The catalytic mechanism of Ntn hydrolases is similar to serine proteases, but with a single N-terminal residue acting both as a nucleophile and a catalytic base. All Ntn hydrolase family members exhibit strikingly similar arrangement of catalytic residues in spite of low sequence homology, and possess one of the nucleophiles such as cys/ser/thr at their N-terminal. The side chain nucleophilic atom of the N-terminal residue attacks the carbonyl group of the scissile peptide in the substrate, resulting in the formation of a tetrahedral transition complex. The active site residues in the vicinity of the nucleophilic residue decide its reactivity. The covalently linked intermediate is stabilized by residues forming an oxyanion hole with the carbonyl oxygen of the scissile amide bond. The α-amino group of the nucleophile then acts as a base, taking up the liberated proton and donates it to the nitrogen of the scissile amide bond; thus completing the acylation step. The deacylation step is facilitated by the involvement of a water molecule, with the formation of a similar tetrahedral intermediate (Oinonen and Rouvinen 2000).

Although all the enzymes catalyze amide bond hydrolysis, their substrates vary widely. As a result, the shape and size of the substrate binding pocket differ, as well as the spatial distribution of interacting residues. However, some of the residues including those that form the oxyanion hole are similar in many Ntn hydrolases (Suresh et al. 1999).

The enzymes in this family are usually activated through autocatalytic mechanism, including penicillin G acylases. (Brannigan et al. 1995). Post-translational auto-proteolysis is known to activate many proteins that play critical roles in biological processes like blood coagulation, cell death, embryonic development, protein targeting and degradation and viral protein processing. The pro-peptide processing in Ntn hydrolases is generally intramolecular, except probably in the proteasome from *Thermoplasma acidophilum* (Seemuller et al. 1996). Details of processing mechanisms have been elucidated, aided by the solution of precursor structures of glycosylasparaginase (Xu et al. 1999), PGA (Hewitt et al. 2000) and β-subunit of proteasome (Ditzel et al. 1998). However, some enzymes like *B. subtilis* PVA and *C. perfringens* BSH possess their N-terminal residue at the second position, thus requiring only the removal of the initial N-formyl methionine to activate the enzyme (Rathinaswamy et al. 2005; Rossocha et al. 2005).

1.4. Penicillin G acylases:

Penicillin G acylases have been isolated and characterized from a wide variety of bacteria, including *Escherichia coli*, *Alcaligenes faecalis*, *Kluvyera citrophila*, *Arthrobacter viscosus*, *Achromobacter xylosoxidans*, *Bacillus megaterium*, *Bacillus badius* and *Providencia rettgeri*. PGA has been reported to hydrolyze non-peptide amide bonds, in benzyl penicillin (Pen G) and related phenyl-acetylated compounds. PGAs from most Gram-negative bacteria are periplasmic, whereas PGAs from *B. megaterium* and *A. viscosus* are secreted extra-cellularly **(Table 1.2)**. Rajendhran et al. (2002) have reported an intracellular PGA from *Bacillus badius.* Even though they possess similar structural organization and high sequence homology, PGAs from different sources exhibit subtle variations in biochemical and kinetic characteristics **(Table 1.2)**. The production of penicillin acylases is usually induced by the addition of phenylacetic acid to the medium and favoured low aeration levels; it is also subject to catabolite repression by glucose (Shewale and SivaRaman 1989).

A number of authors have reviewed the nature of PGAs and their significance in the production of antibiotics and other applications (Shewale and SivaRaman 1989, Parmar et al. 2000, Arroyo et al. 2003, Rajendhran and Gunasekaran 2004, Sio and Quax 2006, Chandel et al. 2008). The penicillin G acylase (*Ec*PGA) from *E. coli* (Duggleby et al. 1995) has been studied extensively and used in various industrial applications. The mature enzyme is heterodimeric (molecular weight 80 kDa), with a 24 kDa α-subunit and 67 kDa β-subunit comprising 209 and 566 amino acid residues, respectively (Duggleby et al. 1995; McVey et al. 2001). The mechanism of catalytic action is similar to that of serine proteases, with the β-chain N-terminal serine residue acting as the main catalytic residue. This serine also plays a vital role as a nucleophile in the post-translational processing of PGA to its mature form (Brannigan et al. 1995).

Penicillin acylases (both PGA and PVA) belong to the protein superfamily Ntn hydrolases, a group which also includes cephalosporin acylases, bile salt hydrolases, proteasome and γ-glutamate transaminases (GGT) among other enzymes (Oinonen and Rouvinen 2000). Enzymes of this family possess a reactive nucleophilic amino acid at their N-terminal which acts as the main catalytic residue, and is revealed by post-translational autocatalytic processing (Duggleby et al. 1995).

Table 1.2. Characteristics of penicillin G acylases from different bacteria.

Source organism	k_{cat}/K_m values ($M^{-1}s^{-1}$)	Cellular location	Special characteristics and applications	References
E. coli	1 x 10^7	periplasmic	Enantioselectivity, resolution of racemic mixtures, antibiotic and peptide synthesis	Margolin et al. 1980; Duggleby et al. 1995
K. citrophila	3.1 x 10^6		Hydrolyze AHLs	Roa et al. 1995; Mukherji et al. 2014
A. faecalis	1.3 x 10^7		Thermostable, enantioselective	Svedas et al. 1997
Providencia rettgeri	Km=19.7 μM		-	Klei et al. 1995; Sevo et al. 2002
Arthrobacter viscosus	Km=0.42 mM	extracellular	-	Ohashi et al. 1988
B. megaterium	Km=1.83 mM		-	De Souza et al. 2005
B. badius	1.025 x 10^6	intracellular	Broad substrate specificity	Rajendhran et al. 2007
Achromobacter xylosoxidans	8.2 x 10^6	periplasmic	thermostable	Cai et al. 2004
Achromobacter sp.	1.5 x 10^7	cytoplasmic	2x active on ampicillin and cephalexin than pen G	Skrob et al. 2003
PAS2	2.08 x 10^6	periplasmic	Isolated from environmental gene pool	Gabor et al. 2005

The *pac* gene coding *E. coli* PGA contains a 26 amino acid periplasmic signal, followed by the α- and β- subunit sequences which are separated by an internal spacer peptide. PGA is initially synthesized as a 90 kDa precursor polypeptide chain in the cytoplasm. Post-translational processing involves transport of the enzyme to the periplasm, and autocatalytic cleavage of the internal spacer peptide **(Fig. 1.4)**. The spacer is first cleaved on the carboxyl side between T263 and S264 to release the α-amino group of N-terminal catalytic amino acid serine of the β-subunit. Subsequently, the C-terminal end of the α-subunit is cleaved and the subunits are reconstituted to give the active enzyme. The processing in PGA is intramolecular,

and requires an intact carboxy terminus. This is found in the maturation of pre-pro insulin and is unique for a prokaryotic enzyme. Based on this auto-catalytic processing mechanism, Duggleby et al. (1995) first proposed the classification of PGAs in the N-terminal nucleophile (Ntn) hydrolase protein family. The active *E. coli* PGA is also produced only at a temperature range of 20-28°C; higher temperatures lead to disruption in folding of α-subunit and the processing mechanism (Deshpande et al. 1994).

Kasche et al. (2003) have studied the folding and maturation of PGA from *Alcaligenes faecalis* (*Af*PGA), which shows 40% sequence similarity to *E. coli* PGA and a higher specific activity. *Af*PGA has a striking difference in the length of the pro-peptide that is removed during processing. Addition of fragments of the internal pro-peptide activated the mature enzyme; and processing mutants containing attached regions of pro-peptide to the α-chain showed the same 2.3 fold increase in activity and a higher turnover number. It is possible that the pro-peptide influences the kinetic constants of the PGA enzyme by stabilizing the active site transition state, although the biological significance of this decrease in activity during maturation is not known (Kasche et al. 2003; Ignatova et al. 2005).

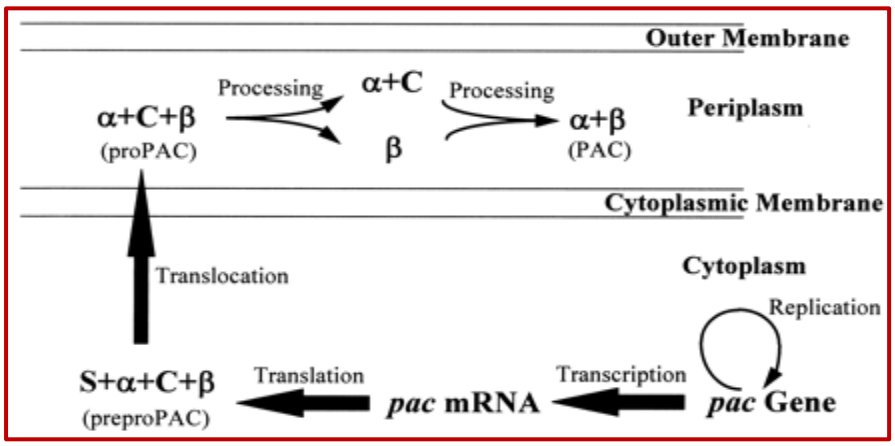

Fig. 1.4. Synthesis and maturation of pen G acylase (PAC) in *E. coli.* [S – signal peptide, α – α subunit, C-connecting/spacer peptide, β – β subunit] (Adapted from Pan et al. 2003)

Subtle differences exist across molecules in the processing pathway and catalytic machinery, even within penicillin G acylases. While *Af*PGA is transported to the periplasm via the Sec-translocation pathway (Kasche et al. 2005), *Ec*PGA is directed to the Tat-pathway with a modified signal peptide (Ignatova et al. 2002). The authors

have also reported that the *E. coli* pre-pro-PGA is recognized by the secretion pathway despite not having the exact twin-arginine Tat recognition sequence.

The structures of different penicillin acylases and their complexes with related ligands have been elucidated using crystallography and X-ray diffraction methods. *Ec*PGA **(Fig. 1.5)** has a kidney-shaped cross-section, with a deep cup-like depression in the centre. The catalytic nucleophile residue β1S sits at the mouth of the binding pocket. The enzyme contains a αββα-fold typical to Ntn hydrolases, with two α-helices flanking a β-sandwich comprising the N-terminal residues of α- and β-chains. The phenyl moiety of penicillin G and other phenylacetylated substrates points towards the interior of the protein into a hydrophobic pocket, as evidenced by co-crystal structures of the enzyme with phenylacetic acid (PAA). The structures of PGAs from *E. coli* and *P. rettgeri* mutants impaired in processing also reveal tightly bound calcium (Ca^{2+}) ion in the protein. The calcium ion has been shown to coordinate two Phe residues in α and β chains (F71 and F146 respectively), thus joining the two chains and defining the structure of the active site (Duggleby et al. 1995; McVey et al. 2001).

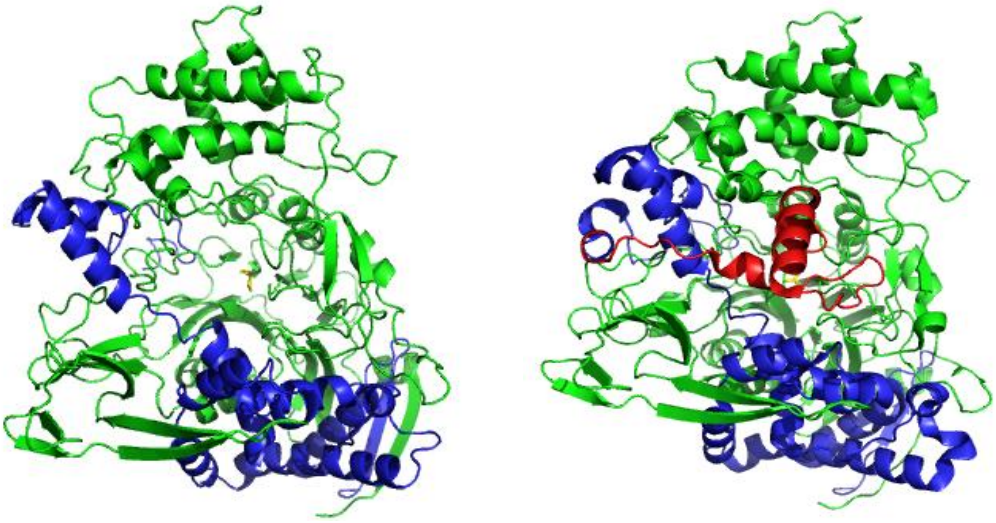

(a) **(b)**

Fig. 1.5. (a) Three-dimensional structure of mature PGA from *E. coli* (PDB ID: 1PNK, Duggleby et al. 1995). (b) Structure of a slow processing mutant precursor of *E. coli* PGA showing the spacer peptide blocking the active site pocket (PDB ID: 1E3A, Hewitt et al. 2000). Colouring scheme – blue: α-chain, green: β-chain, red: spacer peptide, yellow: N-terminal serine (β1S) residue.

Besides β1S, the PGA active site pocket is lined with many other important residues that are involved in substrate binding and catalysis. PGA catalysis proceeds via an acyl-enzyme intermediate (Brannigan et al. 1995). The reaction mechanism involves a direct nucleophilic attack by the β1S residue on the amide bond of the substrate. The hydroxyl oxygen of the serine forms an oxyanion intermediate, which is stabilized via hydrogen bonds by the main chain amide of βA69 (in *E. coli*) and side chain amide of βN241. The enzyme forms a covalent acyl intermediate and is subsequently deacylated by a nucleophile water molecule, through another tetrahedral intermediate to yield free enzyme and the acylation product. Recent studies have also proposed the involvement of βQ23 and βN241 based on quantum mechanical models (Zhiryakova et al. 2009), and demonstrated the crucial role played by the βR145 - βR263 amino acid pair in substrate binding (Guncheva et al. 2004). The reaction can result in hydrolysis (when the nucleophilic attack is performed by water) or in a semi-synthetic antibiotic (when an activated synthetic amide or ester side chain acts as acyl donor). The PGA enzyme is specific for the phenylacetyl group, while remaining tolerant of other features in the substrate. Such flexibility in substrate preference and reaction mechanism makes PGA a valuable enzyme in the pharmaceutical industry.

PGAs from certain other bacteria also display unique kinetic and structural characteristics. The enzyme from *Alcaligenes faecalis* (*Af*PGA) exhibits greater thermostability than *Ec*PGA, which has been attributed to the presence of a disulphide bridge in the enzyme structure (Verhaert et al. 1997; Varshney et al. 2012). Penicillin acylase from *Kluyvera citrophila* (*Kc*PGA) has been recently reported to hydrolyze C_6 and C_8-acyl homoserine lactones (AHLs) involved in bacterial signalling (Mukherji et al. 2014); while *Ec*PGA fails to show such activity (Sio et al. 2006) despite an 80% sequence homology.

Penicillin acylases has been used in a number of industrial applications in both aqueous and organic media. Immobilized preparations of *Ec*PGA have been employed for the production of 6-APA and semi-synthetic antibiotics including ampicillin, amoxicillin and cephalexin. The use of cross-linked enzyme crystals (CLECs, Margolin et al. 1996) and aggregates (CLEAs, Cao et al. 2000) of penicillin acylase has helped develop a kinetically controlled industrial process for ampicillin

synthesis. PGA enzymes and whole *E. coli* cells have been immobilized by covalent binding or entrapment respectively, on a variety of matrices like Eupergit C, Sepabeads and polymethacrylamide beads (Arroyo et al. 2003). Random and site-directed mutagenesis methods have also been employed to improve the characteristics of the enzyme. Alkema et al. (2000, 2002) have reported a βF24A mutant of *Ec*PGA which exhibited a higher synthesis/hydrolysis ratio and reduced inhibition by phenylacetic acid. The demand for penicillin acylase in the pharmaceutical market now exceeds 30 million tonnes per year (Chandel et al. 2008).

In addition, penicillin acylases are enantio-selective in nature; this property has been exploited for use in the resolution of racemic mixtures of amino acids (Ng et al. 2001; Liu et al. 2006), aminoesters (Landis et al. 2002), amines (van Langen et al. 2000) and secondary alcohols (Fadnavis et al. 2006, 2008). Ismail et al. (2007) have developed a fully green procedure for the enantiomeric resolution of amines, using a two-enzyme system of lipase and penicillin G acylase. Penicillin acylases have also been used to protect and deprotect amino groups of amino acids during the synthesis of peptides (Arroyo et al. 2003) and their derivatives. They have been applied in the synthesis of the sweetener aspartame (Fuganti et al. 1986) and D-phenyl dipeptides (van Langen et al. 2000).

In recent years, certain novel penicillin acylases with improved characteristics have been developed through screening and protein engineering methods (Sio and Quax 2006). A penicillin acylase from *Achromobacter* sp. CCM 4824 (Skrob et al. 2005) was reported to hydrolyze ampicillin and other amino-substituted β-lactam compounds faster than penicillin. Gabor et al. (2005) isolated a new penicillin acylase PAS2 through cloning and functional screening of DNA from a sand soil enrichment culture. This enzyme exhibited better potential for synthesis of 6-APA derived antibiotics like amoxicillin, with higher conversion rates and product accumulation. Hybrid penicillin acylases developed by gene shuffling of *E. coli* and *K. citrophila* PGA genes (Jager et al. 2006) displayed better kinetic properties and improved synthetic potential for ampicillin, cephalexin and cefadroxil. These examples illustrate the myriad applications of PGA enzymes in the pharmaceutical industry.

1.5. Penicillin V acylases:

Penicillin V acylases (PVA) act on phenoxymethyl penicillin (Pen V), and share very less sequence homology with PGAs despite acting on similar substrates. PVAs have been characterized from all classes of microorganisms, including bacteria, actinomycetes, yeast and fungi (Shewale and Sudhakaran et al. 1997). A list of PVA sources and their characteristics is given in **Table 1.3**.

Table 1.3. Sources and characteristics of acylases from different organisms active on penicillin V.

Source organism	k_{cat}/K_m values ($M^{-1}s^{-1}$)	Cellular location	Special characteristics and applications	References
Bacillus sphaericus	4.1×10^3	cytoplasm	Hydrolyzes bile salts to 20%	Olsson et al. 1985; Suresh et al. 1999
B. subtilis	0.3×10^4		Specific for Pen V	Rathinaswamy et al. 2005
Aeromonas sp. ACY95	-	intracellular	Production induced by POAA	Deshpande et al. 1996
Fusarium oxysporum	K_m=5.2mM		Production induced by POAA	Lowe et al. 1986
Penicillium chrysogenum	-		Also active on Pen G	Erickson and Bennett 1965
Beijerinckia indica	-		Production induced by sodium glutamate	Ambedkar et al. 1991
Erwinia aroideae	K_m=31mM		Constitutive production	Vandamme and Voets 1975
Rhodotorula aurantiaca	0.24×10^3		monomeric PVA	Kumar et al. 2008
Streptomyces lavendulae	1.65×10^5	extracellular	Pen K acylase	Torres-Guzman et al. 2002
S. mobaraensis	5.19×10^4		Isolated as capsaicin hydrolase	Zhang et al. 2007
Actinoplanes utahensis	4.55×10^3		Aculeacin acylase	Torres-Bacete et al. 2007

PVAs from Gram-positive bacteria and yeast are cytoplasmic, while Gram-negative homologues have been proposed to be periplasmic (Kovacikova et al. 2003). Penicillin V acylases from *Streptomyces* sp. are reported to be extracellular (Torres et al. 2002; Koreishi et al. 2007); however, they are more active on aliphatic

penicillins including octanoyl penicillin (Pen K). Unlike PGAs, the production of PVAs is usually constitutive (Carlsen and Emborg 1981); but in some cases, the activity is enhanced by the addition of phenoxyacetic acid (Sudhakaran and Borkar 1985), sodium glutamate in the medium (Ambedkar et al. 1991) or repressed by glucose (Shewale and Sudhakaran 1997).

The PVA from *Bacillus sphaericus* (*Bsp*PVA) and *Bacillus subtilis* (*Bsu*PVA) have been cloned and structurally characterized (Suresh et al. 1999; Rathinaswamy et al. 2005). The *B. sphaericus* PVA is structurally organized as a well-defined tetramer, with two dimers interacting with each other **(Fig. 1.6)**. Extensions from the upper pair of helices and the C-terminal region interact with other monomers in the molecule and help stabilize the tetramer (Suresh et al. 1999).

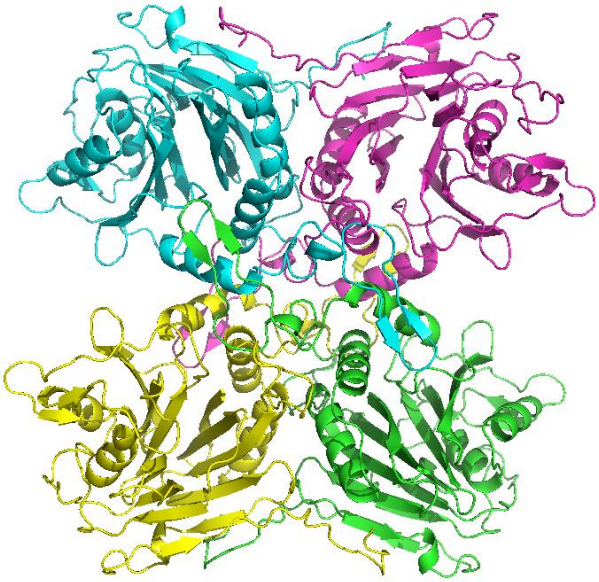

Fig. 1.6. Homotetrameric structure of PVA from *B. sphaericus* (PDB ID: 3PVA, Suresh et al. 1999), coloured by chain.

The catalytic mechanism of penicillin V acylases **(Fig. 1.7)** and the closely related bile salt hydrolases (Kumar et al. 2006) is a little different compared to PGAs, with C1 acting as the nucleophile, favouring direct proton transfer from the bridging water molecule (Suresh et al. 1999). Site directed mutagenesis experiments have shown that *Bsp*PVA needs a conserved N175 as oxyanion hole residue to stabilize the transition state complex during processing and catalysis; while R17 acts as base to deprotonate the Sγ of cysteine (Chandra et al. 2005).

A quantum mechanics simulation-based study (Lodola et al. 2012) offers new insights into this mechanism. These authors have suggested a reaction path involving a chair-like transition state complex, stabilized by various conserved residues in the catalytic site including N82 and R228. In addition, the N-terminal cysteine has been shown to participate in catalysis in a zwitter ionic form ($S^-/NH3^+$ ion pair). The active sites of PGA, cephalosporin acylase and PVA are closely related in terms of the arrangement of residues involved in catalysis (Suresh et al. 1999).

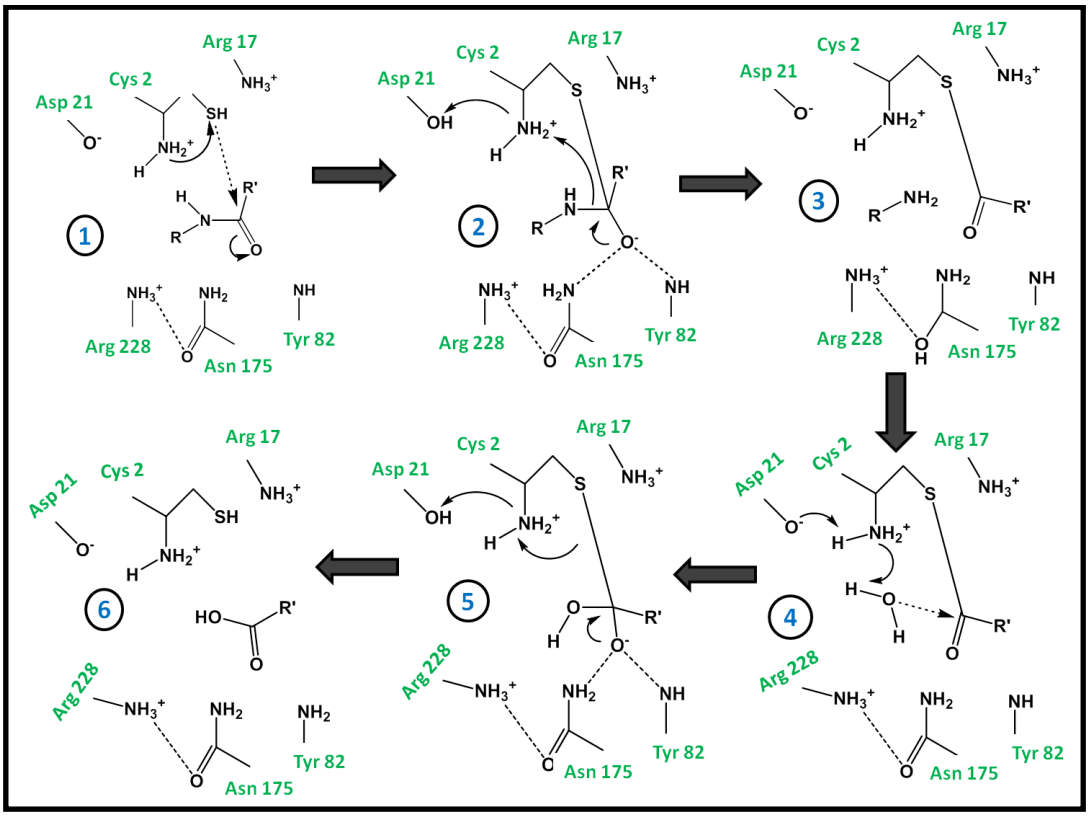

Fig. 1.7. Catalytic reaction mechanism of penicillin V acylases (Residue numbering as in *Bsp*PVA). The nucleophilic attack on the substrate by N-terminal residue (step 1) leads to formation of tetrahedral intermediate stabilized by oxyanion hole (step 2). Removal of the product amine (step 3) is followed by involvement of water molecule (step 4), leading to the release of the carboxyl product (step 5-6). Similar steps occur in most Ntn hydrolases.

The penicillin acylases from *Streptomyces* sp. (Torres et al. 2002; Zhang et al. 2007) are more active against aliphatic penicillins and related compounds, although they also hydrolyze penicillin V to a significant extent. The *S. lavendulae* PVA has been extensively studied with respect to its regulation, catalytic mechanism and substrate specificity. *Sl*PVA hydrolyzes octanoyl (pen K, k_{cat}/K_m = 165.3 mM^{-1} s^{-1}) penicillin

better than Pen V (k_{cat}/K_m = 38.8 mM^{-1} s^{-1}). The Pen V hydrolyzing enyme from *S. mobaraensis* (*Sm*PVA) was originally isolated as hydrolase acting on the plant compound capsaicin (Koreishi et al. 2006). It shows more sequence similarity with AHL acylases and cephalosporin acylases; and has heterodimeric composition similar to PGAs although the N-terminal residue is not serine (Zhang et al. 2007).

Lowe et al. (1986) have partially purified and characterized a PVA from *Fusarium oxysporum* that shows improved stability and solvent tolerance. The PVA from *Rhodotorula aurantiaca* (Kumar et al. 2008) is a functional monomeric enzyme of molecular weight 36 KDa. It is evident that very little is known about the specific mechanism of PVAs and characteristics of such enzymes from organisms other than Gram-positive bacteria. It therefore becomes imperative to study PVA enzymes in greater detail.

Penicillin V acylases have been employed in the production of 6-APA and semi-synthetic antibiotics, although their contribution in the pharmaceutical industry is less compared to PGAs. Nonetheless, some authors (Shewale and Sudhakaran 1997) have reviewed the advantages of using a Pen V - PVA system over PGAs. Penicillin V acylases are more active at acidic pH (5-6) compared to PGAs, which function efficiently at pH 7-8.5. Considering the higher stability of Pen V in aqueous solution at the lower pH range used during extraction, PVAs would be better candidates for the industrial process. PVAs are also more tolerant to phenoxyacetic acid inhibition and exhibit a higher conversion rate at high substrate concentrations. Thus, in spite of the slightly higher costs of Pen V, PVAs are more suited in antibiotic production. However, the development of commercial enzyme preparations has been hindered by the non-availability of improved hyper-producing strains.

Nevertheless, a few industrial preparations of PVAs have been employed in the industry for the production of 6-APA. PVA-producing cells and free enzyme have been immobilized using polyacrylamide entrapment, glutaraldeyde cross-linking and chitosan for kinetically controlled synthesis of antibiotics (Shewale and Sudhakaran 1997). PVA from *S. lavendulae* has been stabilized by covalent immobilization on Eupergit C (Torres-Bacete et al. 2000, 2001). Hydrolysis of Pen V is done at 28-40°C in both batch and continuous modes, and requires strict control of pH during the process. About 15% of total 6-APA is produced using Pen V-PVA system.

1.6. Bile salt hydrolases and choloylglycine hydrolases:

Penicillin V acylases have been observed to share sequence homology and structural similarity with bile salt hydrolases (BSHs), which also belong to the Ntn hydrolase superfamily and occur mostly in intestinal microbiota. BSHs are mainly involved in the deconjugation of bile salts in the intestine; they play a role in negating the antimicrobial activity of bile making it easier for the bacteria to colonize the intestinal epithelium (Begley et al. 2006). Bile salts include glyco- and tauro-conjugates of cholic and deoxycholic acid. Kumar et al. (2006) have elaborated the evolutionary relationships between the bile salt hydrolase and penicillin V acylase enzymes. Together, these enzymes make the choloylglycine hydrolase (CGH) group.

Bile salt hydrolases have been studied extensively with regard to their applications in probiotics. BSH activity has been detected in many bacteria associated with the human gut, including *Lactobacillus* (Christiaens et al. 1992; Lundeen and Savage 1992), *Clostridium* (Gopal-Srivastava and Hylemon 1988), *Bifidobacterium* (Tanaka et al. 2000), *Bacteroides* (Stellwag and Hylemon 1976) and *Enterococcus* (Taranto et al. 1996) spp. Administration of probiotics also helps in the reduction of cholesterol by either diverting its use towards bile acid synthesis or reducing its solubility, a characteristic that has been partially ascribed to the formation of deconjugated bile salts as a result of BSH activity (Klaver and van der Meer 1993). The ability of BSH to enhance the gastrointestinal persistence of bacteria and modulate cholesterol levels renders the presence of BSH activity preferable in a potential probiotic strain (Begley et al. 2006).

On the other hand, BSHs have also been reported to act as virulence factors involved in certain pathogenic bacteria. In *Listeria monocytogenes* (Dussurget et al. 2002), the *bsh* gene was found to be positively regulated by PrfA, a transcriptional activator for many known *Listeria* virulence genes. In addition, the loss of *bsh* gene led to reduced bacterial infection, colonization, and virulence in both intestinal and hepatic phases of listeriosis. The *bsh* gene also doesn't have an orthologue in non-pathogenic strains, thus confirming the importance and role of BSH in pathogenesis. The BSH from *Brucella abortus* too has been shown to confer resistance to bile and play an important role in the infectivity of *Brucella* through the oral route (Delpino et al. 2007, Marchesini et al. 2011).

Structures have been solved for BSHs from *Clostridium perfringens* (Rossocha et al. 2005) and *Bifidobacterium longum* (Kumar et al. 2006). BSHs share appreciable sequence homology and similar tetrameric configuration with PVAs, with an N-terminal catalytic cysteine residue. Other residues critical in the catalytic mechanism are also conserved, like R18, N175 and R228 (numbering as in *Bsp*PVA). Though these enzymes (BSH and PVA) act on the same non-protein amide chemical bond, the substrates are quite different. The steroid moiety of bile salts occupies more space than the corresponding group of Pen V (Lambert et al. 2008). Both the enzymes are usually annotated as conjugated bile acid hydrolases (CBAH) in protein sequence databases (http://pfam.sanger.ac.uk), and it is hard to separate the two enzymes only based on their sequence (Panigrahi et al. 2014).

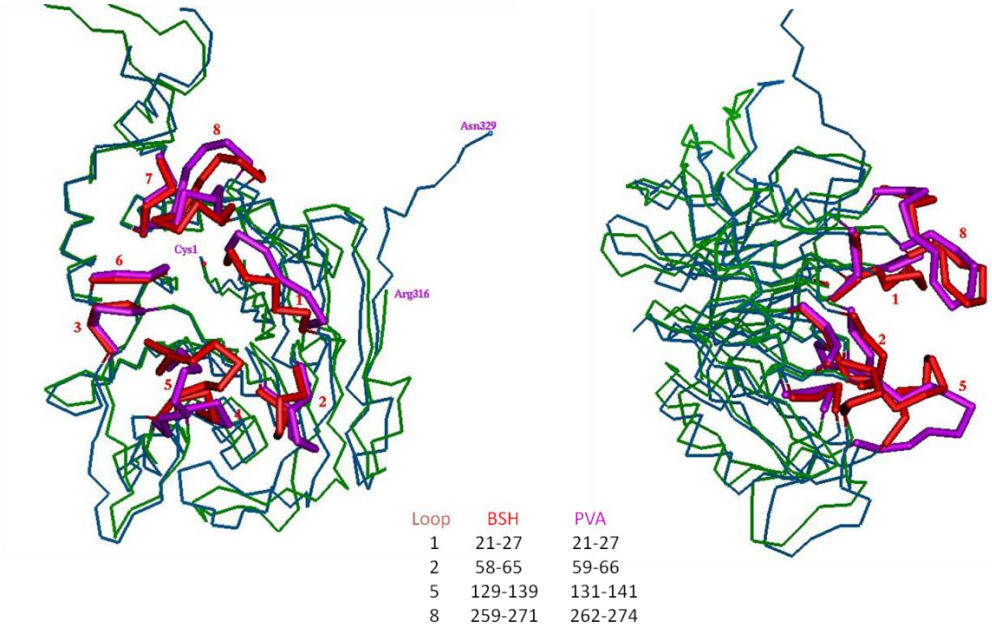

Fig. 1.8. Superposition (front and side view) of the monomer structures of BSH and PVA, showing the variable loop elements surrounding the active site that are involved in determining substrate specificity.

In spite of a similar homotetrameric structure, subtle changes in the structural elements effect changes in catalytic specificity of these enzymes (Lambert et al. 2008). For instance, PVA from *B. subtilis* (Rathinaswamy et al. 2012) hydrolyzes Pen V exclusively, while PVA of *B. sphaericus* (Pundle and Sivaraman 1997) shows up to 20% activity on bile salts. Similarly, *C. perfringens* BSH (Rossocha et al. 2005) can hydrolyze Pen V to some extent, but the *B. longum* enzyme (Kumar et al.

2006) exhibits pure BSH activity. The change in substrate specificity is thought to be effected by the difference in the length of loops flanking the active site (**Fig. 1.8.**, Kumar et al. 2006).

The post-translational processing in cholylglycine hydrolases is also different from other Ntn hydrolases like PGA and cephalosporin acylases. PVA and BSH enzymes usually do not contain a spacer peptide; they either have a single initial methionine before the N-terminal cysteine (as in the case of *Bsu*PVA and *Cp*BSH) or a small prepeptide (MLG in the case of *Bsp*PVA). Generally in bacterial proteins, the initial methionine is removed by native processing by an amino-peptidase. However, it is not clear in cysteine-Ntn hydrolases if the nucleophilic cysteine is uncovered by native or autocatalytic processing. In the case of *Bsp*PVA, Chandra et al. (2005) observed that mutation of cysteine residue impaired processing, while mutants without the propeptide (although inactive) appeared to have their initial methionine removed. It has also been reported that in *Cp*BSH (Rossocha et al. 2005) the mutation of the nucleophilic cysteine resulted in variants that were mostly insoluble and unprocessed.

It is also noted that (Ren et al. 2011) most BSH enzymes occur in Gram positive bacteria (except *Bacteroides*), while PVAs occur widely in all bacteria (Panigrahi et al. 2014). Unlike PVA, the occurrence of multiple BSH homologues in same bacteria has also been reported. In *L. plantarum*, four genes coding bile salt hydrolase proteins are present (Lambert et al. 2008; Ren et al. 2011). The occurrence of variable BSH phenotypes in different isolates of same species (Corzo and Gilliland 1999) and different G+C content with neighbouring genes (Dussurget et al. 2002) have also been observed. This has led to speculations that BSH genes could be potentially acquired by horizontal transfer (Begley et al. 2006).

On account of the homologous nature of BSHs with PVAs, it makes sense to study the cholylglycine hydrolases in tandem, to understand the subtle differences in substrate binding and catalytic mechanism. Such studies on the structural and functional aspects of these enzymes would certainly be useful to devise strategies for protein engineering of Ntn hydrolases.

1.7. In vivo role of penicillin acylases and related enzymes:

Since the emergence of antibiotic resistant bacteria, penicillin acylases have been widely applied in the pharmaceutical industry for the development and production of newer antibiotics. However, there has not been much research on the role of these enzymes in the general physiology of the microorganisms that produce them. Cole (1966) has observed that the production of penicillin acylases doesn't confer resistance against β-lactams to the microbes. The *in vivo* roles of penicillin acylases are not concretely known; but based on the existing information a few hypotheses have been put forward by various authors.

1.7.1. Scavenging for carbon sources:

Hypotheses on the role of PGAs in nature indicate its function as a scavenger enzyme that acts on alternative carbon sources, compounds that have a phenylacetyl group (Valle et al. 1991). The native *E.coli* enzyme is repressed by glucose acting at the transcriptional level while production is induced by phenylacetic acid (PAA) (Merino et al. 1992), furthering this hypothesis. In *E.coli*, the *pac* gene coding for penicillin acylase has been found to be related to the hydroxyphenylacetic acid catabolic operon (Prieto et al. 1996). Kim et al. (2004) have demonstrated that the gene for penicillin acylase in *E.coli* is regulated by the binding of a specific PaaX repressor to the *pac* promoter. The paaX regulator controls the expression of the phenylacetyl coA catabolon, which is located distant along the sequence from the *pac* gene. This process implicates the probable involvement of the PGA enzyme in the metabolism of phenylacetyl-coA related compounds. When phenylacetic acid (PAA) is present, it is converted into PAA-coA by a specific ligase (PaaK), which prevents the PaaX repressor from binding and thus relieves the repression on the synthesis of PGA **(Fig. 1.9)**. In fact, the induction of PGA production by PAA in the medium seems to be achieved through the derepression of *pac* gene by PA-coA. As shown by Galan et al. (2004) and Kim et al. (2004), the *E.coli paa* mutant showed a constitutive high expression and synthesis of PGA. Also, the *pac* promoter has been observed to be a CRP – dependent promoter, leading to the conclusion that cAMP-CRP complex is essential for the activation of *pac* expression.This could explain the repression of PGA production in the presence of glucose in the medium (Valle et al. 1986; Kim et al. 2004).

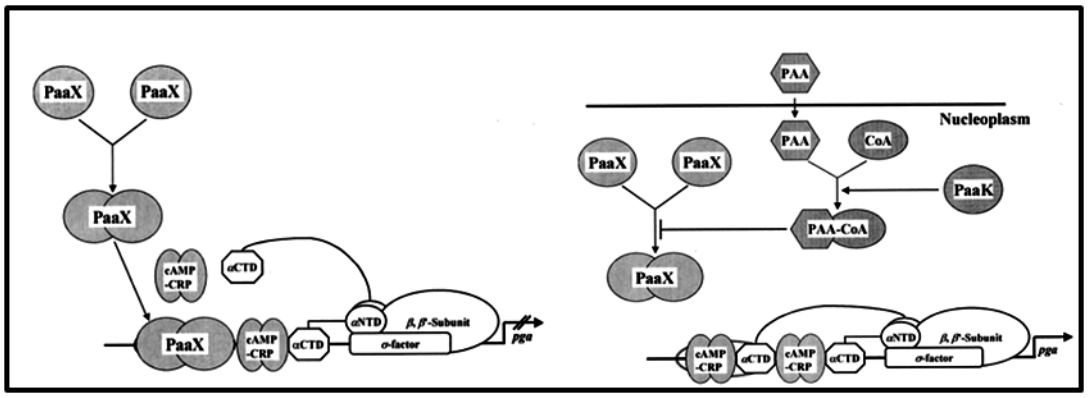

Fig. 1.9. Model of overall regulation of PGA expression. (Left) PaaX represses PGA production during normal growth. (Right) Addition of PAA derepresses PGA synthesis (Adapted from Kim et al. 2004).

Galan et al. (2004) have also studied the presence of paaX regulator homologues in different other PGA producing strains. Bacteria like *K. citrophila, B. megaterium* and *Providencia rettgeri* were found to lack a paaX homologue, explaining the constitutive nature of PGA production in these bacteria. However, the *K. citrophila* gene still retained a paaX recognition sequence, which led to repression of PGA synthesis when the gene was expressed in *E.coli* K12 strains. The presence of a gene coding for PGA even when the bacteria don't have the capability to metabolize PA-coA led the authors to hypothesize that penicillin acylases might also be involved in other unknown roles in nature.

1.7.2. Involvement in bacterial quorum sensing:

In recent years the bacterial cell signalling phenomenon, quorum sensing (Fuqua et al. 2001), has been a subject of widespread interest. Quorum sensing allows bacteria to coordinate gene expression and communicate with other cells and the environment. It is based on the detection of a critical cell density **(Fig. 1.10)**, through the concentration of small signalling molecules produced and released by the bacteria (Miller and Bassler 2001). The silencing of quorum sensing (Dong et al. 2001) allows for control of bacterial virulence and other infection-related phenomena. Acylhomoserinelactone (AHL) acylases (Leadbetter and Greenberg 2001) are a group of enzymes involved in such disruption of signalling, and these enzymes have been found to possess significant sequence and structural similarity with β-lactam acylases and Ntn hydrolases (Sio et al. 2006). AHL acylases act on the acyl chain of acylhomoserine lactones, one of the primary signalling molecules in

bacterial quorum sensing. AHLs consist of a homoserine lactone moiety and an acyl fatty acid chain, the length and substitution of which can vary among different bacteria (Miller and Bassler 2001). Quorum sensing in many Gram-negative bacteria depends on the synthesis and secretion of AHLs, which at a critical concentration bind to specific receptors, ultimately regulating the expression of virulence and other gene systems (Fuqua et al. 2001).

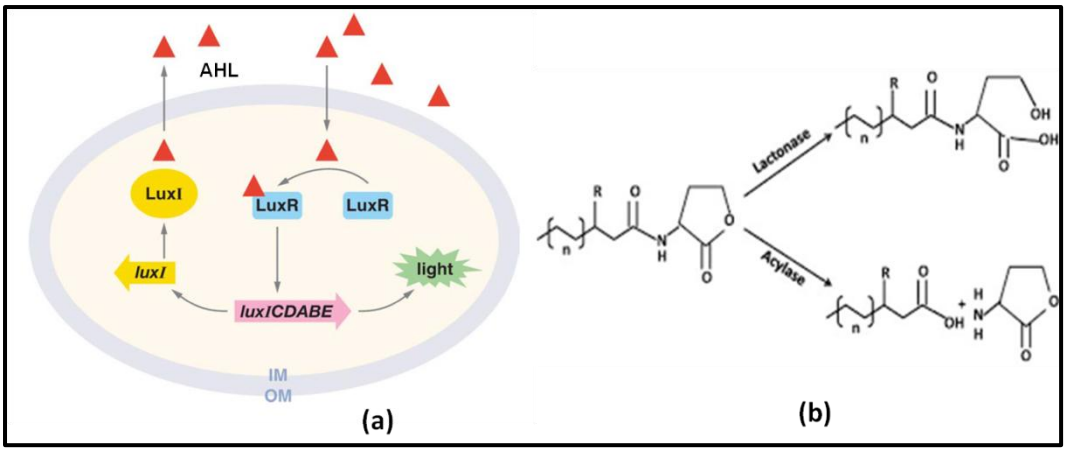

Fig. 1.10. (a) Quorum sensing in *Vibrio fischeri.* AHLs produced by the cells diffuse freely and activate the luxR receptor once a threshold concentration is reached. This leads to activation of lux operon, regulating bioluminescence (Adapted from Waters and Bassler 2005). (b) Quorum quenching: Activity of lactonase and acylase enzymes on AHLs as substrates (Adapted from Helman and Chernin 2015).

AHL acylases have been characterized so far from *Pseudomonas aeruginosa* (Sio et al. 2006), *Rhodococcus erythropolis* (Uroz et al. 2005), *Ralstonia sp.* XJ12B (Lin et al. 2003) and *Streptomyces sp.* M664 (Park et al. 2005). As already mentioned these enzymes show significant sequence homology with β-lactam acylases including PGA and cephalosporin acylase (Matsuda et al. 1987), and Aculeacin A acylase (Inokoshi et al. 1992). *P. aeruginosa* PAO1 reportedly contains no less than four AHL acylase sequences (Sio et al. 2006).

Bokhove et al. (2010) have elucidated the structure of an AHL acylase (PvdQ) from *P. aeruginosa*, which bears striking resemblance to penicillin G acylase structures and shares 24% sequence identity with *E. coli* PGA. It has a αββα structural fold typical of Ntn hydrolases, and is synthesized as a precursor that forms a heterodimeric protein by autocatalytic processing. Though PvdQ also has a serine as N-terminal nucleophile, it differs from PGA in having three disulfide bonds, which

are conserved in aculaecin acylase (Torres-Bacete et al. 2007) and PVA from *S. mobaraensis* (Zhang et al. 2007). The PvdQ catalytic mechanism has been explained to be similar to that of penicillin G acylase, with the activation of β1S by water and the formation of an oxyanion transition intermediate. However, it was also observed that PvdQ contains a hydrophobic pocket near the N-terminal nucleophile in the interior of the enzyme, closed by β24F acting as a gate. This pocket undergoes a volume increase as a result of conformational changes upon binding of the substrate, and this induced fit probably helps the enzyme to catalyze long chain C_{12}-HSLs.The secondary structure elements involved in formation of the substrate-binding pocket of PvdQ are similar as found in PGA and cephalosporin acylase. However, small changes in conformation of amino acid side chains in the active site and the replacement of key substrate-binding residues with smaller side chain amino acids makes PvdQ capable of binding long chain AHLs. The aculaecin acylase from *Actinoplanes utahensis* and PVA from *S. mobaraensis* have a similar substrate spectrum and active site morphology, thus possibly forming a group of Ntn hydrolases that hydrolyze long chain acyl amides.

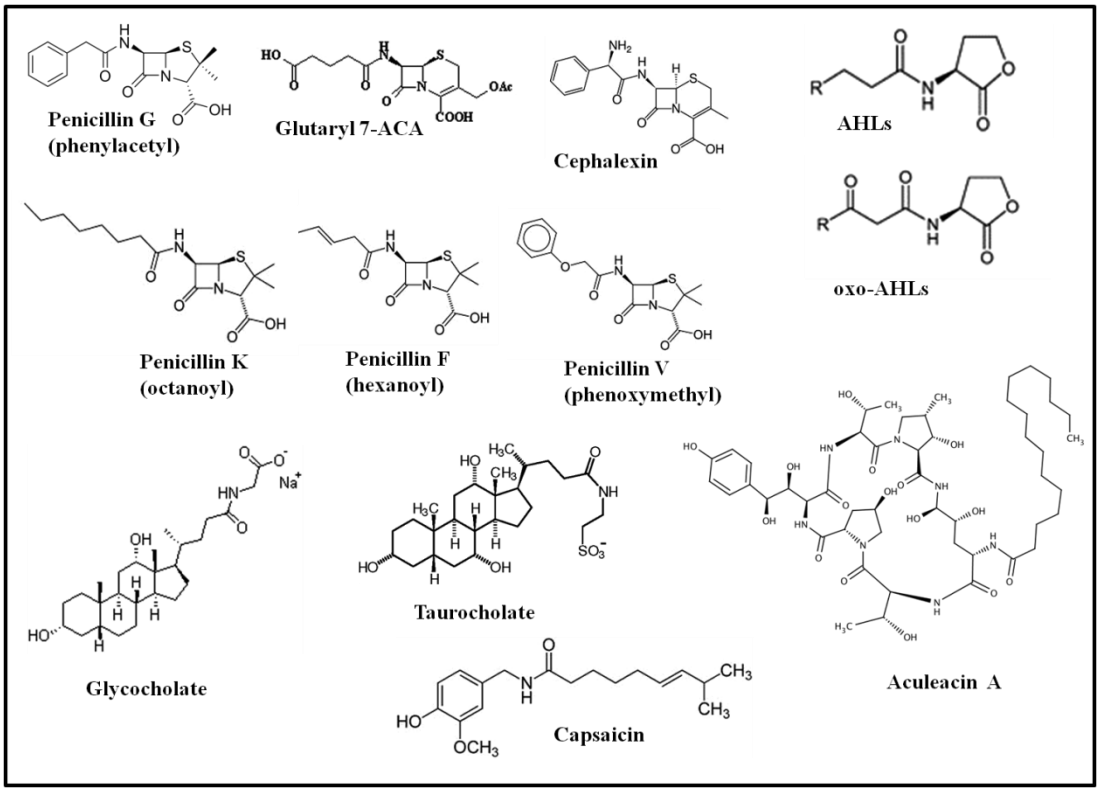

Fig. 1.11. Structures of substrates hydrolyzed by penicillin acylases and related enzymes. The CO-NH amide bond is hydrolyzed.

There are reports about cross-reactivity between cell signalling enzymes and penicillin acylases. AhlM from *Streptomyces* sp. was found to be capable of degrading penicillin G (Park et al. 2005). Recently, the PVA from *S. lavendulae* expressed in *E. coli* has also been reported to hydrolyze aliphatic penicillins and AHLs better than Pen V (Torres-Bacete et al. 2015). The AHL-acylase PA0305 from *P. aeruginosa* shows a low level of activity on penicillin G and penicillin V (Wahjudi et al. 2011). A more recent study (Mukherji et al. 2014) showed that the *K. citrophila* PGA degrades C_6-C_8 HSLs, although at a much lesser rate than AHL acylases. The *E.coli* PGA didn't show any activity towards AHLs (Lin et al. 2003), despite having a high sequence homology with the *K. citrophila* PGA. The differences in the active site organization leading to such a broad and varied substrate spectrum **(Fig. 1.11)** increases the need for extensive research on these Ntn hydrolases, and penicillin acylases in particular, to understand their place in bacterial physiology.

1.7.3. Regulation of PVA expression:

As mentioned previously, penicillin V acylases are vastly different from PGAs in that they possess no appreciable sequence homology, although they contain the same structural elements and show related catalytic mechanisms (Suresh et al. 1999). The metabolic regulation of enzyme production also follows contrasting patterns in these enzymes. While PGA production is induced by the addition of phenylacetic acid to the medium (Merino et al. 1992), PVAs are mostly constitutive (Vandamme and Voets 1974, Shewale and Sudhakaran 1997), with only a few organisms in which the enzyme production is induced by phenoxyacetic acid, including *Aeromonas* sp. (Deshpande et al. 1996), and *Fusarium oxysporum* (Lowe et al. 1986). As in the case of PGAs there are many reports about repression of PVA enzyme synthesis by glucose (Shewale and Sudhakaran 1997); although a few organisms like *B. sphaericus* (Carlsen and Emborg 1981) are not subject to glucose repression. In *Beijerinckia indica,* the PVA production is enhanced by the use of sodium glutamate in the medium (Ambedkar et al. 1991).

Kovacikova et al. (2003) have reported an indirect link between quorum sensing and PVA expression in *Vibrio cholerae,* although there is no close homology between PVAs and AHL acylase-related enzymes. In certain strains of *V. cholerae,* the

quorum sensing system influences the expression of the virulence genes through the activity of the LuxO/HapR response regulators. Activation of the *tcpPH* promoter on the *Vibrio* pathogenicity island by regulators AphA and AphB initiates the *Vibrio cholerae* virulence cascade, and is regulated by quorum sensing through the repressive action of HapR on *aphA* expression. Apart from the tcpPH promoter, AphA was also found to bind efficiently to another region on the small chromosome upstream of a *pva* gene. This results in the negative regulation of *pva* expression in response to cell density. Mutagenesis studies showed that *pva* is repressed at low cell density when AphA levels are high and derepressed at high cell density when AphA levels are reduced. The fact that the regulation of *pva* expression and that of virulence genes expression were mutually exclusive, and thus not observed to play any role in virulence, reiterates the hypothesis that penicillin acylases might function as scavenging enzymes in non-parasitic environments. It is also suggested that though the regulation of PVA might occur by other mechanisms, strains that have functional quorum sensing systems regulating PVA expression would have an advantage in certain environments.

Early studies on pencillin acylases were only focused on their industrial potential, including antibiotic production and other applications such as the resolution of racemic mixtures. However, penicillin acylases also seem to function in myriad roles in nature, which have not been given much attention. Although these enzymes have been described under one cluster with respect to their industrial utility, there is a huge structural and functional diversity exisiting between these homologues despite the presence of the common Ntn fold. Thus, in spite of their continued relevance in antibiotic production, there are compelling reasons that the role of penicillin acylases in natural physiology might not be small to be discounted. It is thus imperative to adopt a holistic approach to study the place of these enzymes in the metabolic network.

1.8. Scope and nature of the work:

The development of penicillin V acylase as a viable system for the industrial production of antibiotics has been hampered by the high cost of substrate (Pen V) and the non-availability of hyper-producing strains. This study offers a viable PVA enzyme for this purpose, from the Gram-negative organisms *Pectobacterium*

atrosepticum and *Agrobacterium tumefaciens.* Recombinant strains with maximum PVA production and high specific activity have been obtained by cloning and expression of the genes in *E. coli*. Development of immobilized systems using these PVAs would help develop a better alternative for the production of 6-APA and semi-synthetic antibiotics.

In addition, this study also aims to unravel the structural characteristics of PVAs from Gram-negative bacteria and understand their differences with their counterparts from *Bacillus* sp. The mechanism of binding of substrates (Pen V and bile salts) has been studied through biochemical techniques, mutagenesis and molecular dynamics simulations. Understanding the basis for high activity and substrate specificity in these PVAs would provide useful information for protein engineering in related enzymes.

Finally, the characteristics of these enzymes also provide several indications toward their possible roles in bacterial physiology and metabolism. The importance of understanding the place of penicillin acylases and homologous enzymes in nature has also been emphasized in this study.

Chapter 2

Cloning, expression and biochemical characterization of penicillin V acylase from *Pectobacterium atrosepticum* (*Pa*PVA)

2.1. Introduction:

The post-genomics era has led to the sequencing of numerous genes from different microorganisms. The availability of a range of techniques in recombinant DNA technology has also helped clone them and over-express many proteins in soluble form in *E. coli* and other microbial hosts, thus paving the way for development of enzymes for commercial applications. Modifications at the gene level (different constructs, codon optimization) and for growth of host strains (optimization of media and inducers) provide further avenues for maximum protein yields and better stability (Rosano and Ceccarelli 2014).

Penicillin acylases (E.C.3.5.1.11) cleave the acyl side chain of the beta-lactam antibiotics (penicillins and cephalosporins) to generate pharmaceutical intermediates 6-amino penicillanic acid (6-APA) or 7-acetoxy cephalosporanic acid (7-ACA) respectively (Shewale and SivaRaman 1989). Although the penicillin G acylase (PGA) from *E. coli* (*Ec*PGA) has a monopoly in the pharmaceutical industry, pen V acylases (PVA) have been reported to be more suitable for the production of semi-synthetic antibiotics (Shewale and Sudhakaran 1997). However, the use of PVA-Pen V combination in industry is limited by the slightly higher cost of substrate and due to the non-availability of large amount of active acylase enzyme preparations.

Penicillin acylases are members of the Ntn hydrolase protein superfamily (Duggleby et al. 1995; Suresh et al. 1999), characterized by a catalytic N-terminal residue and a common αββα-fold. Although most Ntn hydrolases have similar active site geometry, they share a fairly low sequence and structural homology. For instance, PGAs possess a heterodimeric subunit organization, as do cephalosporin acylases and γ-glutamyl transpeptidases (Castellano and Merlino 2013); while PVAs and bile salt hydrolases (BSH) share a homotetrameric structure (Kumar et al. 2006).

Biophysical and structural characterization of PVAs and BSHs has been so far restricted to Gram-positive bacteria. Structures are available for PVAs from *Bacillus sphaericus* (*Bsp*PVA) (Suresh et al. 1999) and *Bacillus subtilis* (*Bsu*PVA) (Rathinaswamy et al. 2005). *Bsp*PVA can also hydrolyze bile salts like glycodeoxycholate (GDCA) to a small extent (20% of Pen V-hydrolyzing activity),

while *Bsu*PVA is specific for Pen V (Kumar et al. 2006). When trying to classify enzymes of cholylglycine hydrolase group based on substrate preference, Lambert et al. (2008) and Panigrahi et al. (2014) have noted the low sequence homology between those from Gram-positive, Gram-negative bacteria and Archaea, even though they carry out similar reactions. Such studies raise the possibility that PVA homologues from Gram-negative bacteria might show different biochemical and structural characteristics from their counterparts from *Bacillus* sp. Screening for novel PVA producing bacteria from different sources identified a few organisms that showed a high level of PVA production. The Gram-negative plant pathogenic bacteria, *Pectobacterium atrosepticum* and *Agrobacterium tumefaciens* produced PVA with a high specific activity. Hence, it could be definitely considered worthwhile to characterize the active PVA enzymes from such Gram-negative bacteria.

The present chapter describes the cloning, over-expression and detailed biochemical characterization of the penicillin V acylase from *P. atrosepticum*. The enzyme displayed unusually high expression in soluble form, and exhibited many fold higher specific activity than that of any known PVA reported till date. Characterization of *Pa*PVA and other Gram-negative homologues would help both in industrial application of PVAs and understanding their substrate spectrum.

2.2. Materials and methods:

2.2.1. Materials:

Bile salts, guanidine hydrochloride (Gdn-HCl), Pen V (potassium salt), phenoxy acetic acid (POAA), kanamycin sulphate and HIS-Select matrix were procured from Sigma (USA). ENrich™ SEC 650 column and molecular weight markers were from BioRad. The synthetic substrate 2-nitro 5-(phenoxyacetamido)-benzoic acid (NIPOAB) was synthesized using the method of Kerr (1993) using the Schotten-Baumann reaction from 2-nitrobenzoic acid and phenoxyacetyl chloride (Sigma). Gdn-HCl was prepared as 8M stock and filtered before use. All DNA manipulation enzymes were procured from New England Biolabs (NEB). DNA isolation and

purification kits, cloning plasmids and *E. coli* strains were from Invitrogen (USA). All media components were procured from Himedia, India. *Pectobacterium atrosepticum* was obtained from DSMZ, Germany (DSM 30186).

2.2.2. Cloning of *pva* gene from *P. atrosepticum*:

The *pva* gene from *Pectobacterium atrosepticum* (annotated as cholylglycine hydrolase) was amplified from genomic DNA using the primers (restriction sites highlighted):

PatF – GGCTAG*ACATGT*GTACGCGGTTCGTTTATCTGGATCC - PciI

PatR - CAATAT*CTCGAG*CCCCGCGAATTCAAACG - XhoI

PCR was performed in a gradient thermocycler (Applied Biosystems) using conditions: 94°C/5min, 30 cycles of [94°C/30s, 52°C/30s, 68°C/60s] and final extension 68°C/10 min. Restriction digestion was carried out using NcoI and XhoI for plasmid pET 28b (Invitrogen) and PciI and XhoI for insert DNA to generate compatible ends. After 4h at 37°C, the DNA was eluted from 1% agarose gel and ligated at 16°C for 12 h. The ligation mixture was transformed into *E. coli* DH5α cells and selected on LB agar containing 35μg/ml kanamycin. Colonies were screened for recombinant plasmids using colony PCR and the gene was sequenced using T7 promoter and confirmed to be in-frame to the vector. The plasmid pET28b-*Pa*PVA was then re-transformed into *E. coli* BL21 star cells for expression using standard calcium transformation procedures (Sambrook et al. 1989). This clone was used for protein preparation, characterization and structural studies.

2.2.3. Expression and purification of *Pa*PVA:

E. coli BL21 star cells containing pET28b-*Pa*PVA were grown in LB medium containing 35μg/ml kanamycin at 37°C and 200 rpm for 2-3 h. At $O.D._{600}$ ~ 0.6, protein production was induced by adding 0.2 mM isopropyl-β-D-thiogalactoside (IPTG) and culture was transferred to 27°C for overnight incubation (18 h). The cells were harvested by centrifugation at 5000 rpm for 15 min. The cells were resuspended and sonicated in lysis buffer containing 25mM Tris-Cl pH 7.0, 300mM NaCl, 10mM $MgCl_2$ and 2mM β-mercaptoethanol. Sonication was done for 5 x 1min

at 50 W using a Branson Digital Sonifier. The expression of *Pa*PVA enzyme in soluble fraction was confirmed using SDS-PAGE and PVA activity assay.

For purification, 1 g *E. coli* – *Pa*PVA cells were sonicated in lysis/binding buffer and the clarified supernatant was loaded on a HIS-Select Ni^{2+}- affinity column equilibrated with the same buffer. After washing out the unbound proteins, *Pa*PVA was eluted using 250mM imidazole. The eluted protein fractions were dialyzed extensively against 20mM acetate buffer pH 5.2 containing 100mM NaCl and 1mM DTT and stored at 4°C. Protein concentrations were estimated using Bradford method (Bradford 1976) and purity was confirmed using SDS-PAGE (Laemmli 1970).

2.2.4. Determination of molecular weight:

The protein was subjected to SDS-PAGE on a 12% polyacrylamide gel with molecular weight markers (BioRad) and stained using Coomassie Brilliant Blue. The subunit molecular weight was ascertained using Matrix-associated laser desorption ionization-mass spectrometry (MALDI, Perkin Elmer) using a sinapinic acid matrix.

SDS-PAGE (12% gel) was also used to determine the subunit molecular weight. The gel was stained with 0.25% Coomassie brilliant blue R250 in 40% (v/v) methanol and 10% (v/v) glacial acetic acid. Electrophoresis was conducted at 25°C at 90 V (constant voltage) till the bromophenol blue tracking dye reaches the end of the gel. The apparent molecular weight was calculated by comparing the migration of the protein with that of marker proteins of known molecular weights.

To determine the native molecular weight of *Pa*PVA, 200 µl of protein (7 mg/ml) was run on size exclusion chromatography column (ENrich™ SEC column, 10 x 300 mm) using a BioRad NGC™ 10 Medium-pressure chromatography system. A similar experiment was used to test the effect of 1M Gdn-HCl on the enzyme.

2.2.5. PVA Enzyme activity assay:

PVA activity was determined by measuring the amount of 6-aminopenicillanic acid (6-APA) formed from penicillin V using p-dimethyl amino benzaldehyde (Shewale et al. 1987). The reaction was carried out for 5 min with 1.2 µM enzyme and 50 mM

Pen V in 100 mM acetate buffer pH 5.0 at 45°C. The reaction was initiated with the addition of the enzyme in a total reaction volume of 0.5 ml and subsequently quenched with equal volume of citrate phosphate buffer (CPB) pH 2.5. All assays were carried out in triplicates. Colour development was performed using p-dimethyl amino benzaldehyde (pDAB) reagent (0.6% w/v in methanol, 0.01% hydroquinone stabilizer) and the absorbance was read at 415 nm, 2 min after addition of pDAB. One unit (IU) of PVA activity was defined as the amount of enzyme required to liberate 1 μmol of 6-APA per min under the mentioned assay conditions. In the case of NIPOAB used as substrate, the enzyme was added to 1ml of 2 mM NIPOAB (2% DMSO effective concentration).

2.2.6. Effect of pH and temperature on *Pa*PVA activity and stability:

The PVA activity was assayed (as detailed above) at different pH values from 4.0 – 9.0 and temperatures (20 – 70°C) to ascertain the optimum conditions for enzyme activity.

*Pa*PVA stability was studied by incubating the protein in 20 mM acetate buffer pH 5.0 for 2 h at different temperatures from 30 to 90°C, and assaying for activity at 45°C after different time intervals. Effect of pH on enzyme stability was studied by incubating the protein in 100 mM buffers of different pH (1-11) for 4 h at 25°C and assaying the residual activity. Buffers used were: HCl-KCl (pH 1-2), acetate (3-6), phosphate (7-8), Tris (8-9) and carbonate-bicarbonate (10-11). All buffers were freshly prepared with pH adjusted at room temperature and filtered before use.

2.2.7. Effect of Guanidine hydrochloride on the enzyme:

The enzyme was also incubated with increasing concentrations of Gdn-HCl (0-6M) for 4h to study its unfolding effect. Renaturation experiments were conducted by diluting the Gdn-HCl concentration 10 times and incubating for 1h at 25°C before checking the activity. The effect of 1M Gdn-HCl on the oligomeric nature of *Pa*PVA was also checked using size exclusion chromatography.

2.2.8. Fluorescence measurements:

Conformational changes that occur in proteins in different conditions can be studied using changes in the fluorescence of sensitive fluorophores, like the aromatic amino acids trp, tyr and phe. Flourescence emission spectra of *Pa*PVA were measured on a Perkin Elmer LS50 B fluorimeter with slit width of 7 nm for both the monochromators. Samples (2 ml) were maintained at constant temperature (± 0.1°C) in a quartz cuvette with the help of a Julabo F 25 circulating cryobath. Samples were excited at 295 nm and the emission spectra were recorded from 310 to 400 nm. All samples were checked for inner filter effect. The fluorescence of buffers, quenchers and various additives were measured at identical wavelengths and corrected for in the observed fluorescence of samples.

2.2.9. Circular dichroism:

Optically active molecules in solution absorb left and right polarized components differentially when circularly polarized light is incident on them, leading to the phenomenon of circular dichroism (CD). Proteins and nucleic acids also display signature CD spectra. The analysis of protein CD spectra in the UV region is commonly used to follow the conformational changes in protein secondary structure, and complements fluorescence spectroscopy and biochemical studies. Far-UV (190-250 nm) CD signals are principally due to absorption by the peptide bond, and can provide an estimation of the secondary structure composition of proteins. Near-UV (250-300 nm) CD signals are contributed by the aromatic amino acids, and are sensitive to the overall tertiary structure of the protein (Kelly et al. 2005).

The enzyme solution filtered through a 0.22 μm membrane and dialyzed against 20 mM acetate buffer at pH 5.0 was used for CD spectroscopy. The CD spectra were recorded on a J-815 spectro-polarimeter with a Peltier Type CD/FL Cell circulating water bath (Jasco, Tokyo, Japan) at 25ºC in quartz cuvettes. All spectra were corrected for buffer contributions and converted to mean residue weight ellipticity. Far-UV CD spectra (0.15 mg/ml *Pa*PVA) were recorded in a rectangular quartz cell of 1 mm path length in the range of 190-250 nm at a scan speed of 100 nm/min with a response time of 1 s and a slit width of 1 nm. Near UV spectra (1.2 mg/ml *Pa*PVA)

were recorded in the range of 250-320 nm with a 5 mm path length quartz cell. Each spectrum was recorded as the average of 3 scans.

To understand the conformational changes taking place in the protein structure and their relation to enzyme stability, fluorescence and CD spectra of *Pa*PVA were measured after subjecting the enzyme to different conditions of pH (1-11), temperature (30-90°C) and increasing concentrations Gdn-HCl (0-6M).

2.2.10. Effect of protein modifiers on enzyme activity:

*Pa*PVA (20 µg) was incubated with reducing agent DTT and metal-chelating agent ethylene diamine tetraacetic acid (EDTA) in a 100µl reaction mixture for 30 min at 25ºC. Enzyme activity was assayed after incubation; untreated enzyme served as control. The effect of divalent metal ions and detergents was studied using similar experiments. Solvents were incorporated at different concentrations into the assay mixture to study their effect on enzyme activity. All experiments were performed independently in triplicates and results expressed as averages with <5% standard deviation.

2.2.11. *Pa*PVA kinetic parameters:

Kinetic behaviour of *Pa*PVA was determined by assaying the enzyme activity with increasing concentrations of penicillin V as substrate, 5-960mM under the optimum conditions. Preliminary determination of Km and V_{max} was done using the method described by Sakoda and Hiromi (1972) and Hill constants were calculated using least squares fitting of ln ($v/(v_{max}-v)$) vs ln (S) plots. These initial values were used to fit the data to equation (2.1) using GraphPad Prism version 5.01 (GraphPad software, La Jolla California USA, www.graphpad.com) to determine Km, V_{max}, h and Ki of substrate inhibition (Chen and Tanaka 2011).

$$v = [V_{max} \cdot S^h] / [K_{0.5} + S^h + (S^{2h}/K_i)] \quad \text{..... (2.1)}$$

In case of the synthetic substrate NIPOAB, the hydrolysis of the substrate was followed at 405 nm in a spectrophotometer with increasing substrate concentrations (0.5-12mM).

2.3. Results and Discussion:

While screening organisms for potential PVA producers, we identified a few bacterial species **(Table 2.1)** that showed high levels of cell-bound activity. Gram negative bacteria like *P. atrosepticum* and *A.tumefaciens* showed much higher activity than other groups including *Bacillus* sp., actinomycetes and yeast. In addition, although PVA enzymes have been isolated from a variety of bacteria and fungi, extensive characterization including structural features is available only for those from *Bacillus sphaericus* (Suresh et al. 1999) and *Bacillus subtilis* (Rathinaswamy et al. 2005, 2012). Based on the sequence homology, the PVAs from Gram-negative bacteria have been shown to cluster separately when compared with their Gram-positive counterparts (Lambert et al. 2008; Panigrahi et al. 2014), and probably possess unique characteristics. In this context, we attempted to clone the genes coding for PVA from Gram-negative plant pathogens and maximize production through heterlogous expression. This chapter details the cloning and expression of PVA from *P. atrosepticum* in *E. coli* and biochemical and biophysical characterization of the enzyme.

Table 2.1. PVA producing bacterial strains identified by screening. * PVA activity (IU/g cells) refers to cell-bound activity of culture grown in nutrient broth.

Bacterial identification	Strain designation	Source	PVA activity (IU/g cells)*
P. atrosepticum	DSM 30168	DSM	22.5
A. tumefaciens	DSM 30205	DSM	19.3
Bacillus cereus	ATUAVP1846	Soil (Pune, India)	6.4
Enterobacter hormaechei	APS3	Sulphur spring water (Dehradun, India)	3.2
Aeromonas enteropelogenes	SPA1	Soil (Pune, India)	14.1

2.3.1. Cloning and expression of *pva* gene from *P. atrosepticum*:

The gene ECA3205 from the genome sequence of *Pectobacterium atrosepticum* is annotated in the GenBank database (www.ncbi.nlm.nih.gov) as cholylgycine hydrolase, a group of enzymes which includes penicillin V acylase and bile salt hydrolases. Phylogenetic analysis and biochemical assays confirmed the enzyme as a penicillin V acylase. The *pva* gene contained a 29-amino acid signal sequence that directs the enzyme to the periplasm. This signal peptide is present in most Gram-negative cholylglycine homologs; however, the length and sequence is dependent on the bacterial species. *Pa*PVA has only 25% sequence identity with already characterized PVAs from *Bacillus* and BSHs from Gram-positive bacteria, which furthers the argument for the necessity of studying such enzymes from Gram-negative bacteria.

The *pva* gene was cloned without the periplasmic signal sequence, with a methionine residue added before the N-terminal cysteine **(Fig. 2.1a)**. The recombinant gene was identical to the reported sequence (NCBI accession number NC_004547.2) without any mutation. The protein expressed in *E. coli* with a C-terminal 6X His-tag, in the cytoplasmic soluble fraction; this suggests that the processing of *Pa*PVA occurs by the simple removal of methionine in the recombinant *E. coli* and by removal of the periplasmic signal peptide in the wild type *P. atrosepticum*. Ntn hydrolases usually are processed to their active form by post-translational autocatalytic mechanism (Brannigan et al. 1995; Oinonen and Rouvinen 2000). Chandra et al. (2005) prepared various processing-impaired mutants of the PVA enzyme from *B. sphaericus*, which possesses a MLG pro-peptide before the N-terminal cysteine. Mutants with the prosequence retained the tripeptide; however, mutants lacking it appeared to have their initiation formyl methionine (fMet) removed. In the case of BSH from *Clostridium perfringens* (Rossmann 2008), cysteine mutants expressed in mostly insoluble form with the N-terminal methionine intact; neither native nor autocatalytic processing was observed. Structural analysis of *Cp*BSH indicated the importance of the position of C1 for nucleophilic attack and the role of R18 and D69 residues in autocatalytic processing. These residues are highly conserved in many cholylglycine

hydrolases characterized so far. Mutagenesis of such residues could shed more light on the processing mechanism of cholylglycine hydrolases in Gram-negative bacteria.

*Pa*PVA was hyper-expressed in *E. coli*, with protein yields comfortably reaching 250 – 300 mg per litre of culture. This is very high compared to model recombinant proteins in *E.coli* (Rosano and Ceccarelli 2014); the enzyme did not accumulate in inclusion bodies even after overnight incubation at 27°C.

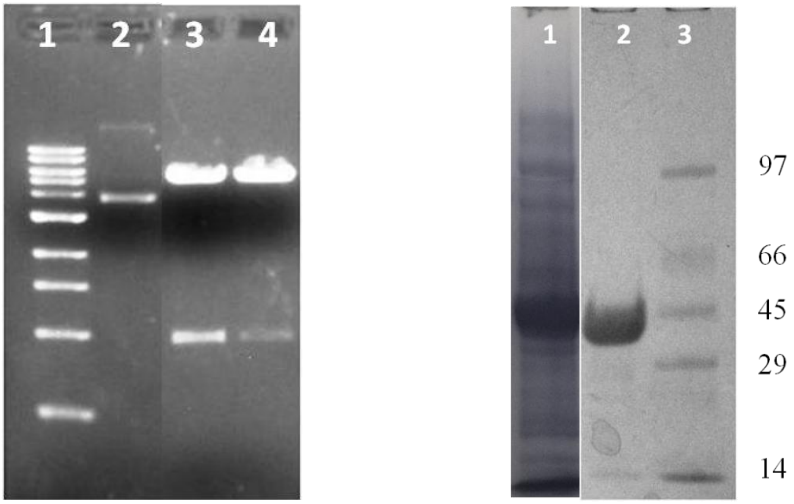

(a) **(b)**

Fig. 2.1. (a) Restriction digested *Pa*PVA-pET28b on 1% agarose gel (Lane 1 – Invitrogen 10 kb DNA ladder, 2 – *Pa*PVA-pET28b, 3, 4 – recombinant *Pa*PVA-pET28b digested with XbaI/XhoI for 3 h at 37°C). (b) *Pa*PVA on 12% SDS-PAGE gel (Lane 1 – Sonicate of *Pa*PVA expressing BL21 clone, soluble fraction, 2 – purified *Pa*PVA, 3 – BioRad protein molecular weight marker, MW in KDa).

2.3.2. Purification of *Pa*PVA:

The protein was purified to homogeneity **(Fig. 2.1b)** using Ni^{2+} affinity chromatography. A small amount of precipitate was formed on dialysis, which was clarified by high speed centrifugation. Before characterization, the enzyme was also passed through a size exclusion column to remove any soluble aggregates present. The enzyme (3 mg/ml) stored at 4°C retained 90% of its activity after 30 days. The final yield of protein was 72 mg/ g wet cells, with a specific activity of 430 IU/mg with 50mM Pen V. The catalytic reaction was linear till 10 mins for 1.2 μM enzyme.

*Pa*PVA exhibits many fold greater specific activity for Pen V than other PVAs from Gram-positive bacteria, actinomycetes, fungi and yeast (Shewale and Sudhakaran 1997). Such high activity and increased protein yields make *Pa*PVA a valuable enzyme for use in the pharmaceutical industry. The targeting of such a highly active PVA enzyme to the periplasmic space in *P. atrosepticum* also provides possible pointers to the physiological role of the enzyme. Periplasmic proteins generally interact actively with compounds in the environment, functioning as signaling receptors, binding proteins and hydrolytic or detoxifying enzymes. Valle et al. (1991) have hypothesized the role of penicillin acylases in the environment as scavengers for alternative carbon sources, while Kovacikova et al. (2003) have studied the modulation of *pva* gene expression in *Vibrio cholerae* by bacterial signalling (quorum sensing) mechanism.

2.3.3. Molecular weight determination:

MALDI showed a single peak of 39, 191 Da, corresponding to the subunit molecular weight of *Pa*PVA enzyme **(Fig. 2.2)**. The native molecular weight was estimated to be 154 kDa using size exclusion chromatography, which confirmed a tetrameric subunit association similar to that reported for other PVAs (Suresh et al. 1999). The isoelectric point of the enzyme was 8.4.

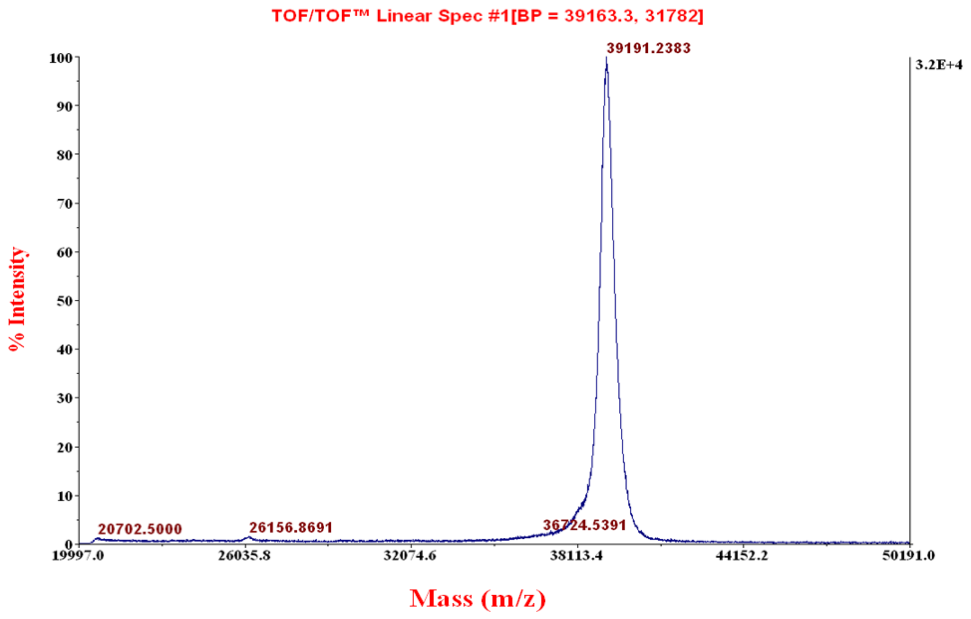

Fig. 2.2. *Pa*PVA subunit molecular weight (39.19 kDa) determined by MALDI.

2.3.4. Effect of pH and temperature on PaPVA activity:

The *Pa*PVA enzyme exhibited maximum activity at an optimum pH of 5 (acetate buffer) in the assay **(Fig. 2.3a)**. The enzyme showed a narrow pH spectrum (4-6) of activity and was most active in the acidic pH range. The PVA from *B. sphaericus* (Olsson et al. 1985) shows a similar optimum pH, while PVAs from *Fusarium oxysporum* (Lowe et al. 1986) and *Streptomyces lavendulae* (Torres et al. 2003) are more active at pH 7-9. The optimum temperature for activity of *Pa*PVA was 45°C **(Fig. 2.3b)**; the enzyme showed very little activity when temperatures reached 60°C.

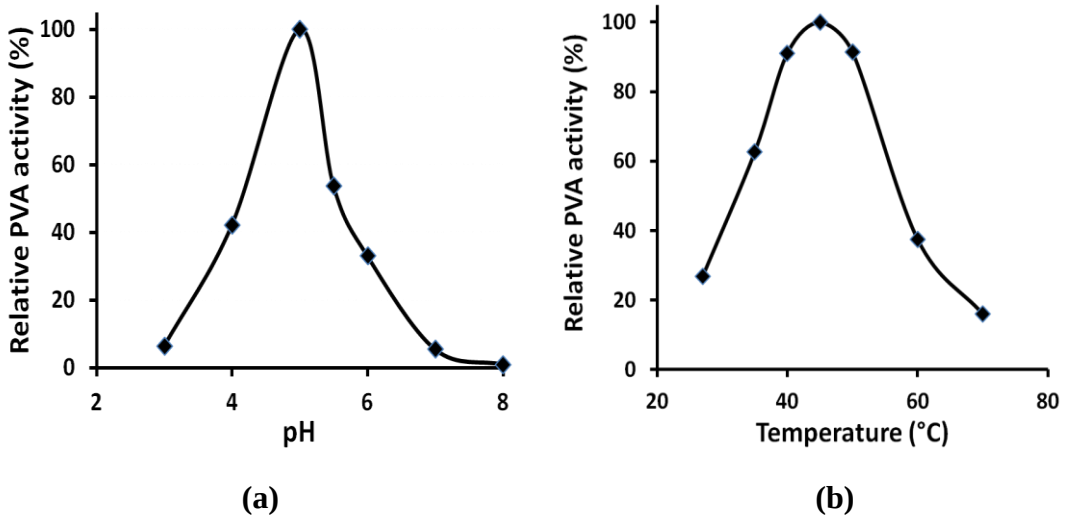

Fig. 2.3. Optimum pH (a) and temperature (b) for *Pa*PVA enzyme activity. Activity at pH 5 and 45°C (430 IU/mg) taken as 100%.

2.3.5. pH stability of *Pa*PVA:

The enzyme was functionally stable in the pH range 3-7 **(Fig. 2.4a)** with than 80% retention in activity after 4 h. There was significant reduction in activity at pH 9-11, with only 40% of the original activity retained. The enzyme was rapidly inactivated at pH 1-2. The stability of *Pa*PVA and optimum activity in acidic pH signify the potential of the enzyme to be used in large-scale production of 6-APA (Shewale and Sudhakaran 1997).

The fluorescence intensity of the enzyme showed emission maxima (λ_{max}) at 335 nm. The intensity significantly decreased at extreme pH (1-2 and 9-11),

corresponding to a reduction in enzyme activity **(Fig. 2.4b)**. The far UV CD spectrum of the native *Pa*PVA enzyme at pH 5 **(Fig. 2.4c)** showed a minimum at 218 nm and was typical of a protein with β-sheet and α-helix structure. Some rearrangement of the structure was evident at pH 1 with minima of 213 nm and significant reduction in negative minima. In the case of CD spectra in the aromatic region (250-320 nm), the enzyme was featureless at pH 1 indicating a loss of structure **(Fig. 2.4d)**. These results agree well with the modulation of *Pa*PVA activity observed at different pH.

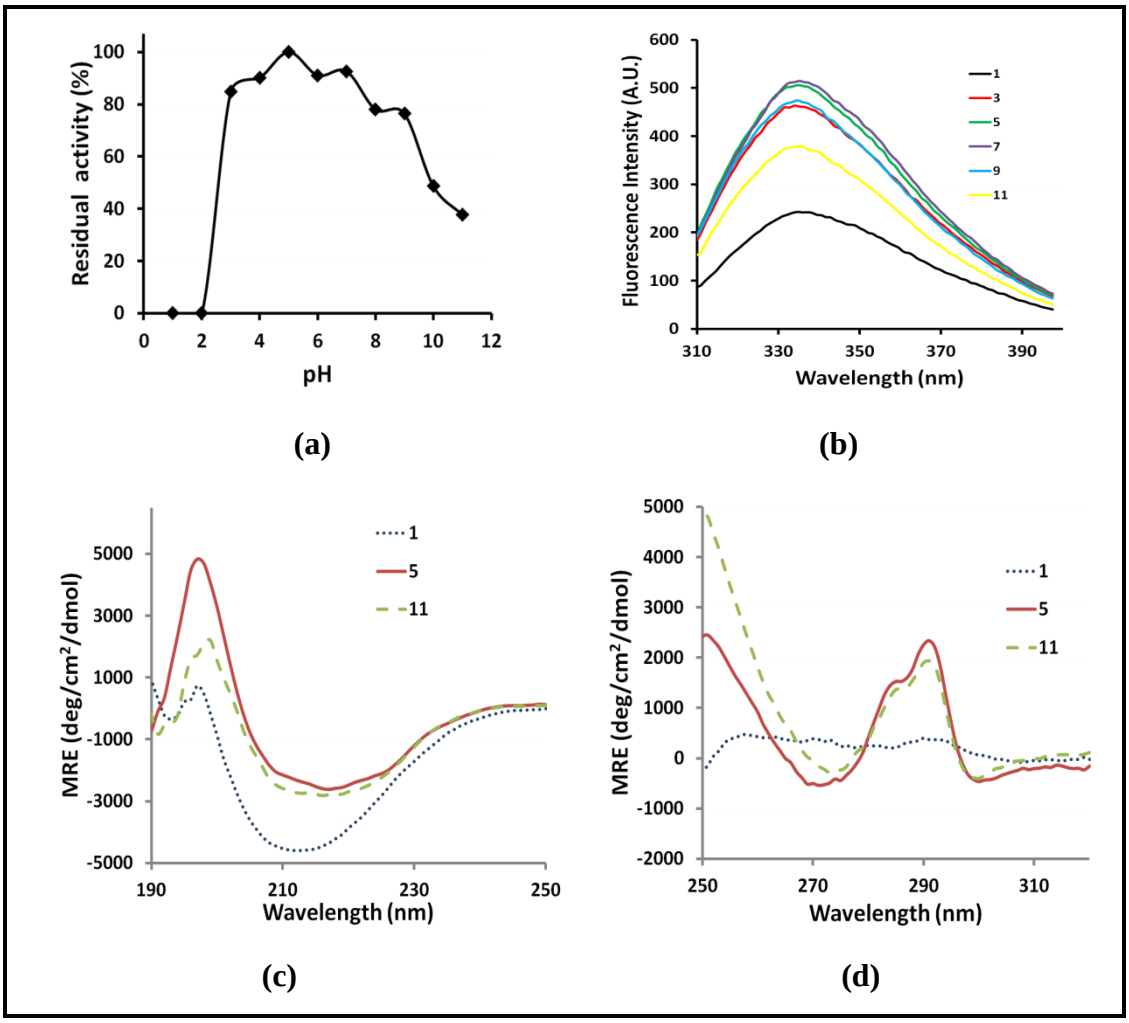

Fig. 2.4. (a) *Pa*PVA stability at different pH: Residual activity after 4h at 25°C. (b) Fluorescence spectrum of *Pa*PVA at different pH at 25°C. (c) Far-UV CD spectra of *Pa*PVA after 4 h incubation at different pH. (d) Near-UV CD spectra of *Pa*PVA after 4 h incubation at different pH.

2.3.6. Thermal stability of *Pa*PVA:

There was a gradual reduction in the enzyme activity with increase in temperature **(Fig. 2.5a)**. The enzyme (40 µg/ml) retained 87% of its original activity at 30°C and 50% activity at 50°C after 2h. *Pa*PVA showed significant loss of activity only at 80°C; it lost 90% activity within 15 min. There is a marginal improvement in stability at 60°C over previously reported bacterial PVA/BSH enzymes.

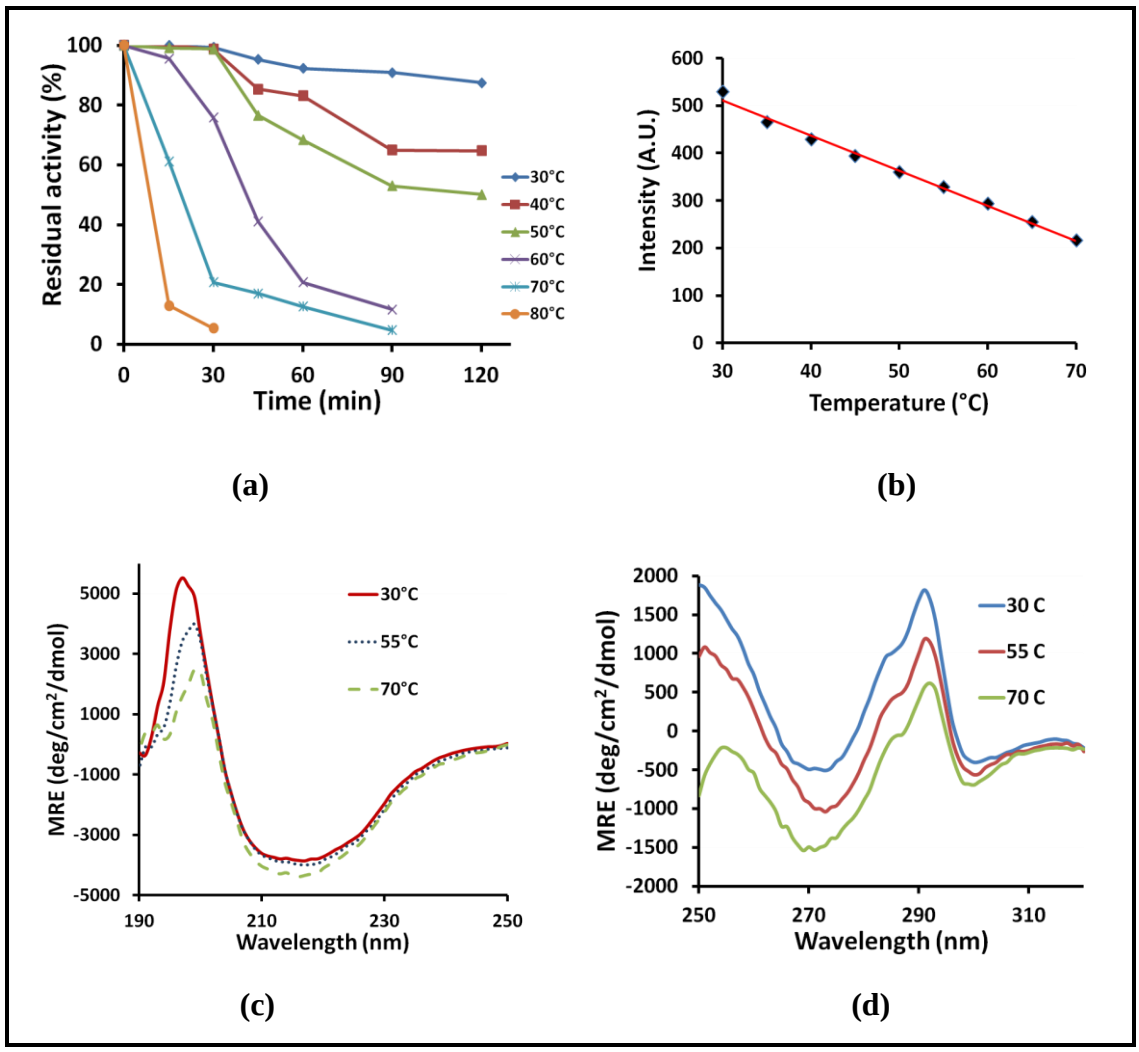

Fig. 2.5. (a) Effect of temperature on *Pa*PVA stability: Residual activity after incubation at 30-70°C for different time intervals. (b) *Pa*PVA fluorescence intensity at λ_{max} as a function of temperature (incubation time 15 min) (c) Far-UV CD spectra of *Pa*PVA after incubation at 30-70°C for 15 min. (d) Near-UV CD spectra of *Pa*PVA after incubation at 30-70°C for 15 min.

While the PVAs from *Bacillus* spp. or BSHs show loss of activity and collapse of tertiary structure within 15 min at 60°C (Rathinaswamy et al. 2012), *Pa*PVA was observed to retain at least 80% of original activity till atleast 30 min. At higher concentrations (0.4 mg/ml) and in the presence of 100mM NaCl, the *Pa*PVA enzyme was able to retain its full activity up to 6 h at 50°C. This is an additional favourable feature for industrial applicability of *Pa*PVA, besides high yield and specific activity.

Increase in temperature led to a linear reduction of fluorescence intensity of *Pa*PVA **(Fig. 2.5b)**, without any change in λ_{max}. The intensity decreased to 40% of the original at 65°C. The *Pa*PVA enzyme contains 8 trp residues per monomer, two of which are situated in the active site. The decrease in intensity might be due to quenching of tryptophan fluorescence and exposure of aromatic residues to the solvent, as a result of thermal inactivation.

The enzyme also showed no significant loss of secondary or tertiary structure till 70°C as revealed by the CD spectra **(Fig.2.5 c, d)**.

2.3.7. Effect of Guanidine hydrochloride on *Pa*PVA:

*Pa*PVA showed enhanced activity in the presence of low concentrations of Gdn-HCl (up to 1M) **(Fig. 2.6a)**. Using size exclusion chromatography, we observed that the enzyme formed soluble aggregates in the absence of NaCl; the aggregates disappeared when the protein was incubated in low concentrations of Gdn-HCl till 1M **(Fig. 2.6b)**. Gdn-HCl at low concentrations has been known to confer effective charge shielding (Monera et al. 1994) and prevent aggregation in proteins (Hevehan et al. 1997). In the case of dihydrofolate reductase (Fan et al. 1996), activity enhancement by Gdn-HCl has been attributed to increased conformational flexibility in the active site, thus helping in more favourable binding of the substrate. Thus, it is possible that the increase in *Pa*PVA activity could be a consequence of interaction with Gdn-HCl leading to deaggregation and conformational changes at the active site of the enzyme. The enzyme started progressively losing activity after 1.5M Gdn-HCl, and was totally inactivated at concentrations over 2M.

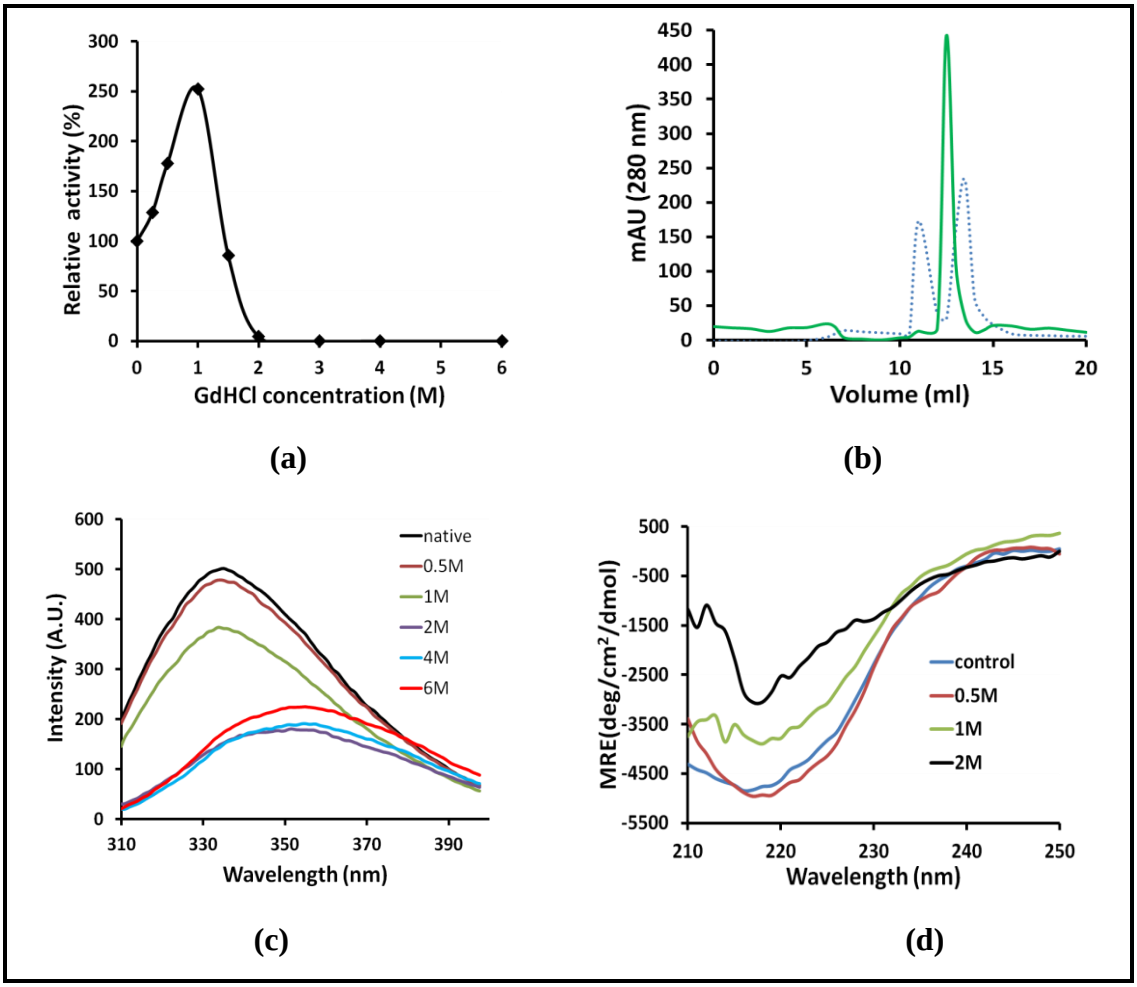

Fig. 2.6. (a) Relative activity of *Pa*PVA after incubation with increasing concentrations of Guanidine hydrochloride (Gdn-HCl, 0-6M) for 4 h. (b) Size exclusion chromatography of *Pa*PVA in 20 mM acetate buffer pH 5 (...) and Gdn-HCl treated enzyme (–). (c) Fluorescence spectrum of *Pa*PVA after incubation with Gdn-HCl for 4 h. (d) Far UV CD spectra of Gdn-HCl treated *Pa*PVA.

The fluorescence λ_{max} shifted to 355 nm **(Fig. 2.6c)** with increase in Gdn-HCl concentrations above 1.5 M. The 335/355 OD ratio decreased from 1.36 to 0.93 indicating the exposure of tryptophan residues to the polar environment. Unfolding was maximum at 2 M, as indicated **(Fig. 2.6d)** by the far-UV CD spectra; this correlates well with the complete inactivation of the enzyme from this concentration of the denaturant. However, dilution of Gdn-HCl led to revival of the original enzyme activity within 1h, indicating that unfolding was completely reversible. The duration of treatment with Gdn-HCl and increasing temperatures have been known to influence the yield of protein on renaturation (Kathir et al. 2005).

2.3.8. Effect of protein modifiers on PaPVA activity:

The presence of 1mM DTT enhanced the enzyme activity by 14%, indicating active sulfhydryl group of cysteine present in *Pa*PVA. The enzyme was stored in buffer containing 100 mM NaCl and 1mM DTT to ensure that the protein stays in active state with catalytic cysteine remaining in reduced form. There was no significant change in *Pa*PVA activity in the presence of EDTA (**Table 2.2**). In the presence of metal ions that bind to sulfhydryl groups (Hg, Ag), the enzyme was completely inactivated within 15 min.

Table 2.2. Effect of additives (Reducing agents, chelating agents and detergents) on *Pa*PVA activity. Enzyme without any modifier served as control (100%).

Additives	Concentration	Relative activity (%)
DTT	1 mM	114.5 ± 0.4
	10 mM	123.2 ± 6.1
βME	1 mM	119.0 ±5.8
	10 mM	105.3 ± 3.2
EDTA	1 mM	101.1 ± 4.5
	10 mM	101.1 ±6.3
CTAB	0.1 %	250.1±4.7
	0.5 %	270.6±0.6
Triton X-100	0.1 %	180.4±1.3
	0.5 %	185.3±0.5
Tween 20	0.1 %	175.1±4.3
	0.5 %	153.3±2.9
SDS	0.1 %	8.9±1.7
	0.5 %	0

The activity of *Pa*PVA was significantly enhanced by treatment with detergents for 30 min at room temperature. (**Table 2.2**) Cationic detergent CTAB increased the

enzyme activity by 250%, while mild non-ionic surfactants (Tween 80, Triton) enhanced the activity by 175%, at concentrations higher than their CMCs. Enhancement of PVA activity in *R. aurantiaca* in the presence of detergents has been reported recently (Kumar et al. 2008). Detergents interact with the enzyme surface and play a role in enhancing the solubility and stability of proteins (Neugebauer 2000), and could also modulate kinetic behaviour of enzyme reactions in micelles (Abuin et al. 2007). The anionic detergent SDS, however, rapidly deactivated the *Pa*PVA enzyme at 0.1% concentration.

*Pa*PVA activity was also enhanced in the presence of organic solvents like isopropanol, acetone, butanone, acetonitrile, hexane and ethyl acetate at 5% (v/v) concentration in the assay mixture (**Table 2.3**). The protein was stable for 4 h in 10% isopropanol, retaining 80% of its original activity; higher concentrations deactivated the enzyme rapidly (data not shown). Aprotic solvents (DMSO, DMF, dioxan and tetrahydrofuran), and non-polar hydrocarbons (chloroform, dichloromethane) inhibited or deactivated the enzyme.

Table 2.3. Modulation of *Pa*PVA activity in presence of organic solvents. Enzyme with water served as control (100%).

Solvent	Relative activity (%)	
	5% (v/v)	10%(v/v)
Methanol	74.9 ± 2.1	34.7 ± 1.0
Ethanol	82.0 ± 0.8	69.9 ± 1.6
Isopropanol	194.6 ± 3.6	167.7 ± 1.9
Acetone	106.1 ± 1.6	103.4± 1.8
Butanone	174.0± 2.7	74.7± 2.2
Acetonitrile	165.0 ± 3.4	81.4 ± 1.9
Ethyl acetate	147.5 ± 3.0	59.7± 2.1
Hexane	113.0 ± 1.8	77.1± 1.3
DMSO	57.5± 1.4	27.8± 0.6

Arroyo et al. (1999) have studied the enhancement of *S. lavendulae* PVA activity and its stability in water-organic co-solvent monophasic systems. Solvents like dioxan, tetrahydrofuran (THF) are hydrophobic with high salvation capacity and thus are strong denaturants. On the other hand, alcohols are highly nucleophilic and could replace water in the deacylation step of Pen V hydrolysis, thus ensuring faster removal of product and enhanced activity (Arroyo et al. 1999, 2000). However, it is to be noted that in *Pa*PVA only isopropanol was observed to increase the enzyme activity.

2.3.9. Kinetics of Pen V binding:

PVAs and BSHs reported so far have followed normal Michaelis-Menten (MM) kinetics (Olsson et al. 1985; Rathinaswamy et al. 2012; Kumar et al. 2006). However, substrate binding in *Pa*PVA was more complex with distinct deviation from MM kinetics, showing cooperative behaviour and substrate inhibition **(Fig. 2.7a)**. Chen and Tanaka (2011) have reported a similar behaviour in the case of *Lactococcus lactis* prolidase, an enzyme which hydrolyzes proline-containing dipeptides. The hexameric enzyme Aspartate transcarbamoylase (ATC) has also been reported to show substrate inhibition at pH 7.8-9.1, along with its cooperative nature (Pastra-Landis et al. 1978). *Pa*PVA showed normal allosteric saturation behaviour in the 5-80 mM concentration range, while the 120-960 mM region is due to the inhibition at high substrate concentrations. The intermediate 80-120 mM section exhibits two opposing effects – activity due to normal Pen V binding and inhibition due to possible unproductive binding of the substrate in the enzyme active site. The substrate inhibition in *Pa*PVA was near complete, with the activity nearing zero at very high Pen V concentrations.

The kinetic parameters for *Pa*PVA enzyme ($K_{0.5}$, K_i, h and Vmax) were computed using equation (2.1) as described earlier **(Fig. 2.7a)**. The maximum velocity for *Pa*PVA (V_{max} = 758.5 IU/g) is greater than any other acylase active on Pen V reported so far. The substrate concentration at half-maximum saturation ($K_{0.5}$) was 40.8 mM, which is comparable to the K_m of *Bsp*PVA (40 mM).

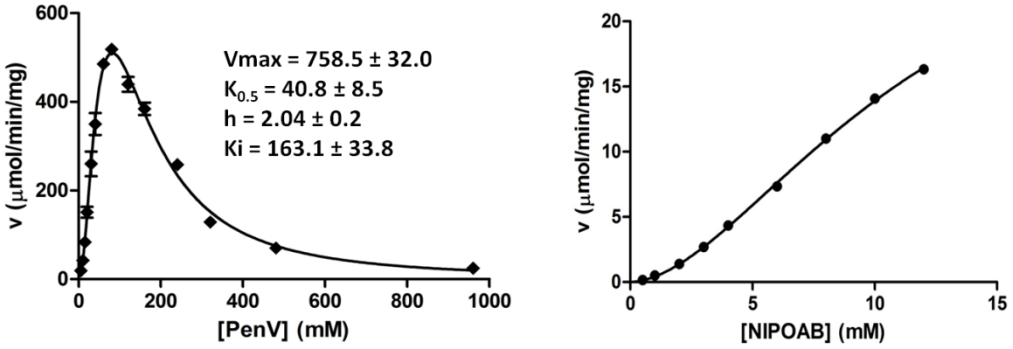

(a) **(b)**

Fig. 2.7. Kinetic analysis of *Pa*PVA. (a) *v* vs [S] curve with Pen V as substrate (5-960 mM); inset: kinetic parameters. (b) *v* vs [S] curve with synthetic substrate NIPOAB (0.5-12 mM).

*Pa*PVA showed a Hill's coefficient of 2.04, indicating apparent positive cooperativity. Cooperative behaviour of bile salt hydrolase has been reported in *Lactobacillus salivarius* (Bi et al. 2013), while the enzyme showed curves similar to MM kinetics when DTT was present in the assay mixture. However, in the case of *Pa*PVA, the presence or absence of DTT did not cause any significant change in the allosteric nature of the enzyme. In addition, the occurrence of substrate inhibition (Ki = 163.1 mM for *Pa*PVA) is possibly unique to Gram-negative PVAs. Substrate inhibition has rarely been reported in any cholylglycine hydrolase so far (Rathinaswamy et al. 2012; Kumar et al. 2006). Kinetic studies using washed cells of PVA producing fungi *Fusarium oxysporum* have indicated weak substrate inhibition (Ki = 900mM) (Lowe et al. 1986). Efforts are being made to further understand the dynamics of Pen V binding and the structural mechanism of cooperative behaviour substrate inhibition in *Pa*PVA. In the case of PGA, Novikov et al. (2013) have proposed that the apparent substrate inhibition is a result of unproductive substrate binding, although it happens at the same active site.

The enzyme rate also showed allosteric behaviour with increasing concentrations of the synthetic substrate NIPOAB **(Fig. 2.7b)**. However, the v/[S] curve couldn't reach saturation, since the solubility of NIPOAB was restricted to 12mM in 2% DMSO; higher DMSO concentrations proved deleterious for enzyme activity.

In conclusion, the *Pa*PVA isolated from the Gram-negative plant pathogen *P. atrosepticum* shows certain interesting properties so far not reported in PVAs. Both the yield of recombinant protein and the specific activity of the enzyme are very high, auguring well for application in the pharmaceutical industry for 6-APA production. The enzyme exhibited uncharacteristic kinetic behaviour, showing positive cooperativity coupled with substrate inhibition. Further biochemical and structural analysis on *Pa*PVA could help unravel the dynamics of similar enzymes from other Gram-negative bacteria, so as to develop them for industrial applications and also understand the place of such enzymes in microbial physiology.

Chapter 3

Crystallization and structural analysis of penicillin V acylase from *Pectobacterium atrosepticum* (*Pa*PVA)

3.1. Introduction:

X-ray crystallography is a powerful method to elucidate macromolecular structures, especially for the three-dimensional structure determination of proteins. It uses the diffraction pattern of X-rays by a protein crystal to determine the structure of the protein. Structures obtained through X- ray diffraction provide accurate information on interactions between proteins and the cognate ligands. The knowledge of accurate protein structures is prerequisite for understanding structure-function relationships and development of new strategies for protein engineering, drug designing and many other applications. The application of X-ray crystallography for studying structures of enzymes like penicillin acylases holds great value, owing to their industrial importance.

The Ntn hydrolase protein family comprises a group of enzymes that cleave non-protein amide bonds. In spite of low sequence homology, they share a common αββα structural fold and possess a catalytic nucleophilic residue at the N-terminal (Oinonen and Rouvinen 2000). Penicillin acylases that hydrolyze amide bonds in beta-lactam antibiotics are also members of the Ntn hydrolase family (Brannigan et al 1995; Suresh et al. 1999). Penicillin G acylases (PGA) act on benzyl penicillin (pen G), while penicillin V acylases (PVA) preferentially act on phenoxymethyl penicillin (Pen V). Both the reactions release 6-amino penicillanic acid (6-APA), a pharmaceutically important intermediate that is industrially used for the production of newer semi-synthetic antibiotics with favourable properties (Arroyo et al. 2003).

Penicillin acylases also undergo post-translational autocatalytic processing to expose the α-amino group of the N-terminal residue, which then acts as the base in the catalytic reaction (Duggleby et al. 1995). However, the processing mechanism differs in different penicillin acylases. PGAs and PVAs show minimal sequence homology and different subunit composition, although they share important catalytic residues and act on similar substrates. Serine is the catalytic N-terminal nucleophile residue in PGAs; whereas PVAs contain cysteine (Suresh et al. 1999). PVAs share an evolutionary relationship with bile salt hydrolases (BSH) that catalyze the deconjugation of bile salts in intestinal microbiota. Together, PVAs and BSH form the choloylglycine hydrolase group of enzymes (Kumar et al. 2006).

One of the first structures of Ntn hydrolases to be determined was that of the penicillin G acylase from *E. coli* (Duggleby et al. 1995). Since then, structures of many other Ntn hydrolases and ligand-bound enzyme complexes have been elucidated through X-ray crystallography. In the case of choloylglycine hydrolases, the structure of a functional PVA from *Bacillus sphaericus* (*Bsp*PVA) was first reported by Suresh et al. (1999); followed by PVA from *B. subtilis* (*Bsu*PVA, Rathinaswamy et al. 2005) and BSHs from *Clostridium perfringens* (*Cp*BSH, Rossocha et al. 2005) and *Bifidobacterium longum* (*Bl*BSH, Kumar et al. 2006). However, all these structures are from Gram-positive bacteria, although PVAs are known to be produced by both Gram-positive and Gram-negative bacteria. Lambert et al. (2008) and Panigrahi et al. (2014) have classified choloylglycine hydrolases from different bacteria and observed that the enzymes from Gram-negative bacteria cluster separately. In addition, penicillin acylases and their close homologues from different bacteria have been reported to show a varied substrate spectrum, sometimes cross-reacting with each other's substrates (Kumar et al. 2006; Mukherji et al. 2014). Many other Gram-negative PVA homologues also share significant sequence similarity and with *P. atrospeticum*, hence *Pa*PVA could be considered a representative of functional Gram-negative choloylglycine hydrolases. This chapter describes the crystallization of *Pa*PVA and determination of the three-dimensional structure of the enzyme. It also details the unique structural features of *Pa*PVA and differences with respect to other cholylglycine hydrolases.

3.2. Materials and methods:

3.2.1. Crystallization of *Pa*PVA:

In general, X-ray crystallography involves placing a protein crystal in the path of an intense X-ray beam and the collection of diffracted X-rays with a detector. The first step of this process requires growing a suitable protein crystal, which can be defined as a well-ordered arrangement of molecules in a lattice held together by non-covalent interactions. Due to the difficulty in growing diffraction quality crystals, the crystallization step still remains a major bottleneck in X-ray based structure determination that requires utmost attention. There is no fixed method to obtain a protein crystal, and it is required to optimize many factors that might affect the

quality of the crystals including pH, temperature, precipitating agents, ionic strength, presence of impurities, nucleating agents and additives. Protein crystals are usually soft and fragile owing to their high solvent content (30-80%) and weak binding energies between the stacked molecules in the crystal. Protein crystals are therefore grown in optimum conditions that cause little or no perturbations in their molecular properties (Matthews 1985; Littlechild 1991).

Crystallization of proteins from solution is a reversible equilibrium phenomenon. Growing a protein crystal requires the generation of a certain degree of supersaturation in the solution. The supersaturation zone occurs when the protein exceeds its solubility limit **(Fig. 3.1)**, leading to nucleation and formation of crystals. Supersaturation can be achieved by different approaches including altering the pH, temperature, protein and precipitant concentration. Nucleation helps to cross the free energy barrier for crystal formation, and the decrease in free energy acts as the thermodynamic basis for molecular ordering and growth of crystals (McPherson 1982).

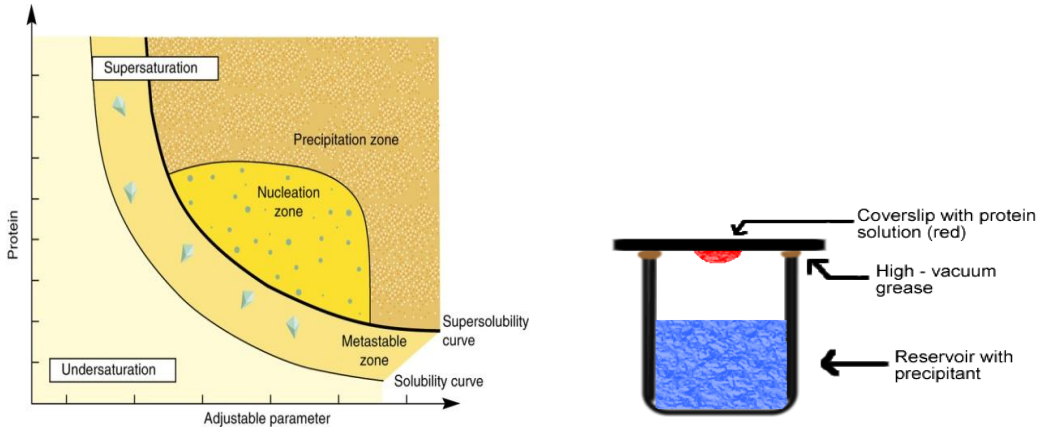

(a) **(b)**

Fig. 3.1. (a) Schematic illustration of a protein crystallization phase diagram (Chayen 2004). (b) Hanging drop technique (Source: www.bio.davidson.edu)

A popular experimental set up for the crystallization of proteins is based on vapour diffusion, using either hanging drop or sitting drop technique. Vapour diffusion is an efficient means of protein crystallization, owing to the ease of performing the experiment and the relatively small volumes of protein required. In the hanging drop method, small droplets of protein and precipitant solutions are mixed and placed over a well with a larger volume of the precipitant solution in an airtight chamber, to

allow for vapour equilibration **(Fig 3.1)**. As water vaporizes from the drop over time, the precipitant concentration in the drop rises till the optimum level for crystallization is reached (Rhodes 2000; McRee and Duncan 1993). There are also a variety of other techniques available such as sitting drops, dialysis buttons and microbatch techniques. More recently, crystallization robots have been introduced that are useful for automatic screening and optimization of crystallization conditions.

Purified *Pa*PVA enzyme was concentrated to 10-20 mg/ml using Amicon ultra-15ml centrifugal filters (Millipore, USA). Conditions for crystal formation were screened at 22° C using sitting drop vapour diffusion. Mosquito Crystal Nanolitre protein crystallization robot (TTP Labtech, UK) was used to prepare the drops by mixing 300 nl each of the protein and precipitant on 96-well plates. JCSG (Molecular Dimensions, UK), Index, Crystal screen I and II and PEG-Ion screens (Hampton Research, CA, USA) were used to identify the crystallization conditions. Further manual optimization was done using hanging drop vapour diffusion with larger drops (2 µl + 2 µl) equilibrated against 1 ml precipitant solution at 22 °C. Drops were set up on siliconized coverslips and allowed to equilibrate in multiwell trays rendered air-tight using silicone grease.

3.2.2. X-ray diffraction and data collection:

X-ray crystallography involves the use of X-rays, which are electromagnetic radiation generated when electrons accelerated with high voltage collide with atoms of a metal target like copper. The wavelength of X-rays (in the range 1- 100 Å) is in the same order of magnitude as the bond length between atoms (0.5 -1.6 Å) in the protein molecules; this makes it convenient to use X-rays for protein crystal diffraction (Blow 2002). Each molecule in the crystal contributes to the diffraction, resulting in intense X-ray diffraction beams that can be measured using detectors (Rhode 2000). Home sources such as rotating anode generators with copper as the metal anode produce X-rays of wavelength 1.542 Å. Synchrotrons produce high intensity X-rays using particle accelerators, and the diffraction pattern is recorded on charge coupled device (CCD) detectors. Synchrotron gives better resolution than home sources, and data collection can be done in shorter time period (Drenth 1994).

Intense X-rays can cause extensive damage to crystals through the generation of free radicals that cause chemical changes in the protein. To subvert the radiation damage,

data collection is usually done at low temperatures (-160°C). The crystals are subjected to flash cooling, and exposed to a liquid nitrogen jet after mounting, to keep the crystal frozen. Cooling of crystals also requires the use of cryoprotectants to minimize lattice damage. Glycerol, ethylene glycol, low molecular weight PEGs, MPD (2-methyl-2, 4-pentanediol), sucrose, xylitol etc. are used as cryoprotectants to ensure proper freezing of the crystals (Garman and Scheider 1997).

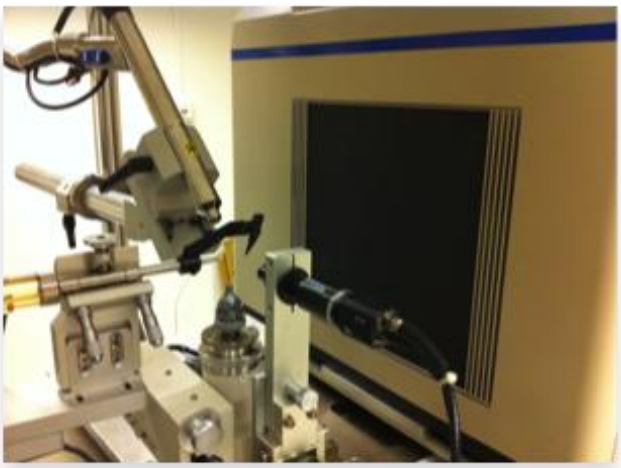

Fig. 3.2. In-house laboratory instrumentation for protein X-ray crystallography.

The crystals are mostly handled mounted in cryoloops, made from fine nylon fibers of diameter 0.05-1mm and thickness 10-20 μm. The crystals are picked up from the crystallization drop and placed in the cryosolution for a short period of time, after which they were plunged into liquid nitrogen for flash freezing (Parkin and Hope 1998). The crystal is then mounted on the goniometer head and kept at -160°C. An initial image of X-ray diffraction pattern (exposure time 120 seconds) is usually analyzed to determine the resolution limit, space group and unit cell parameters. Diffraction data are collected by exposing the crystal to the X-ray beam, and rotating it over a spindle axis over a given oscillation range **(Fig. 3.2)**. The electron density of the molecule is calculated by inverse Fourier transform of phased reflection data.

The *Pa*PVA crystal was soaked in a reservoir solution containing 20% glycerol, and flash-cooled under liquid nitrogen (-190°C). The diffraction data were collected at synchrotron source (INDUS-II) at Indore, India. Data were collected for 180° in 0.5° intervals of oscillation frames with exposure times of 15 s each.

3.2.3. Data processing:

Investigation and scaling of the diffraction data was performed using XDS (Kabsch 2010) and SCALA (Evans 2006).

3.2.4. Matthew's number:

With knowledge of the crystal space group and unit cell dimensions, it is possible to estimate the number of molecules in the asymmetric unit and the solvent content of the crystal using the equation by Matthew (1968).

$$Vm = \text{unit cell volume} * z / (MW * n)$$

where *Vm* is the Matthew's number, MW is molecular weight of the protein (156000 Da for *Pa*PVA), n is the number of molecules per asymmetric unit and z is Avagadro's number. For proteins, *Vm* is usually between 1.7 and 3.5 $Å^3$ Da^{-1}, mostly ~2.15 $Å^3$ Da^{-1}. The solvent content of the crystal is equal to (1 – (1.23/ *Vm*)).

3.2.5. Structure solution:

Accurate solution of the protein structure from diffraction data is dependent on tackling the phase problem, which is to determine the phase angle of each reflection. Isomorphous replacement (heavy atom method), Multiwavelength anomalous dispersion (MAD) and Molecular replacement (MR) are different methods used to determine the phases and solve the protein structure (Ladd and Palmer 2013). While heavy atom derivatives are used in isomorphous replacement, MAD relies on data at different wavelengths from the same protein crystal, probably having a natural heavy atom or seleno methionine.

Molecular replacement (Rossman and Blow 1962) is the easiest technique for structure solution and uses an available protein structure homologous to the molecule of interest. This makes use of the fact that primary sequences of proteins determine their three-dimensional structure and therefore, proteins possessing homologous sequences could be expected to share structural homology as well. Placement of the molecule in the target unit cell requires its proper orientation and precise position, involving two steps: rotation and translation. In the rotation step, the spatial orientation of the known and unknown molecule with respect to each other is

determined, whereas in the next step, the translation needed to superimpose the now correctly oriented molecule onto the other molecule is calculated. MR also exploits the presence of non-crystallographic symmetry to improve phase information and reduce phase uncertainties.

With the expansion of the Protein Data Bank, MR has been used recently in successfully solving many new protein structures. Programs like AMoRe, Phaser and MolRep use MR for structure solution. In the case of *Pa*PVA, the structure was solved using Phaser ver 2.5.6 (McCoy et al. 2007) with the crystal structure of choloylglycine hydrolase from *Bacteroides thetaiotomicron* (PDB ID: 3HBC, 45% sequence identity with *Pa*PVA) as the MR template.

3.2.6. Structure refinement and validation:

After getting the atomic coordinates using a preliminary structural model, it is required to refine the structure. Refinement fits the parameters of the model to minimize errors in phase estimates, and achieve a closer agreement between observed and calculated structure factors. The crystallographic R-factor provides an index of the correctness of the structure and is calculated using the formula below [F(h,k,l) = structure factor]

$$R - factor = \frac{\sum_{(h,k,l)} \| F_{obs}(h,k,l) | - | F_{calc}(h,k,l) \|}{\sum_{(h,k,l)} | F_{obs}(h,k,l) |}$$

Refinement involves incrementing the positional parameters and temperature factors of the atoms by applying restraints on the structure, including stereochemistry, bond lengths and angles and van der Waals contacts (Engh and Huber 1991). Structure refinement is carried out by the Refmac5 (Murshudov et al. 1997) software using a restrained maximum likelihood refinement process. Model building and structure refinement of the *Pa*PVA structure were done using Coot and Refmac5 (CCP4 suite), respectively. **Table 3.1** details the crystallographic data processing and refinement parameters.

Structure validation was carried out to assess the correctness and precision of atomic placements in the structure. The resolution and R-factor are initial indicators of the reliability of the structure and general fit with the observed data. However, the R-

factor can be sometimes biased due to exclusion or over-fitting of the data (Brunger 1992). A better assessment of the fit involves the use of the statistical parameter R-free. In this scheme, about 5% of the experimental observations (test set) are removed from the data set before refinement. The other 95% (constituting the working set) are subject to refinement, and R-free is calculated on how well the model predicts the remaining 5% data in the test set. For an ideal model, the R-free value is supposed to be close to the R-factor.

Isotropic temperature factors (B-factors) relate to the vibration of atoms in the lattice and can thus reflect the precision of measurement of atomic coordinates. Stereochemistry of the final refined models can be checked by measuring the phi-psi angles (Ramachandran plot). PROCHECK (Lakowski et al. 1993) software was used to check the geometry of the *Pa*PVA model and estimate the fractions of residues within or outside the allowed regions of the Ramachandran plot (Ramachandran and Sasisekharan 1968). Unusual ω angles, eclipsed dihedral angles in side chains, exceptionally high B-factors and abnormal van der Waals contacts all need further checking for proper refinement.

3.2.7. Structure analysis:

Structural homology search was performed using the DALI server (Holm and Rosenstrom 2007). Analysis of oligomeric interactions was performed using PDBsum or PISA web servers. All structural figures were prepared using PyMol (The PyMOL Molecular Graphics System, Version 1.7.4, Schrödinger, LLC) or CCP4*MG* (McNicholas et al., 2011).

3.3. Results and Discussion:

3.3.1. Crystallization of *Pa*PVA:

Recombinant *Pa*PVA was expressed and purified using techniques mentioned in Chapter 2. Preliminary trials for crystallization were performed using a high throughput crystallization robot on 96-well plates with different commercially available screens. Thin needles and plates appeared after 3 days in many conditions with PEG-salt combinations. Further manual optimization was done on 24-well

plates to grow bigger and morphologically better crystals. Crystals were grown by vapour diffusion at 22°C. The protein at 11 mg/ml concentration (in 20 mM acetate buffer pH 5.0 containing 100 mM NaCl and 1 mM DTT) was used to set up hanging drops (2µl protein + 2µl well solution). Long cuboid crystals measuring 400-500 µm **(Fig. 3.3)** grew in 4 days in 0.2M sodium potassium tartrate, 0.1 M HEPES (pH 7.5) and 14% PEG 3350. The crystals diffracted at 2.5 Å resolution, and diffraction data was collected with 20% glycerol as cryoprotectant. The crystals belonged to $P2_12_12_1$ space group with two tetramers per asymmetric unit (2226 amino acids, 46 water molecules).

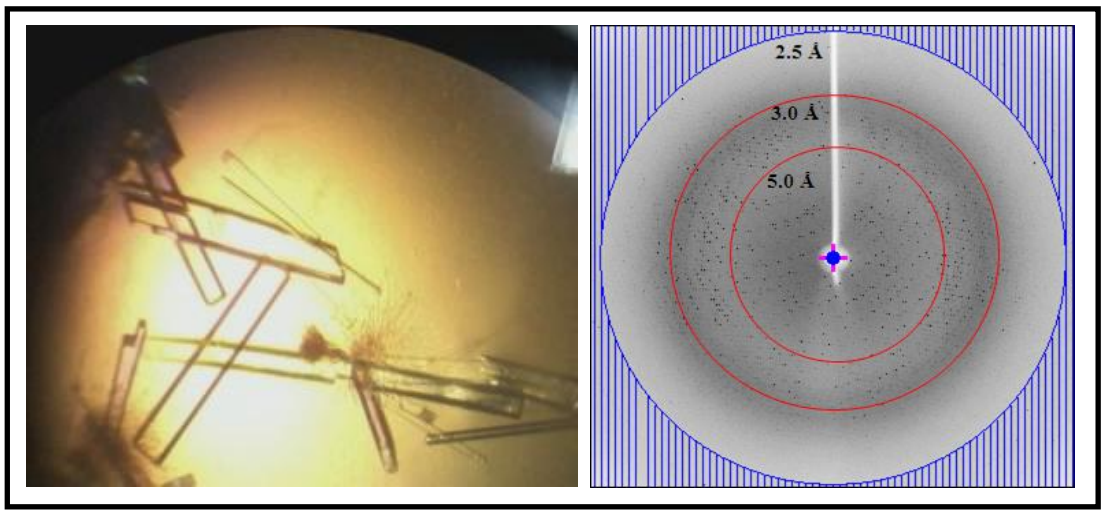

Fig. 3.3. (a) Crystals of *Pa*PVA grown under optimum crystallization conditions. (b) Diffraction pattern of *Pa*PVA crystals.

To understand the influence of structural changes on PVA enzyme function, we tried to crystallize the enzyme-substrate complex. Ligands Pen V and GDCA (glycodeoxycholic acid, a bile salt) were used for soaking the crystals or included in the crystallization experiment at 1-10 mM concentration, with the native *Pa*PVA or inactive C1S mutant. However, soaking led to cracking or dissolution of the crystals within seconds. Crystals were observed with the native enzyme in a few conditions of Hampton Crystal Screen I and II containing GDCA, but they were smaller compared to those of apoenzyme and showed diffuse and poor diffraction. No crystals were formed in the case of C1S mutant. It is possible that the dynamic state and flexibility incurred during the binding of substrates could have led to dissipation of crystal packing.

Table 3.1. X-ray diffraction data collection and structure model refinement of *Pa*PVA. Values in parentheses represent outer shell.

X-ray diffraction and data collection	
X-ray source	INDUS –II
Space group	$P\ 2_12_12_1$
Resolution range	65.70-2.5 Å
Unit cell parameters (Å)	a=118.45, b= 150.21, c = 185.63
Molecules per asymmetric unit	2 tetramers
Matthews coefficient ($Å^3Da^{-1}$)	2.65
Solvent content (%)	53.55%
Total no. of reflections	734773 (57445)
No. of unique reflections	101210 (11504)
Multiplicity	7.3 (5.0)
Completeness (%)	88.5 (70.1)
Average I/σ(I)	11.7 (1.8)
R-merge (%)	0.117 (0.786)
Structure refinement:	
R-factor	0.2149
R-free	0.2478
Number of atoms:	
Protein	21696
Water	46
Average B-factors:	
Protein	40.11
Water	25.94
Ramachandran plot:	
Most favourable	97.9
Allowed	2.1
Outliers	0

3.3.2. *Pa*PVA structure solution and refinement:

The initial structural model of *Pa*PVA was built using molecular replacement, with the structure of choloylglycine hydrolase from *Bacteroides thetaiotamicron* (*Bt*BSH, PDB ID: 3HBC) as the template. This structure is the outcome of a structural genomics project by Kim et al. (2007), and has gaps and breaks in some loop regions; it is also thought to represent a BSH. The best solution had a Z-score of with 8 monomers (2 tetramers) in the asymmetric unit. The initial model of *Pa*PVA was subject to further model building and refinement, using Coot and Refmac5 softwares (CCP4) respectively. The calculated R-factor for the final refined model was 0.215 and R-free 0.248. The geometric precision of the atomic coordinates was confirmed from Ramachandran plot **(Table 3.1, Fig. 3.4)**. The overall G-factor output by PROCHECK is -0.1, which serves as a measure of the stereochemical quality of the structure.

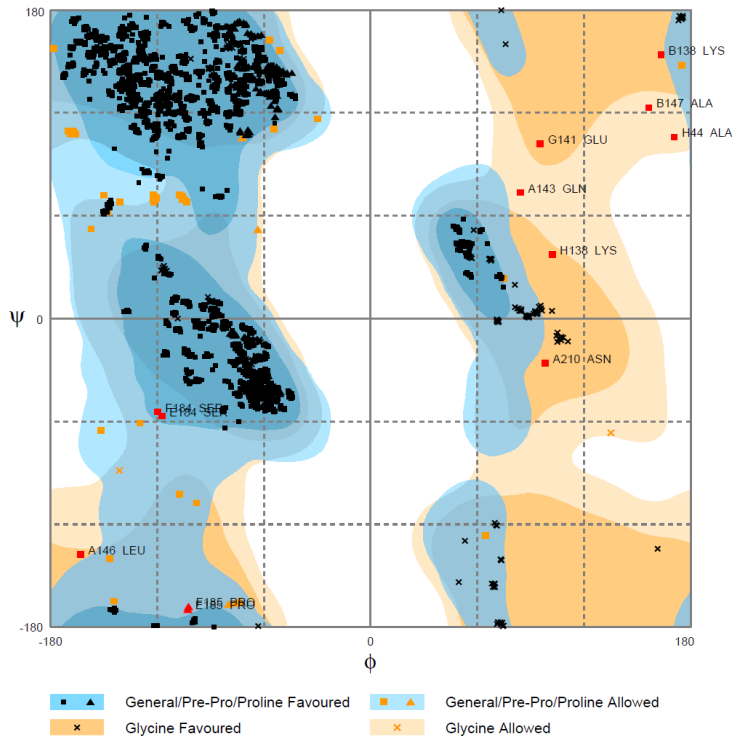

Fig. 3.4. Ramachandran (phi-psi) plot of final refined *Pa*PVA model.

3.3.3. Description of overall structure of *Pa*PVA:

The overall structure of *Pa*PVA was a homotetramer, similar to structures of previously reported CGHs. The *Pa*PVA structure displays the characteristic αββα

core catalytic fold of Ntn hydrolases (Oinonen and Rouvinen 2000), comprising two anti-parallel β-sheets packed against each other and sandwiched between two α-helices. The approximate dimensions of the monomer were 47 x 55x 47 Å, forming a tetramer with a buried surface area of 9552.7 $Å^2$. Each monomer was composed of 19 β-strands making up two sheets, and five α-helices and four 3_{10} helices **(Fig. 3.5, 3.6)**. The connecting segments form 9 β-hairpins, 6 β-bulges, 35 β-turns and 1 γ-turn. The coordinates of *Pa*PVA structure have been deposited in the PDB under the accession codes **4WL2**.

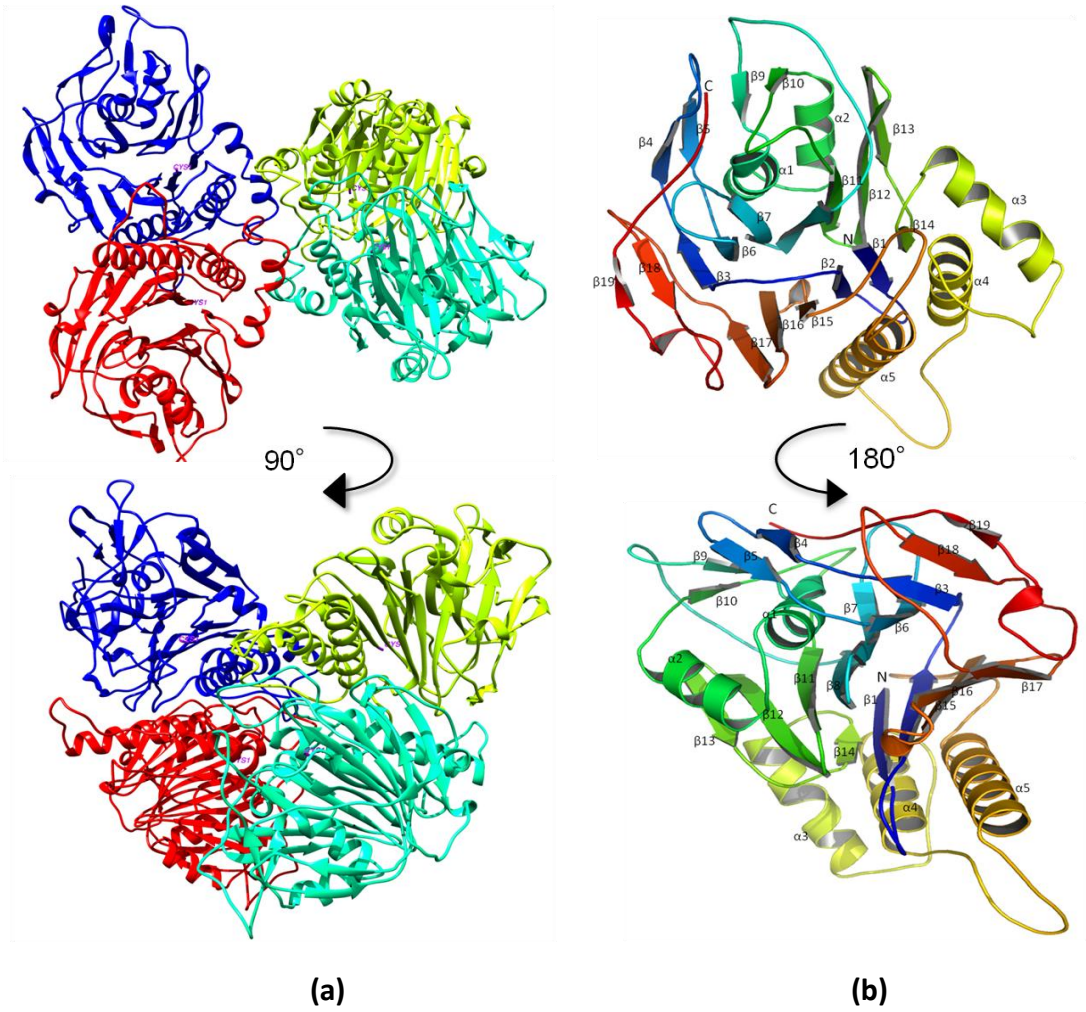

(a) **(b)**

Fig. 3.5. (a) Quaternary structure of *Pa*PVA tetramer after refinement (front view and rotated 90°). The four subunits are shown in different colours. (b) Cartoon representation of secondary structural elements in *Pa*PVA monomer color-ramped from N- to C-terminus (blue to red) from the front and rotated 180°.

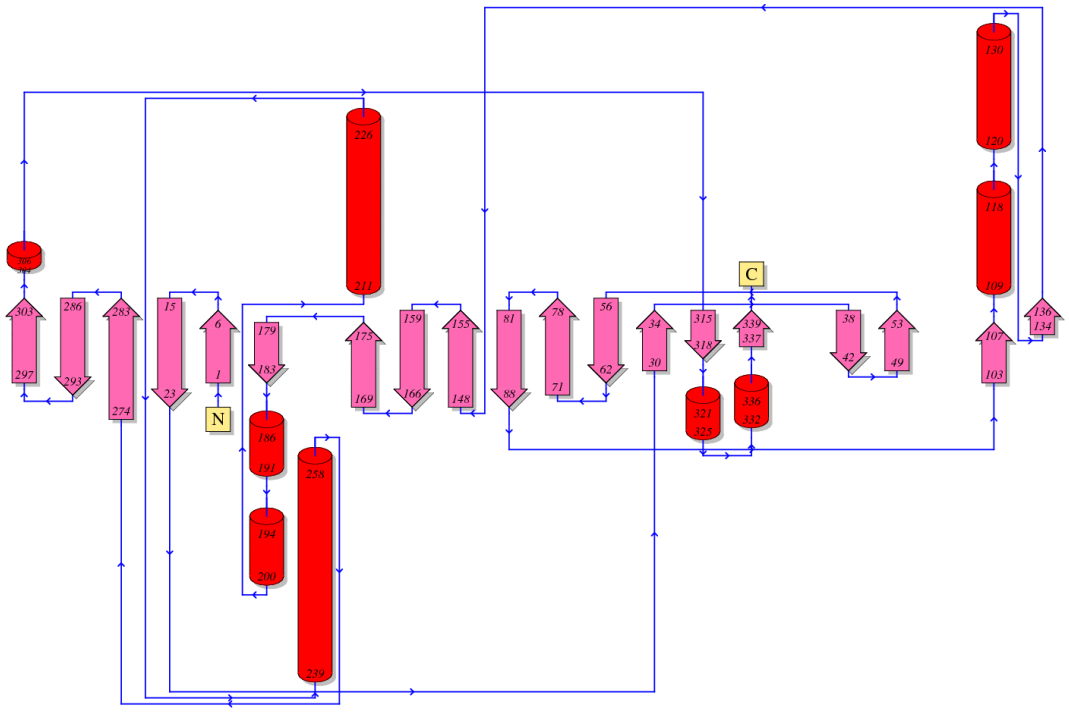

Fig. 3.6. Topology diagram of the secondary structure content of *Pa*PVA (from PDBsum). The α-helices are represented by cylinders and the β-strands are represented by flat arrows.

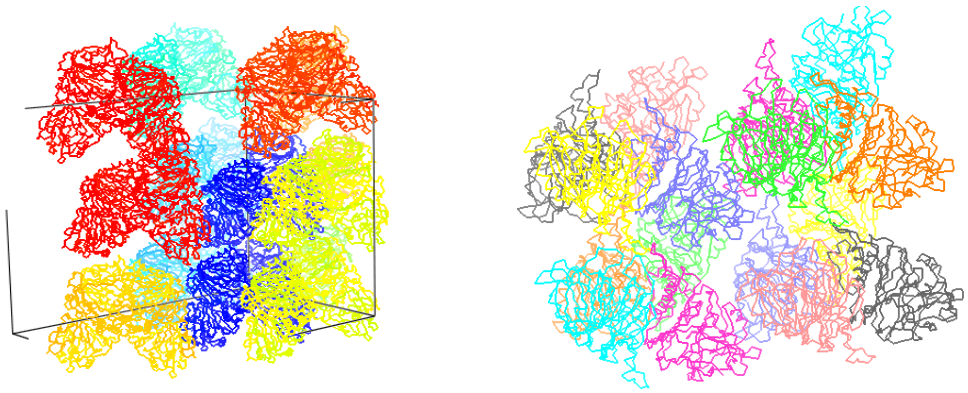

Fig. 3.7. *Pa*PVA crystal packing diagram in orthorhombic form.

The average B-factor for the main chain atoms for the entire protein calculated using Protein Server Analysis Package (PSAP) web server (http://iris.physics.iisc.ernet.in/psap/) was found to be 40.11 Å^2. The residues 137-148 corresponding to a loop region near the active site (which had poor electron density) showed significantly higher average main-chain temperature factors, suggesting that such regions could have independent mobility.

The monomers were assembled into a homotetramer, which can be considered a dimer of dimers. Katre and Suresh (2009) have classified the features of molecular association in homotetrameric proteins. PVAs have been observed to usually display a planar orientation with the four monomers lying in one plane and any two adjacent subunits facing opposite directions. Although *Pa*PVA has a similar structural composition, the subunits are farther from the centre of the molecule; and the angles between the adjacent monomers of different dimers are higher by 10° **(Fig. 3.8)**. In addition, angle between diagonally opposite monomers is 157°, in contrast to 170-180° in *Bsp*PVA, resulting in a slightly non-planar orientation of the tetramer. Dihedral angles measured by taking the Cα atoms of Cys1 of each subunit showed the location of D subunit below the BCA subunit plane by 72°, while the corresponding subunit in *Bsp*PVA was located below the plane by 48.3°. Biochemical characterization of *Pa*PVA has revealed the unique kinetic behaviour of the enzyme, showing allosteric behaviour and substrate inhibition kinetics (Chapter 2). Although *Pa*PVA shows a different structural orientation compared to other choloylglycine hydrolases, it is not clear if this change is in any way responsible for the allosteric behaviour of the enzyme.

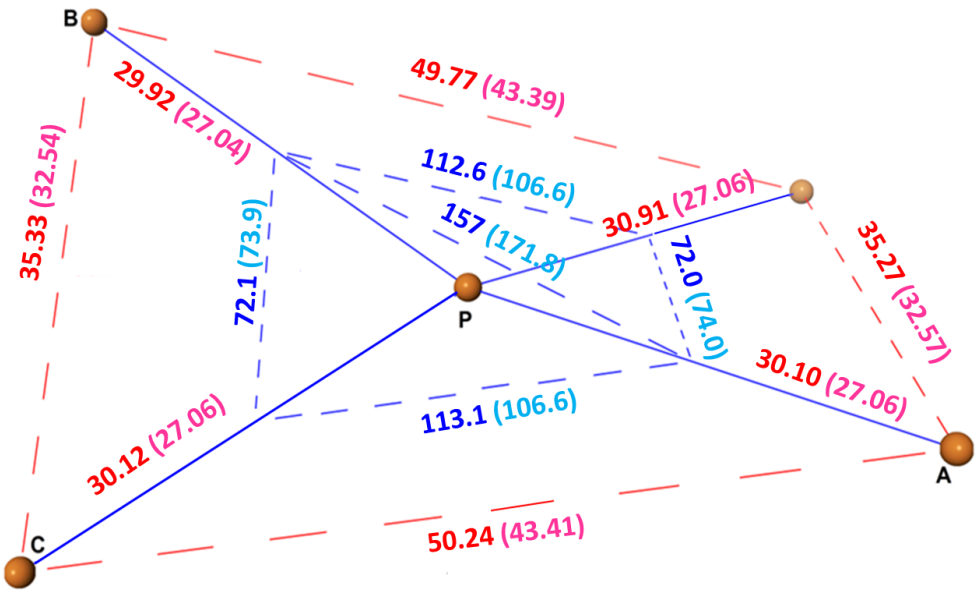

Fig. 3.8. Distances (red) and angles (blue) between the centres of mass of subunits in *Pa*PVA and *Bsp*PVA (values shown in parentheses).

3.3.4. Comparison of *Pa*PVA structure with other Ntn hydrolases:

This is the first complete structure of a functionally characterized penicillin V acylase from Gram-negative bacteria. The *Pa*PVA structure was similar (RMSD 1.7 Å, **Table 3.2**) to the structure of *Bacteroides thetaiotamicron* choloylglycine hydrolase (*Bt*BSH, 45% sequence identity with *Pa*PVA) that emerged from a structural genomics project (PDB ID: **3HBC**). Although *Bacteroides* sp. is Gram-negative, it is thought to produce a BSH, and the available PDB structure contains breaks with residues 48–49, 157–162 and 271–273 missing near the substrate binding site **(Fig. 3.9)**. The PVA and BSH structures from Gram-positive bacteria were less similar to *Pa*PVA, with RMSD values for Cα atoms in the range 2.4-2.7 Å (DALI server, Holm and Rosenstrom, 2007). Superposition of *Pa*PVA with other choloylglycine hydrolase monomers **(Fig. 3.9)** highlights the differences between these enzymes from Gram-positive and Gram-negative bacteria. Two major structural changes set apart the two clusters of enzymes – a reduction in tetrameric interactions and changes in substrate binding elements in the active site.

Table 3.2. Structural alignment of *Pa*PVA with other Ntn hydrolases (DALI server, Holm and Rosenstrom 2007)

PDB ID	Z	RMSD	LALI	LSEQ2	%Identity	Protein
3HBC	42.9	1.7	304	309	47	CGH (*Bacteroides thetaiotamicron)*
2OGC	33.7	2.4	291	317	22	PVA (*Bacillus subtilis)*
3PVA	33.6	2.5	291	334	23	PVA (*B. sphaericus)*
2BJF	32.6	2.6	285	329	25	BSH (*Clostridium perfringens)*
2HF0	32.1	2.7	287	316	19	BSH (*Bifidobacterium longum)*
2X1E	19.8	2.8	224	350	12	Acyl coA: isopenicillin N acyl transferase
3FGT	16.4	3	221	344	10	Putative phospholipase B-like
2WVC	15.3	3.6	224	546	8	AHL acylase PvdQ subunit
1FM2	14.2	3.6	224	520	6	Glutaryl 7-ADCA acylase
1AI6	13.6	3.6	212	557	12	PGA
1PMA	9.4	3.5	162	203	9	proteasome
1GPH	2.1	5.0	106	465	6	Glutamine PRPP-amido transferase

3.3.5. Quarternary structure and inter-subunit interactions:

In the case of choloylglycine hydrolases from Gram-positive bacteria, a loop consisting of 20-25 residues extends from one monomer into the opposite subunit, thus making a major contribution to the formation of the tetramer. In contrast, Panigrahi et al. (2014) have observed the presence of an indel mutation of approx. 20 amino acids in the loop region in the case of CGH from Gram-negative bacteria. *Pa*PVA and *Bt*BSH share this mutation, and possess a corresponding shorter loop in the region leading to a reduction in the oligomeric interactions between the monomers **(Fig. 3.9)**.

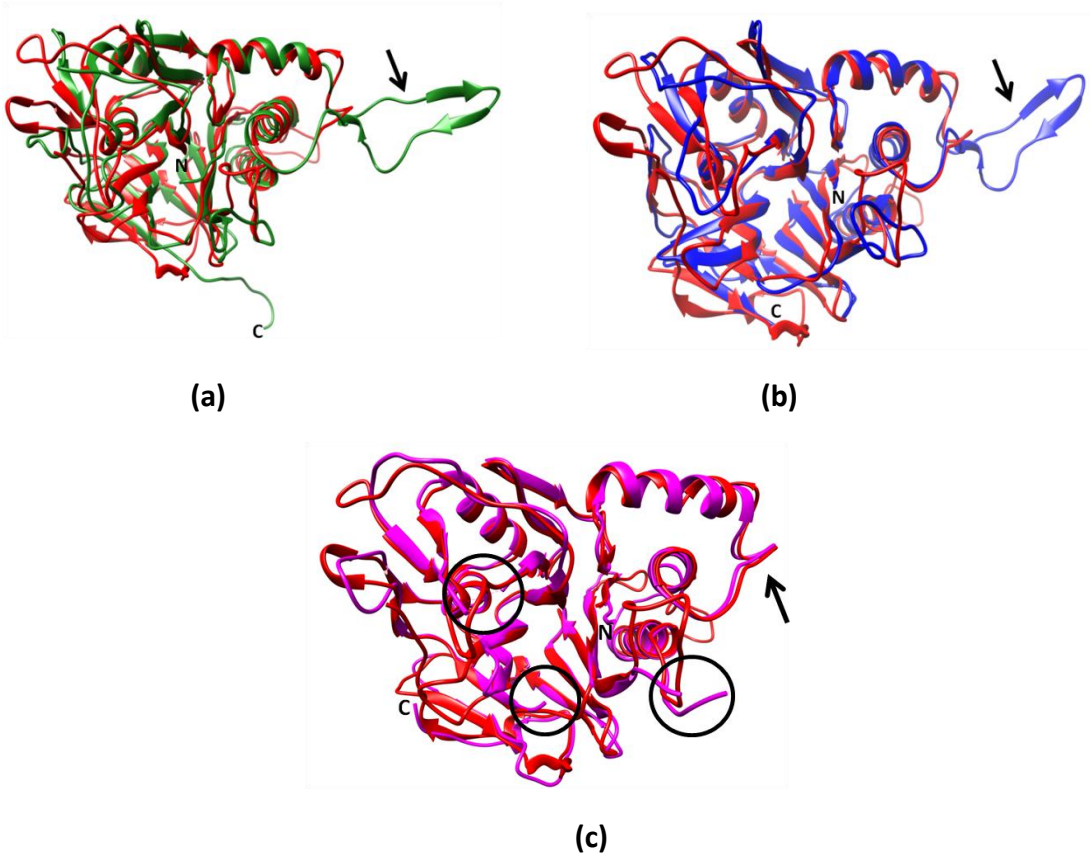

Fig. 3.9. Superposition of the monomers of *Pa*PVA (red) with *Bsp*PVA (green), *Bl*BSH (blue) and *Bt*BSH (magenta). Arrows mark the location of the assembly motif, while circles mark the breaks in *Bt*BSH structure.

The number of hydrogen bonds and non-bonded interactions are considerably reduced **(Table 3.3)** between the opposite subunits (AB/CD) and the components of the dimers (AD/BC). In the *Pa*PVA structure, the opposite subunits are linked merely through van der Waals and hydrophobic contacts; while many such

interactions and hydrogen bonds occur in *Bsp*PVA and *Bl*BSH (CGH from Gram-positive bacteria) primarily with the assembly motif (residues 190-210) extending from the opposite monomer. *Bl*BSH also contains cluster of reciprocal interactions between W181 and D185, two residues which are highly conserved in Gram-positive choloylglycine hydrolases, but are missing in their Gram-negative counterparts. Only 3 residues (V204, M205 and Y196) are involved in non-bonded contacts in *Pa*PVA. Some residues that were strictly conserved in Gram-positive CGHs have been replaced by similar amino acids in *Pa*PVA (L193, I200), but these interact with the adjacent rather than the opposite subunit **(Fig. 3.10)**. The large interface forming the dimers (AD/BC) comprises many interacting residues (including a stretch from M206 to T209) which are highly conserved across all choloylglycine hydrolases. The E291:R256 ion pair, on the other hand, is conserved only in Gram-negative CGHs. Other conserved residues in the dimer interface in Gram-negative CGHs include T250, S253, P261, Y262, R246 and R278.

On the other hand, the interface area between two adjacent subunits (AC/BD) and the number of contacts is higher in *Pa*PVA than Gram-positive CGH. Many new interactions have been formed with new residues including Y196, W197, T192, Q189, Q199, L193, I200, R211 and D214; probably to compensate for the loss of the assembly motif. The loss of the assembly motif has also been reported to decrease the thermodynamic stability of the tetramer (Panigrahi et al. 2014) in Gram-negative PVAs. Nevertheless, *Pa*PVA did not dissociate into dimers in the presence of denaturing agents like Guanidium hydrochloride (1M Gdn-HCl).

Table 3.3. Quantitative estimation of interface area and no. of interactions between individual subunits of *Pa*PVA and *Bsp*PVA in their quaternary structures.

Property	***Pa*PVA**			***Bsp*PVA**		
	AB/CD	**AC/BD**	**AD/BC**	**AB/CD**	**AC/BD**	**AD/BC**
Interface area	142.6	574.2	1686.5	1209.6	352.3	3248.4
Δ G (kcal/mol)	-3.3	-7.2	-14.1	-27.2	-2.3	-34.7
Interface residues	3	13	29	22	7	60
Hydrogen bonds	0	2	14	8	2	29
Salt bridges	0	0	2	0	0	4
Non-bonded contacts	5	49	112	87	46	369

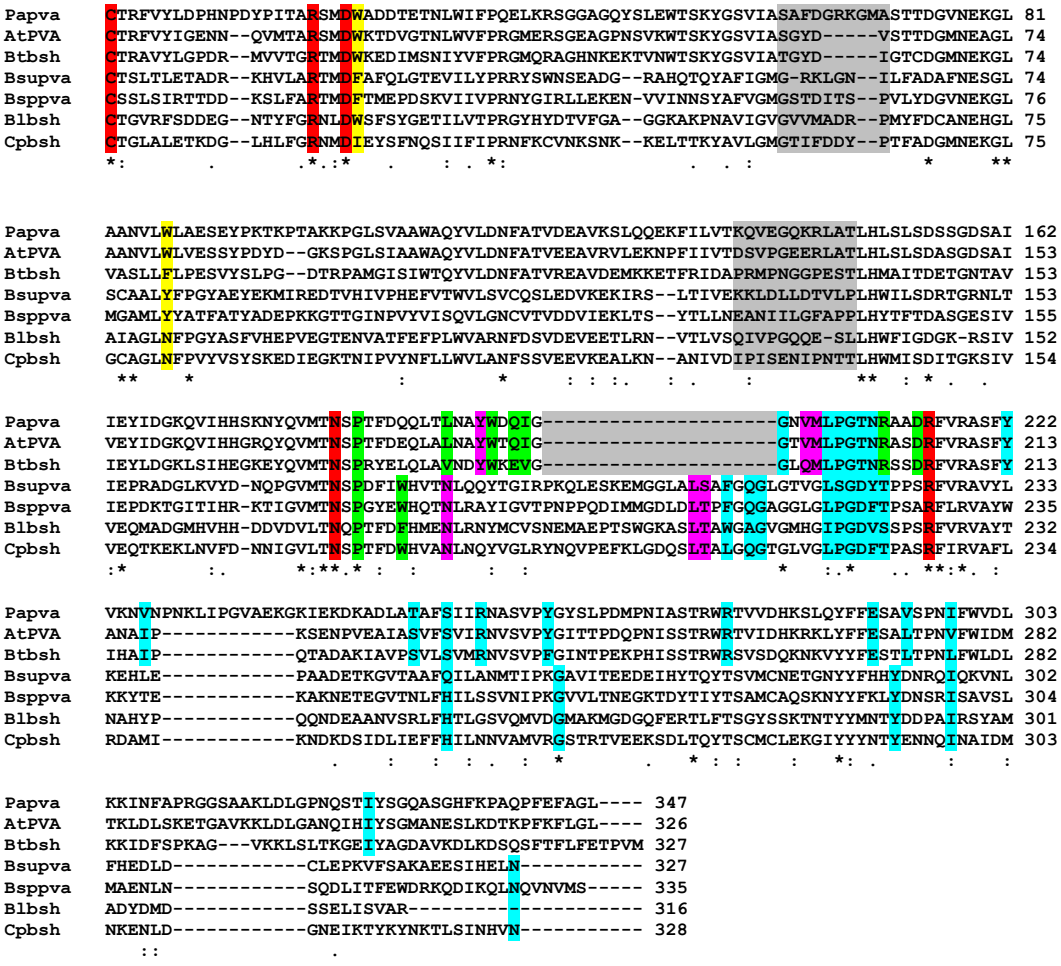

Fig. 3.10. Sequence alignment of CGH enzymes. PVAs from *Pectobacterium atrosepticum* (*Pa*PVA), *Agrobacterium tumefaciens* (*At*PVA), *Bacillus subtilis* (*Bsu*PVA) and *B. sphaericus* (*Bsp*PVA); BSHs from *Bacteroides thetaiotamicron* (*Bt*BSH), *Bifidobacterium longum* (*Bl*BSH) and *Clostridium perfringens* (*Cp*BSH). The alignment highlights conserved active site residues (red and yellow), loops (grey) flanking the active site and assembly motif, and conserved residues involved in oligomeric interactions between opposite subunits (pink), adjacent dimers (green) and within dimer (cyan).

Compared to cholylglycine hydrolases of Gram-positive bacteria where the surface charge is predominantly negative, *Pa*PVA shows a clear difference by exhibiting neutral or positive charges on the surface **(Fig. 3.11)**. However, the contrast in electrostatic pattern is less pronounced at the interface. Most of the oligomeric interactions (also in *Pa*PVA) involve residues near the C-terminal end. In contrast, most of the strictly conserved active site residues in CGHs are concentrated in the N-terminal part **(Fig. 3.10)**. The length of the C-terminal also varies in CGHs with PVAs having longer ends than BSH. As a result, further experiments on truncation

of the protein sequence could help to understand the interaction between the subunits in formation and stabilization of the tetramer, without affecting the PVA activity.

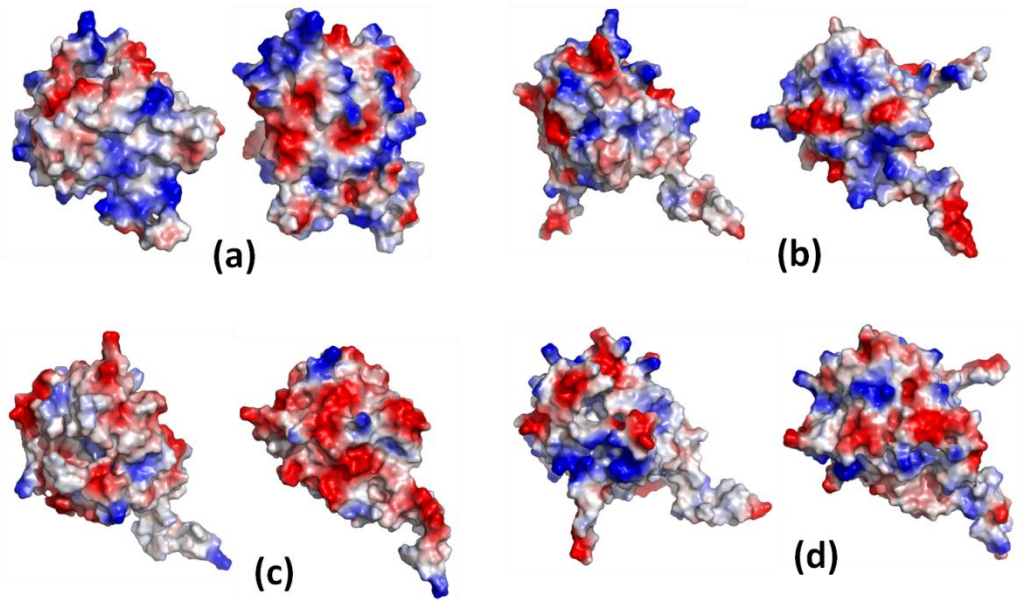

Fig. 3.11. Electrostatic surface charge distribution in (a) *Pa*PVA, (b) *Bsp*PVA, (c) *Bl*BSH and (d) *Cp*BSH.

3.3.6. Active site residues and substrate binding interactions:

The organization of the active site residues in *Pa*PVA and the surrounding loops are shown in **Fig. 3.12.** Most of the important catalytic residues involved in the Ntn hydrolase reaction mechanism are conserved in *Pa*PVA. The reaction mechanism of PVAs involves a nucleophilic attack on the amide bond by the N-terminal catalytic cysteine residue, followed by the stabilization of a tetrahedral intermediate by the formation of an oxyanion hole. The deacylation phase and release of the second product necessitates the involvement of a water molecule (Suresh et al. 1999). The N-terminal cysteine and other residues involved in the catalytic reaction like R19, N183 and R215 are fully conserved in all cholylglycine hydrolases, including *Pa*PVA. While C1 (with its side chain and α-amino group) and D22 form the Ntn catalytic dyad, the oxyanion hole is formed by main chain NH of W87 and N183. The N-H groups of W87 and N183 are 3.6 and 6.4 Å from the catalytic S of cysteine, and 6.6 Å away from each other **(Fig. 3.12)**. The amino group of the nucleophilic cysteine forms a hydrogen bond with the side chain carboxyl oxygen of D22.

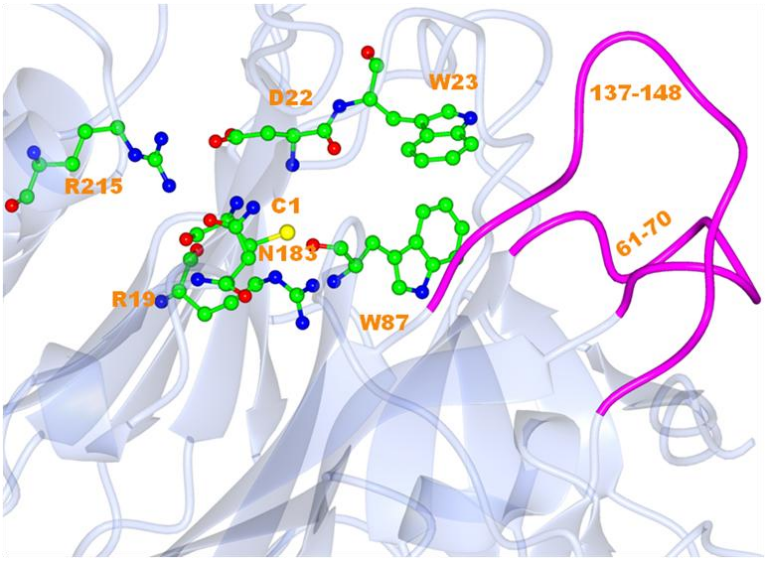

(a)

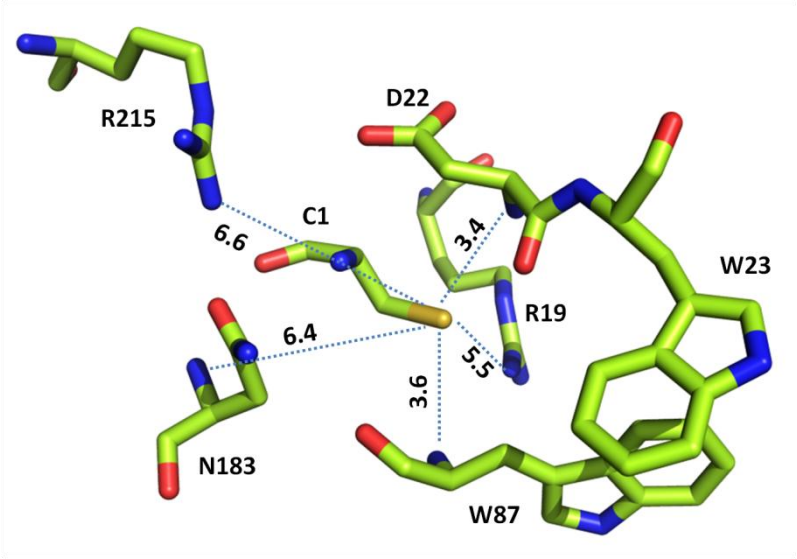

(b)

Fig. 3.12. (b) Organization of the *Pa*PVA active site and flanking loops. (b) Distance (in Å) of different active site residues from sulfhydryl group of the N-terminal cysteine.

The active site geometry of *Pa*PVA shows two major deviations from the reported choloylglycine hydrolases. Firstly, the length of the loops surrounding the active site is increased in the case of *Pa*PVA. Four major loops enclose the active site in CGHs (Kumar et al. 2006). In *Pa*PVA, these loops are comprised of residues 22-35 (loop1), 61-74 (loop2), 137-148 (loop3) and 263-275 (loop4). The sulfhydryl group of the N-terminal cysteine is 10.3 and 15.7 Å away from the termini of loop2 and loop3, respectively. The loops surrounding the active site are thought to influence the variation in substrate specificity between PVA and BSH (Lambert et al. 2008); these

loops are folded inward in PVAs, forming a closed and reduced size binding site pocket whereas the pocket is comparatively large and open in the case of BSH. In *Pa*PVA, Loop2 is about 3 residues larger than the corresponding loop in BlBSH, CpBSH and BspPVA enzymes, and about 4 residues larger compared to BsuPVA. This insertion causes the loop to fold further inwards towards the active site, decreasing the size of active site to a greater extent (**Fig. 3.13)**. Except BspPVA, all other enzymes have one or two residue shorter Loop3 compared to PaPVA. The loop3 region contains stretches of hydrophobic residues in PVAs (as opposed to hydrophilic in BSH), which also serves to decrease the size of the pocket for phenoxyacetate group of Pen V (Rossmann 2008).

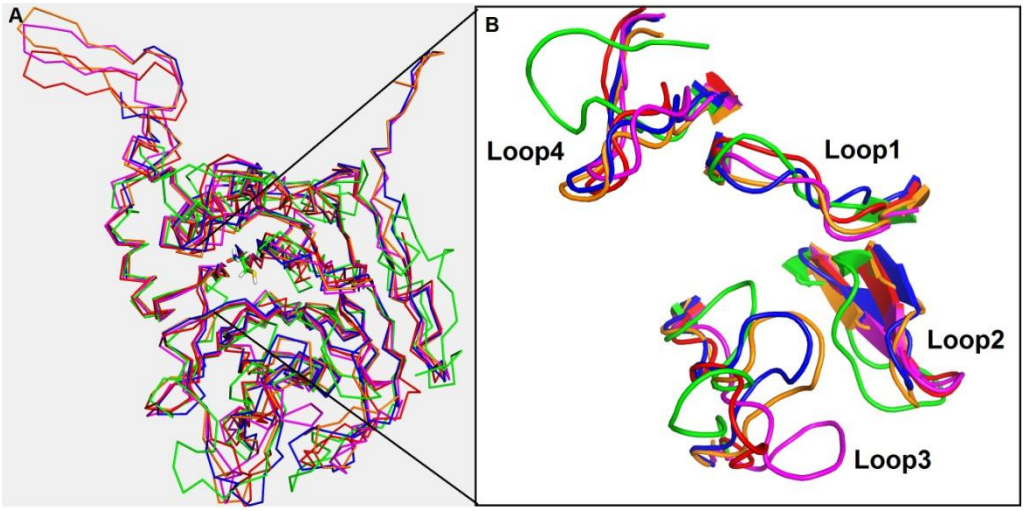

Fig. 3.13. (a) Superposition of CA-trace of *Pa*PVA enzyme (green) with *Bl*BSH (red), *Cp*BSH (magenta), *Bsp*PVA (orange) and *Bsu*PVA (blue). The N-terminal catalytic residue Cys1 is shown in stick representation. (b) Zoom view of the catalytic site showing the differences in the orientation of the four substrate binding site loops.

*Pa*PVA has two tryptophan residues at positions 23 and 87 that are thought to interact closely with the phenyl ring of Pen V. While the latter (W87) is known to participate in the formation of oxyanion hole through its main chain amide group during the catalytic reaction, the significance its side chain and the role of the other residue (W23 in *Pa*PVA) has not been studied so far. Apart from the size of the active site, the nature of these residues plays a major role in determining the substrate specificity of the CGH towards Pen V or bile salts. Both these residues are aromatic in PVAs, whether from Gram-positive or Gram-negative bacteria; they are thought to interact with the phenoxy ring of the Pen V side chain through stacking

interactions. In the case of BSHs (where the substrate GDCA has a bulky steroid group), the residue involved in oxyanion hole is non-aromatic (N79 in *Bl*BSH). However, in BlBSH, the upper amino acid is aromatic (W21) and this is thought to play a role in the binding of Pen V to the enzyme as indicated by fluorescence quenching (Kumar et al. 2006). The BSH from *Clostridium perfringens* shows minimal cross-reactivity towards Pen V; where a nearby phe residue (F24) is thought to interact with the Pen V molecule (Rossocha et al. 2005; Kumar et al. 2006). Aromatic amino acids in many proteins are known to interact via pi-stacking interactions; such networks have been shown to be important for structure stability and folding, protein recognition and ligand binding (Lanzarotti et al. 2011).

PVAs from *B. sphaericus* and *B. subtilis* possess phe and tyr in the corresponding positions, which has been substituted to a trp-trp pair in most Gram-negative bacteria. The occurrence of the homologous trp-trp aromatic pair is very rare in proteins (3% of all aromatic networks), while the phe-tyr pair is the most abundant (31%). Tryptophan is one of the most conserved amino acids in protein binding sites (Thomas et al. 2002; Ma et al. 2003), and is quite distinct from other protein rings, being a heteroatomic fused-ring system (Samanta et al. 1999). Although the residues in both PVAs are positioned in the *edge-face* or T-shape orientation, the substitution to a trp-trp pair in *Pa*PVA results in a modulation in the distance and angles between the aromatic residues. While the centroid distance between the aromatic residues is shortened from 5.8 Å in *Bsp*PVA to 4.83 Å in *Pa*PVA, the angle between them increased from 50-60° to 76° in *Pa*PVA **(Fig. 3.14)**. PVA enzymes from Gram-negative bacteria additionally have a conserved aromatic residue (F63 in *Pa*PVA) in the loop near the active site, leading to the formation of an aromatic network with the trp pair.

Superposition of the active sites also shows the placement of W87 residue farther from the nucleophilic cysteine and nearer to W23in *Pa*PVA, as compared to tyr or asn at the same position in *Bsp*PVA and *Bl*BSH respectively **(Fig. 3.14)**. These subtle changes could lead to stable and better stacking when the substrate binds to the enzyme, with this juxtaposition enhancing the Pen V hydrolysis activity of the enzyme. Indeed, *Pa*PVA has a manifold enhanced PVA activity (Avinash et al. 2015) and is highly specific to Pen V compared to its counterparts from *Bacillus* spp.

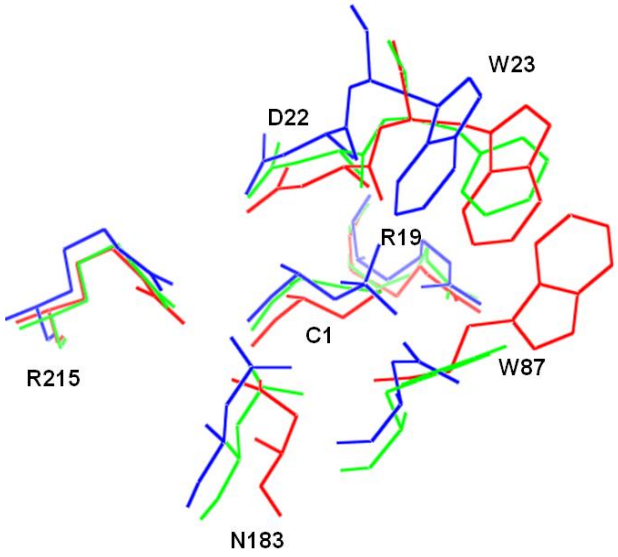

Fig. 3.14. Superposition of active site residues in *Pa*PVA (red), *Bsp*PVA (green) and *Bl*BSH (blue) respectively (numbering according to *Pa*PVA).

Docking of Pen V with the enzyme shows that apart from W23 and W87, a few other residues are also involved in hydrogen bonding and electrostatic interactions with the 6-APA part of the Pen V molecule **(Fig. 3.15)**. The main chain oxygen atom of N271 acts as an acceptor for amide NH of Pen V. While residues R215 and A212 interact with the side chain carboxylate of the beta-lactam, R211 is close to the ring and is probably involved in indirect electrostatic interaction with the substrate. The oxygen atom connected to the penam ring is involved in hydrogen bonding with A273. Certain residues like E90 and R276, which are strictly conserved only in Gram-negative CGHs, could also interact with the Pen V molecule.

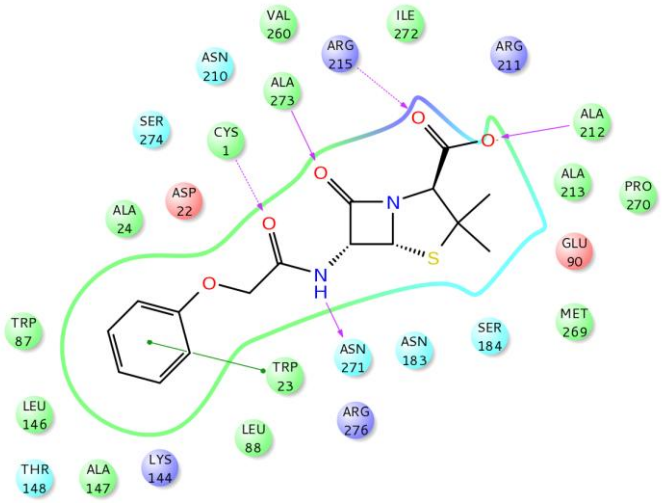

Fig. 3.15. Protein-ligand interaction diagram of *Pa*PVA with Pen V molecule.

Chapter 4

Analysis of substrate binding in *Pa*PVA using docking, mutagenesis and molecular dynamics simulations

4.1. Introduction:

Protein-ligand interactions, including antigen-antibody interactions, receptor recognition and enzyme-ligand interactions, are cornerstones of cellular metabolism. The term ligand usually refers to any small molecule interacting with the protein; ligands are involved in reversible, non-covalent interactions with the enzyme thereby modulating its biological role in a controllable way. Understanding the mechanics of ligand binding to an enzyme, including the amino acids and interactions involved, is very crucial to explore different facets of enzyme function (Harding and Chowdry 2001). The information from ligand binding studies can also help in protein engineering to modify the substrate spectrum of the enzyme, or in drug designing, to develop newer enzyme inhibitors.

The details of ligand binding to proteins can be studied through a variety of experimental and *in silico* techniques. Site-directed mutagenesis of specific residues in the binding site or active site of the enzyme can be used to produce variants that possess unique properties different from the native enzymes, including changes in activity, stability and substrate specificity. This can determine with precision the role of the mutated active site residue in ligand binding or catalytic mechanism of the enzyme (Plapp et al. 1995). Apart from X-ray crystallography or NMR, studies like fluorescence spectroscopy and isothermal titration calorimetry (ITC) can help explore the free energy and conformational changes in the enzyme during ligand binding (Mocz and Ross 2013; Damian 2013). *In silico* methods to study ligand binding in proteins include docking and molecular dynamics simulations. Docking predicts the preferred orientation of the substrate or inhibitor molecule in the enzyme active site, which could be used to further predict the binding affinity through scoring functions. Computer simulations can be used to model the physical movements of a dynamical system of atoms or molecules, and then calculate their trajectories through solving Newtonian equations of motion (Becker and Watanabe 2001). The molecular dynamics of enzymes in presence of the substrate or inhibitor could trace the interactions involved in ligand binding, and the effect of mutations on such interactions.

Penicillin V acylases are evolutionarily and structurally related to BSHs, and they show cross-reactivity of their substrates as described earlier (Chapter 1). While

*Bsp*PVA is active on bile salts and *Cp*BSH on Pen V to a small extent, *Bsu*PVA and *Bl*BSH are very specific only for their respective substrates. Therefore, as a representative of Gram-negative choloylglycine hydrolases, it is important to explore the substrate specificity of *Pa*PVA and understand the interaction of the enzyme with other substrates such as bile salts and other compounds similar to Pen V. In addition, *Pa*PVA was observed to be highly active on Pen V with unique kinetic behaviour; it would be interesting to trace the important interactions involved in Pen V binding and catalysis that lead to the enhancement in activity. We have determined the three dimensional structure of *Pa*PVA and observed some structural features that are different from available CGH structures. This chapter details the studies on binding of Pen V and GCA to *Pa*PVA and the significance of the enzyme-substrate interactions involved, through site-directed mutagenesis, docking and molecular dynamics (MD) simulations.

4.2. Materials and methods:

4.2.1. Expression and purification of *Pa*PVA enzyme:

*Pa*PVA was expressed in *E. coli* BL21 star cells with a C-terminal His-tag, and was purified to homogeneity using a HIS Select Ni^{2+} affinity column and ENrich^{TM} 650 (BioRad) size exclusion column, as described in Chapter 2. All *Pa*PVA variants were also expressed in *E. coli* BL21 star cells and purified using the same procedure.

4.2.2. *Pa*PVA enzyme activity assay:

The Pen V hydrolysis activity of native and mutant *Pa*PVA enzymes was estimated by studying the formation of Schiff's conjugate with the product 6-APA and p-dimethyl amino benzaldehyde (Shewale et al. 1987). One unit (IU) of enzyme activity was defined as the amount of enzyme producing 1 μmol 6-APA in 1 min under standard conditions (0.1 M acetate buffer pH 5, 45°C).

4.2.3. Substrate specificity of *Pa*PVA:

The hydrolytic activity of purified *Pa*PVA towards various penicillins and cephalosporins was determined by incubating the enzyme with different substrates at 5 mg/ml concentration.

Activity on bile salts was examined by incubating the enzyme with 10 mM of different bile salts for 1 h. The amino acid moiety released was quantified by reacting with nihydrin reagent (Kumar et al. 2006).

4.2.4. Modulation of *Pa*PVA activity by bile salts:

The effect on PVA activity by the presence of bile salts was estimated using a range of concentrations of the compound (5μM to 40mM) and Pen V at a constant concentration (50mM). Plots of v/[S] were prepared at 0.1, 1 and 10mM GDCA concentration with Pen V as substrate.

4.2.5. Docking of Pen V and GCA to *Pa*PVA structure:

The 3D conformation of Glycocholic acid (GCA) and Penicillin V (Pen V) used in the docking study was obtained from PubChem compound database (Bolton et al. 2008) with their CID 10140 and 6869, respectively. Partial atomic charges of each ligand atom were determined from OPLS_2005 all-atom force field using LigPrep. Grid based ligand docking program Glide (Freisner et al. 2006) was used for docking these ligands in the binding site of receptor. The binding site was defined as a grid box of dimension 26x26x26 Å, centered on Cys1 residue. Receptor grid generation was followed by ligand docking where the ligands were docked flexibly using Glide's extra precision. Free energy of binding is roughly estimated by using an empirical scoring function called GlideScore, which includes electrostatic, van der Waals interaction and other terms for rewarding or penalizing interactions that are known to influence ligand binding. All structural figures were prepared using PyMol.

4.2.6. Site-directed mutagenesis:

Mutation of different residues in the active site (C1, R19, D22, W23, R215) in the active site was done using ExTaq enzyme (TaKaRa Bio Inc.). The primers designed for each mutant are given in Table 2. PCR was performed in a gradient thermocycler using conditions: 94°C/5min, 20 cycles of [94°C/30s, 55°C/30s, 72°C/390s] and final extension 72°C/10 min. The PCR products were transformed in *E. coli* DH5α and positive mutants were confirmed by sequencing (First Base Laboratories, Malaysia). The mutant plasmids were further transformed into BL21 star cells for

protein expression. Enzyme activity was determined using the assay system described above.

4.2.7. Determination of binding constants for Pen V:

Steady-state fluorescence measurements were also made for the native enzyme and W23 and W87 mutants. Change in fluorescence intensity after the binding of substrate was monitored at λ_{max} of the protein (335 nm). At the highest concentration of substrate, volume change was less than 5% of the solution in the cuvette. To 2 ml of the protein sample in 20 mM acetate buffer pH 5.0, 2-4 µl aliquots of 0.1M Pen V stock solution were added in increments and the fluorescence intensity monitored before and after addition. Linear fits and graphs were generated using Microcal Origin 8.1 software.

The fluorescence intensity of PVA saturated with substrate (F_∞) was extrapolated from the plot $F_o /(F_o-F_c)$ against 1/[C] where F_o and F_c are the fluorescence of the enzyme in the absence and presence of substrate at a given concentration, C. The association or binding constants (K_a) for the protein-substrate interactions were determined from the titration data by assuming the relation that pK_a of the complex equals the value of [C] when log $[(F_c-F_o)/ (F_\infty-F_c)] = 0$. The abscissa intercept of the log $[(F_o- F_c)/(F_c-F_\infty)]$ versus log[C] plot was used to calculate K_a.

4.2.8. Molecular dynamics simulations:

MD simulations involve the computational study of time-dependent behaviour of a molecular system. This method has been used to provide detailed theoretical information on the fluctuations and conformational changes in proteins and nucleic acids. Computer simulations provide a bridge between microscopic length and time scales and the macroscopic world of lab experiments, by starting from experiment-based guess of molecular interactions to predict bulk properties of macromolecules (Allen 2004). During MD simulations, a system of N interacting atoms is studied by solving the Newtonian equations of motion. Such simulations are increasingly being used in the exploration of folding and stability of proteins, molecular recognition and ligand binding, enzyme reactions, drug designing and so on (Sabonmatsu and Tung 2007). **Fig. 4.1** shows the steps involved in a typical MD simulation process.

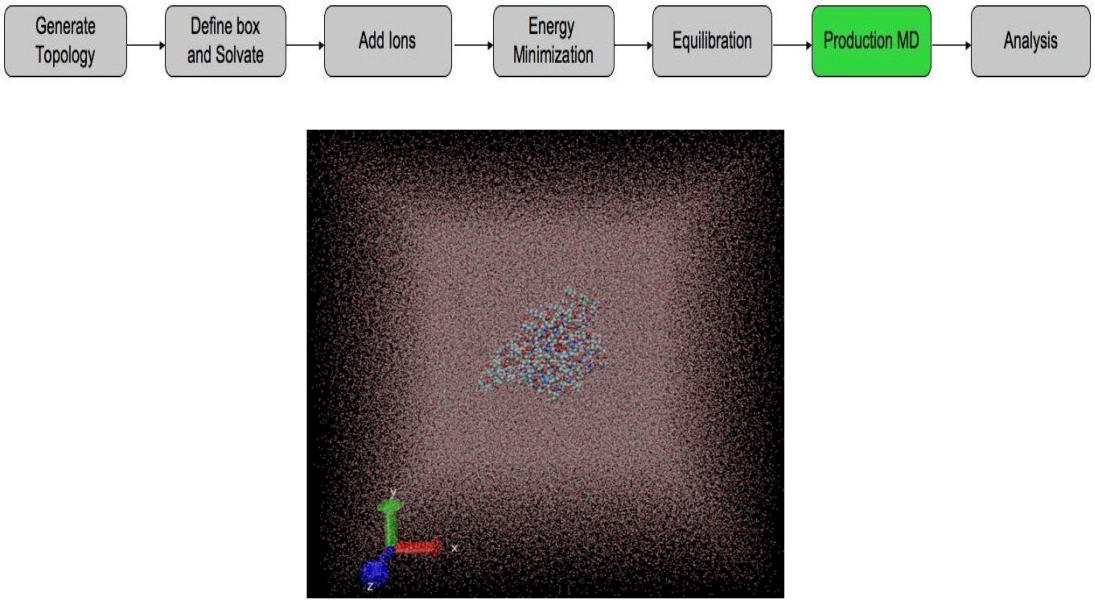

Fig. 4.1. Steps involved in a typical MD simulation of protein molecules, and a solvated grid box with a representative protein, ready for simulation.

Chain A of the *Pa*PVA structure was used as the initial model for docking and MD simulation. The Pen V-bound complex structures were obtained by docking the substrates in *Pa*PVA binding site using Glide (Freisner et al. 2006). Based on the estimated binding affinity values in the form of GlideScore, the best pose in each case was considered as the productive mode of substrate binding. In order to explore the role of W23 and W87 residues towards Pen V binding, a total of six molecular dynamics simulations (MDS) were carried out: *Pa*PVA_apo (*Pa*PVA wild type structure without Pen V bound), *Pa*PVA_penV (*Pa*PVA wild type structure with penV bound), *Pa*PVA_penV_W23F, *Pa*PVA_penV_W23I, *Pa*PVA_penV_W87Y, and *Pa*PVA_penV_W87N (respective *Pa*PVA mutants with Pen V bound). All simulations were carried out using Gromacs 4.5 (Pronk et al. 2013) with amber99sb force field. The program *acpype* (da Silva and Vranken 2012) was used to generate the topology and parameter files for Pen V molecule using General Amber Force Field. Each structure was solvated in a cubic box with tip3p water models and appropriate counter-ions were added to neutralize the system. The system was first energy minimized using steepest descent followed by conjugated gradient minimization (maximum force for convergence: 10 kJ/mol/nm). The resulting system was then equilibrated in NVT ensemble for 100ps at 300K using V-rescale temperature coupling followed by 100 ps NPT ensemble at 1 atmosphere pressure using Parrinello-Rahman pressure coupling. The equilibrated system was finally

subjected to production simulation for 15ns time scales using leap-frog integrator. Grid-based search algorithm was employed to generate the non-bonded interaction pair-list with update at every 5 steps. A 10Å cut-off was considered for Short range neighbor list, electrostatic and VdW interactions. Long-range electrostatic interactions were measured using Particle Mesh Ewald method (0.16 nm Fourier spacing with cubic interpolation).

4.3. Results and Discussion:

4.3.1. Substrate specificity of *Pa*PVA:

Penicillin V was found to be the best substrate for *Pa*PVA since the enzyme showed highest specificity towards Pen V. All other β-lactam substrates, including penicillin G, ampicillin, cephalexin, cloxacillin and dicloxacillin were hydrolyzed by PVA at a rate less than 10% of that of Pen V. Pundle and SivaRaman (1997) have also reported high specificity towards Pen V in the case of *Bsp*PVA. Since PVA and BSH enzymes are structurally and evolutionarily related, the abililty of *Pa*PVA enzyme to hydrolyze bile salts was also explored. However, the enzyme failed to show any activity with glyco- or tauro- conjugated bile salts **(Fig. 4.2)**.

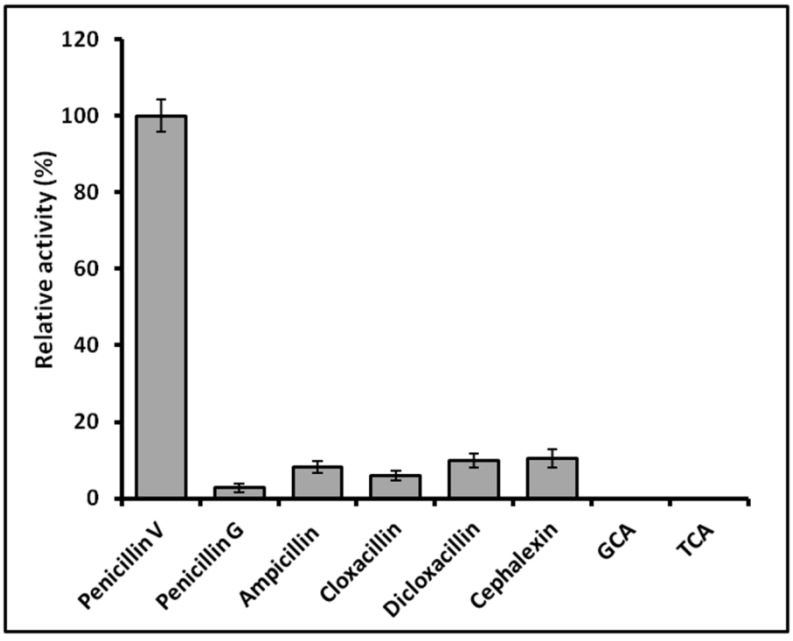

Fig. 4.2. Activity of *Pa*PVA on Pen V and related substrates.

4.3.2. Nature of *Pa*PVA binding pocket:

The observations on substrate specificity of *Pa*PVA could be explained by examining the binding of different substrates to the active site of the enzyme. There is a significant change in the nature of the binding pocket of *Pa*PVA as compared to reported CGHs. One of the major structural changes in *Pa*PVA includes the presence of longer loops surrounding the active site, as explained in Chapter 3. This leads to a difference in physical nature of binding site pocket. The binding site pocket of *Bsp*PVA is large and more hydrophobic compared to that of *Pa*PVA **(Fig 4.3)**. Similarly there is a difference in the electrostatic potential, observed between the active sites of *Pa*PVA and *Bsp*PVA. The hydrophobic binding site surface area in *Bsp*PVA, as calculated by tool *SiteMap*, is 261.78 $Å^2$whereas in case of *Pa*PVA, it is 145.09 $Å^2$. The approximate binding site volume in *Bsp*PVA is 399.59 $Å^3$, which is slightly larger than *Pa*PVA where the binding site volume is 329.6 $Å^3$.The change in nature and surface area of the hydrophobic pocket could influence the binding on substrates in the PVA active site. While *Pa*PVA is highly specific for Pen V and does not hydrolyze bile salts, it has been observed that *Bsp*PVA is able to hydrolyze GDCA (glycodeoxycholate) up to 20% of its Pen V hydrolytic activity (Kumar et al. 2006).

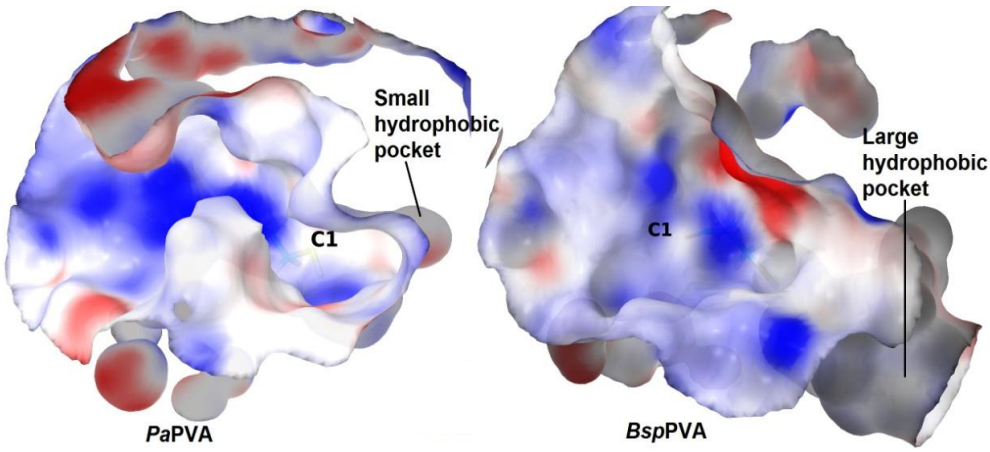

Fig. 4.3. Binding site cavity of *Pa*PVA and *Bsp*PVA, where the electrostatic potentials are mapped on to the surface. (red = regions rich in negative potential, blue = region rich in positive electrostatic potential). Position of N-terminal catalytic residue Cys1 is labelled. The smaller hydrophobic pocket in *Pa*PVA is also shown. The figure on the right corresponds to similar representation of binding site pocket of *Bsp*PVA.

4.3.3. Binding modes of Pen V and GCA:

Docking of Pen V and GCA to the binding site of *Pa*PVA depicts the binding modes of these substrates **(Fig. 4.4)**. The estimated values for free energy of binding suggested a favourable binding for both the molecules but Pen V exhibited higher binding affinity as compared to GCA (Pen V: -4.4, GCA: -3.4 kcal/mol). Both molecules interact with the key catalytic residues such as C1, D22, W23, W87, N183 and R215. In the case of Pen V, the residues C1 and R215 are involved in hydrogen bonding interaction with its carbonyl oxygen of the amide bond and the carboxylate group of β-lactam ring. Similarly, the aromatic residues W23 and W87 interact with the phenyl ring of Pen V. GCA also interacts with residues C1 and W87 (main chain nitrogen atom acts as donor) via hydrogen bonding interaction. It could be inferred from these observations that GCA can bind to the enzyme at the site where Pen V binds, although the enzyme didn't show any activity on GCA. The binding of GCA was also supported by fluorescence quenching experiments.

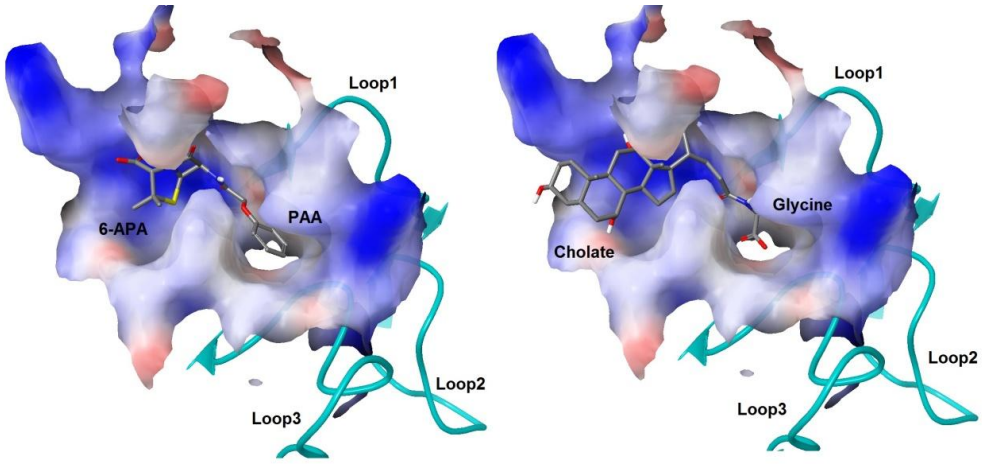

Fig. 4.4. The mode of binding of Pen V (left panel) and GCA (right panel) in the active site of PaPVA. The substrate binding site loops of the enzyme, along with the leaving and tetrahedral intermediate forming groups of each ligand are labelled. Binding site is shown in electrostatic surface.

Interestingly, a different mode of binding was observed for GCA compared to Pen V in the *Pa*PVA active site **(Fig 4.4)**. In Pen V, after the cleavage of its amide bond, the putative group which leaves first, or the **Leaving Group (LG),** is 6-amino penicillanic acid (6-APA); where as in case of GCA it is the glycine moiety which leaves first. After the LG is removed, the remaining groups which form a tetrahedral

intermediate with the enzyme, henceforth called **Tetrahedral intermediate forming group (TG)**, are phenoxy acetic acid (POAA) and cholate respectively in Pen V and GCA. It was observed that the location of LG and TG between substrate Pen V and inhibitor GCA were interchanged and hence the direction of amide bond (CO-NH direction) got reversed. The binding mode of GCA in *Pa*PVA is significantly different from that of *Cp*BSH, for which a complex structure with GCA (PDB ID: **2RLC**) is available. It is likely that this mode of GCA binding is not optimal for GCA cleavage, hence the absence of catalytic activity although it binds at the same site as Pen V. Structural superposition of *Pa*PVA with *Cp*BSH **(Fig. 4.5)** showed heavy steric clashes between the bound product cholate of *Cp*BSH and the residues of *Pa*PVA loop2 (residues 61-74) and loop3 (137-148) near the active site.

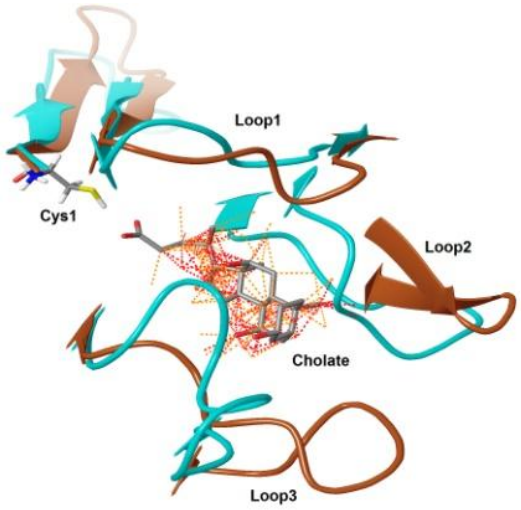

Fig. 4.5. Structural superposition of *Pa*PVA (cyan) and *Cp*BSH (brown) structures. The cholate moiety bound to *Cp*BSH structure is showing heavy steric clashes (shown as dotted lines) with the Loop2 (61-74) and Loop3 (137-148) residues of *Pa*PVA. The conserved N-terminal catalytic Cys1 residue is shown in stick representation.

4.3.4. Modulation of *Pa*PVA activity by binding of bile salts:

The binding of bile salts to *Pa*PVA was further experimentally confirmed by checking the Pen V hydrolysis activity of the enzyme in presence of different bile salts. The PVA activity was modulated by the action of bile salts; it was observed that low concentrations of bile salts (5 to 500 μM) activated the enzyme to a maximum of 140% **(Fig. 4.6)**, while concentrations from 1 mM inhibit the enzyme at

fixed substrate concentration ([Pen V] = 50 mM). Such a "biphasic" regulation has been discussed for epidermal phosphofructokinase enzyme with ATP (Kondo and Adachi 1972). It is possible that the binding of bile salts at low concentrations to the enzyme active site (although unproductive) could function similar to the substrate Pen V in activating an allosteric mechanism, thereby enhancing the enzyme activity. The allosteric behaviour of *Pa*PVA on Pen V has been mentioned in Chapter 2. At higher concentrations (>1mM), the excess binding of bile salts probably inhibits the Pen V binding, leading to decreased PVA activity. Kinetics curves of *Pa*PVA for Pen V hydrolysis at three different GDCA (glycodeoxycholate) concentrations (0.1 mM, 1 mM and 5mM) indicate changes in both V_{max} and K_m (Fig. 4.7), signifying a competitive inhibition component.

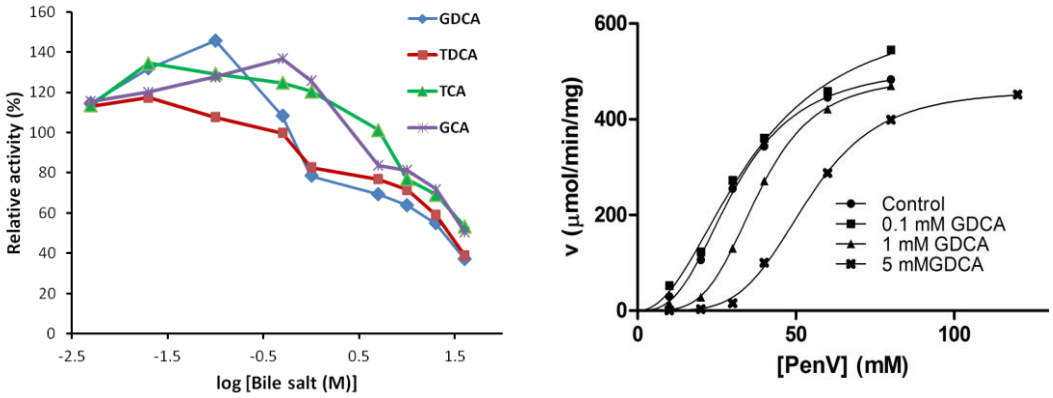

Fig. 4.6. (a) Inhibition of *Pa*PVA activity in the presence of bile salts. (b) v/[S] plots for PaPVA with increasing concentrations of Pen V in the presence of 0.1,1 and 5 mM GDCA.

4.3.5. Exploration of residues involved in binding of Pen V to *Pa*PVA using site-directed mutagenesis:

PVAs from Gram-negative bacteria exhibit some striking structural differences from their Gram-positive counterparts. They also exhibit a considerably enhanced Pen V hydrolysis activity, and are very specific for Pen V over bile salts or related β-lactam compounds. The mutagenesis of specific residues in the active site of *Pa*PVA could help explore their importance in substrate binding and the catalytic mechanism. In this context, we performed site-directed mutagenesis of some of these residues and studied their effect on PVA activity.

Mutating most of the active site residues led to a drastic reduction in activity, and a loss of protein yield in many cases **(Table 4.1)**. Replacement of N-terminal cysteine in the C1S mutant led to complete loss of PVA activity. Although the R19H variant was stable, it showed only 6% of the native PVA activity. It has been suggested that the R19 residue is involved in lowering the pKa of the N-terminal cysteine, thus increasing its nucleophilicity. It has also been implicated in processing mechanism of *Cp*BSH (Rossmann 2008). Other variants such as D22E, D22N and R215L all showed a drastic reduction in activity, attesting to the importance of these residues in maintenance of active site geometry and transition state stabilization (Lodola et al. 2012).

Table 4.1. Protein expression yields and relative specific activity of *Pa*PVA variants. Specific activity of native *Pa*PVA (430 IU/mg) was taken as 100%.

Enzyme variant	Protein expression (mg/L)	Relative specific activity (%)
Native	262	100
C1S	2.1	0
R19H	121	6
D22N	2.5	5.1
D22E	34	10.9
R215L	5.6	7.4
W23F	6.9	4
W23I	7.1	0.9
W87Y	6.7	1.5
W87N	196.8	81.2
W23F/W87Y	3.3	0.13
W23I/W87N	3.6	0.02

*Pa*PVA and other such sequences from Gram-negative bacteria contain a trp pair at the positions 23 and 87 (Chapter 3). While W87 is known to participate in the formation of oxyanion hole through its main chain amide group during the catalytic reaction, the significance of its side chain and the role of W23 are not clear, although they are thought to be involved in Pen V binding. We generated variants of *Pa*PVA

with mutations in these tryptophan residues to better understand their interactions with the Pen V molecule. Specific mutations were chosen based on the evolutionary preference of residues at these positions in different cholylglycine hydrolases. Change at the 23 position led to drastic reduction both in protein expression and activity. W23F and W23I showed only 4% and 0.9% of the native PVA activity, respectively **(Table 4.1)**. The W87 mutants on the other hand were ambiguous, with a significant reduction in activity with W87Y while W87N showed good expression and activity similar to the native enzyme. Regardless, the trp double mutants – W23F/W87Y and W23I/W87N – both exhibited lower activity than single mutants. In spite of their differences in specific activity, all the mutants were observed to display a similar kinetic behaviour as wt-*Pa*PVA, with cooperative nature and substrate inhibition (Avinash et al. 2015).

4.3.6. Molecular dynamics simulations of *Pa*PVA - Structural changes related to Pen V binding:

Due to the loss of protein yield in tryptophan mutants and difficulty in getting a enzyme-ligand complex structure, we followed computational docking and molecular dynamics simulations (MDS) to understand the role of the Trp residues in Pen V binding. The parameters of the simulation were first analyzed to validate its results. All the simulations were observed to be stable based on their Cα RMSD values throughout the simulations (average 0.2 Å; **Fig.4.7**). Pen V was observed to bind firmly in the active site throughout the simulation (avg. RMSD 0.3-0.5 Å).

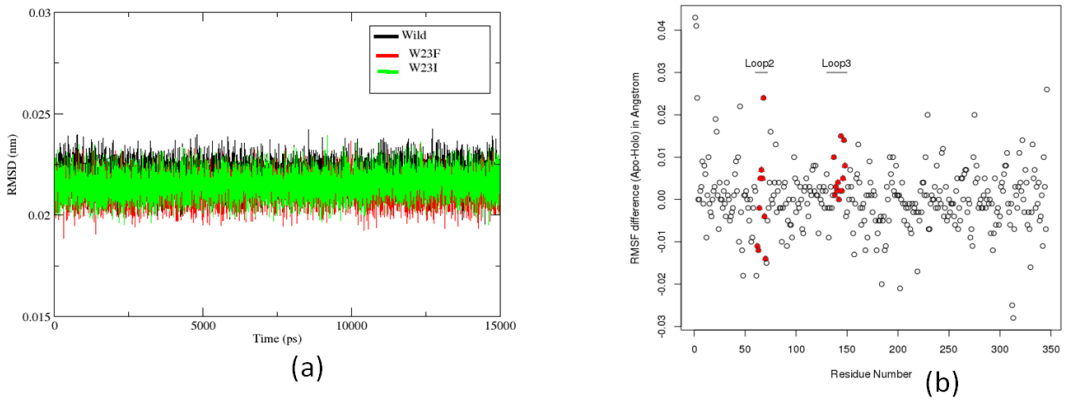

Fig. 4.7. (a) RMSD of Cα atoms in native *Pa*PVA and variants during the course of MD simulation. (b) RMSF of Cα atoms in apo and holo – *Pa*PVA. Loop regions near the active site are highlighted in red.

No significant conformational flexibility to explain the allosteric behaviour of *Pa*PVA (Chapter 2) was observed in the overall structure upon Pen V binding, as inferred from the root mean square fluctuation (RMSF) values of the active site loop regions (61-70 and 137-148) **(Fig. 4.7)**. However, these loop regions are different with respect to their conformational folding and orientation compared to other CGH enzymes (Panigrahi et al. 2014; Lambert et al. 2008). It is also possible that the *Pa*PVA enzyme could display allosteric behaviour even in the absence of conformational change. Recently, certain proteins have been explained to manifest allosteric behaviour as a result of cumulative dynamic entropy changes (Cooper and Dryden 1984) without visible structural change. Ligand binding causes fractional decreases in the rms coordinate fluctuation of atoms in the active site, leading to a minute but global rigidification of the protein domain. This generates a free coupling energy in the range of 1.5 kcal/mol that could lead to allosteric interaction, although minute to be detected experimentally (Kern and Zuiderweg 2003). Also, studies have shown that changes in regions distant from the functional active site could also propagate dynamic effects to influence substrate binding affinity and catalysis (Luque et al. 2002; Petit et al. 2009). Considering these observations, it seems possible that the deletion of the assembly motif (Chapter 3) in CGHs from Gram-negative bacteria might also be relevant to the alloteric nature of *Pa*PVA.

During the simulation of the native *Pa*PVA-Pen V complex, a strict geometrical arrangement was observed between the aromatic rings of Pen V, W23 and W87 **(Fig.4.8)**. However, there was a difference in the modes of interaction of the trp residues with the Pen V molecule – while W23 stacks in parallel above the Pen V phenyl ring, the W87 residue interacts edge to face with an orthogonal geometry. Binding energy in parallel stacked complexes are thought to involve repulsion-dispersive interactions causing π-π complexation, in contrast to T-shape interactions that are dominated by electrostatic and van der Waals contributions with the $\delta(+)$ hydrogen atom pointing towards the $\delta(-)$ π-electron cloud (Gervasio et al. 2002). Parallel stacking has been reported to be 1kcal/mol more stable than the T-shaped interaction in aromatic amino acid interactions in proteins (McGaughey et al. 1998), suggesting that the W23-Pen V interaction might relatively contribute more to binding energy than the W87-Pen V interaction.

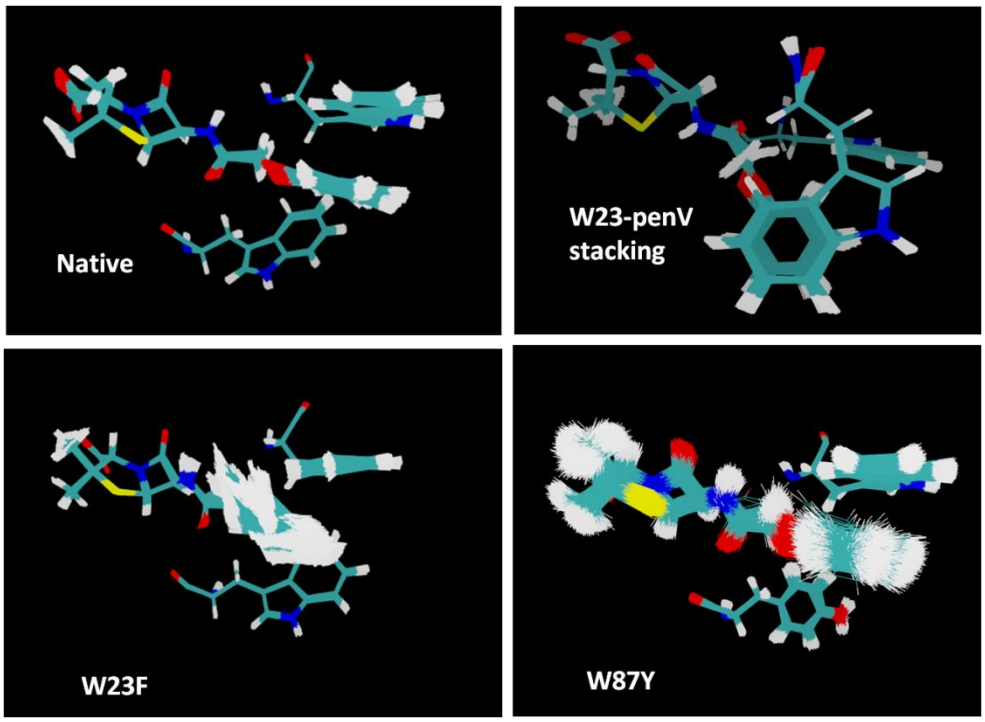

Fig. 4.8. Fluctuations and stacking interactions of Pen V at the active site in native and mutant *Pa*PVA (W23F and W87Y) during 15 ns simulation.

Mutation and computational analyses seem to indicate that the enzyme stability is probably dictated by the strength of aromatic interaction between these trp residues, while the PVA activity depends on the combination of the interactions of Pen V phenyl ring with W23 and W87. The importance of the tryptophan residues in stacking was quantitatively estimated by measuring the RMSD of phenyl ring atoms as well as the whole Pen V molecule during the simulation. W23F, W23I and W87Y mutants showed significant increase in the average RMSD values, indicating loss of proper stacking interactions with the substrate. These observations and the loss of enzyme activity of these variants corroborated well with a change of binding constants obtained through fluorescence quenching experiments **(Table 4.2)**. In the W23F and W87Y mutants, a definite increase in the centroid distances and the dihedral angles was also observed between the planes of the aromatic residues **(Fig. 4.9)**. The W87N mutant was an exception, exhibiting good PVA activity with RMSD of Pen V molecule and substrate binding constant closer to that of the native enzyme **(Table 4.2)**. In this instance, it might be possible that the NH group of asn is involved in amino-aromatic interaction with the W23 residue, and Pen V phenyl ring during substrate binding, thus replacing W87 to an extent. Amino-aromatic

interactions have been known to be analogous to T-shape interactions between aromatic residues in proteins (Burley and Petsko 1986). On the other hand, substitution with tyr in the W87Y mutant led to disruption of the aromatic interaction, probably due to the change in distance from the Pen V molecule and dihedral angles. Interestingly, both W23F/W87Y and W23I/W87N double mutants showed near complete loss of activity **(Table 4.1)**. This attests to the possibility that the coordination of residues at both these positions is important to interact with and position the Pen V molecule in the active site.

Table 4.2. Average RMSD (Mean ± s.d.) of Pen V molecule and its phenyl ring observed over the course of the simulation in native and mutant *Pa*PVA. Pen V binding constants (K_a) for all variants (calculated from fluorescence titrations) are also displayed.

Enzyme	Phenyl ring	Pen V molecule	Association constant (Ka, M^{-1})
Native	0.56 ± 0.22	0.67 ± 0.15	292.11
W23F	0.70 ± 0.36	0.77 ± 0.23	20.04
W23I	0.80 ± 0.47	0.87 ± 0.24	18.02
W87Y	0.75 ± 0.47	0.85 ± 0.37	64.26
W87N	0.61 ± 0.33	0.71 ± 0.19	134.84

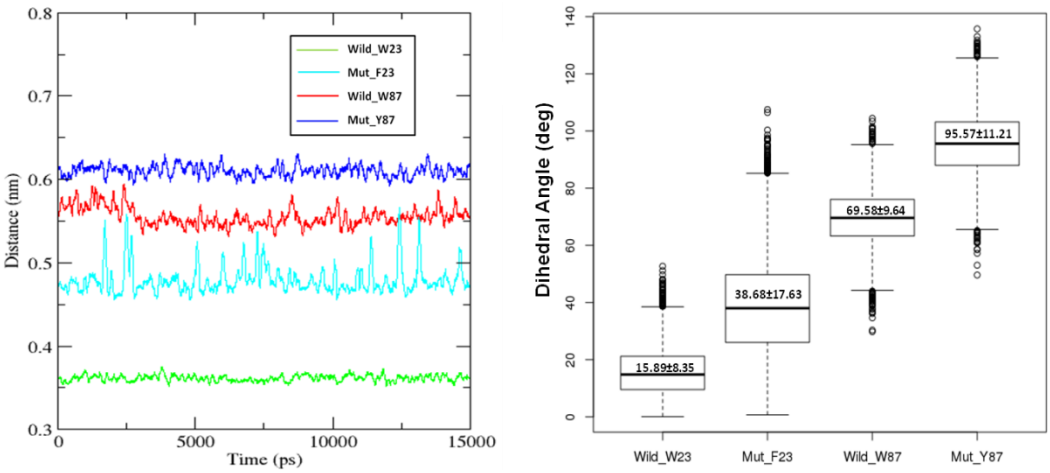

Fig. 4.9. (a) Centroid distance and (b) angles between W23 (F23) or W87 (Y87) and phenyl ring of Pen V during the course of the simulation in native and variant (W23F or W87Y) *Pa*PVA, respectively.

In order to assess the binding strength of Pen V in the active site, the hydrogen bonding pattern was also monitored throughout the simulation. Pen V was observed to form hydrogen bonds with active site residues over 50% of the simulation time scale in the native enzyme. The residues R215, N183 and A273 were found to dominate in terms of hydrogen bonding interactions with Pen V in the active site **(Table 4.3)**. The essential roles of these residues in PVA catalytic mechanism have been explored; R215 interacts with the carboxyl-side chain of β-lactam ring, while N183 forms the oxyanion hole with W87 (Suresh et al., 1999, Lodola et al., 2012).

Table 4.3. Number of frames (% of 7500) in which hydrogen bonds were formed by Pen V molecule with different residues in the active site, in native *Pa*PVA and variants (W23F, W23I, W87Y and W87N).

Residue	Native	W23F	W23I	W87Y	W87N
N183	1.56	0.11	0.32	0.08	0.12
R215	40.10	18.48	15.96	20.38	32.56
A273	16.12	14.17	30.39	23.43	26.87
A212	-	0.09	5.31	-	0.17
N271	0.25	3.07	0.07	-	1.28
No. of bonds	**Native**	**W23F**	**W23I**	**W87Y**	**W87N**
0	49.89	67.86	54.43	58.20	48.49
1	37.08	27.63	38.50	34.66	40.30
2	11.60	4.24	6.74	6.78	10.27
3	1.40	0.25	0.33	0.35	0.75
4	0.03	0.01	-	-	-

Other residues such as A212 and N271 were also found to participate in substrate interactions; these residues mainly form hydrogen bonds with the 6-APA part of the Pen V molecule. Hydrogen bond formation with R215 and N183 was considerably reduced in the mutant variants (W23F, W23I and W87Y) that showed a drastic

reduction in activity. R215 was observed to interact with Pen V in 40% of frames in the native enzyme and lower than 20% in these mutants. In contrast, Pen V was involved in hydrogen bonding with R215 in 32% of frames in the case of W87N. The number of frames exhibiting one or more hydrogen bonds between the Pen V molecule and the active site residues was also measured. Native *Pa*PVA and W87N mutant exhibited more than 50% of frames with at least one hydrogen bond with Pen V, while the other three trp mutants showed a reduction in hydrogen bond formation.

Analysis of the residues at positions 23 and 87 (in *Pa*PVA) using mutagenesis and MD simulations strongly suggests that the nature and position of these amino acids in cholylglycine hydrolases play a vital role in Pen V binding. Both the trp residues appear to act in tandem to properly position the Pen V in the active site relative to the N-terminal cysteine for maxium activity, and subtle changes disrupting these interactions lead to drastic reduction in activity. However, the W23 residue seems to be irreplaceable due to its parallel stacking interaction with the phenyl ring of Pen V; while the W87 residue could be substituted by asparagine with minimal loss of enzyme activity.

4.3.7. Substrate binding in PVAs from Gram-negative bacteria:

Panigrahi et al. (2014) have reported the segregation of choloylglycine hydrolases from Gram-positive and Gram-negative bacteria into different clusters, based on a new binding site profile-based scoring system. The two groups show low sequence homology (<30%) and significant structural differences, including the loss of the assembly motif and inclusion of a periplasmic signal pre-peptide in Gram-negative CGHs. Decrease in the size of active site and substitution of aromatic residues help the PVAs from Gram-negative bacteria to be more specific and highly active on Pen V. This chapter details the subtle structural features involved in substrate binding that explain the high activity and specificity of *Pa*PVA for Pen V, and the modulation of Pen V hydrolysis through binding of bile salts. Through mutagenesis and MD simulations, the importance of W23 and W87 residue side chains in Pen V binding has also been emphasized. These residues play a significant role in interacting with substrates like Pen V at the active site through aromatic interactions, modulating the PVA activity and specificity.

An analysis of PVAs and Ntn hydrolases in general (Avinash et al. 2014) illuminates the distinctive quality of the family of enzymes to maintain the catalytic αββα fold even in the absence of appreciable sequence homology. A few important amino acids responsible for the catalysis (including N-terminal nucleophile and residues involved in oxyanion hole formation) are strictly conserved, thus preserving the reaction mechanism. However, subtle changes in residues involved in substrate binding and loops near the active site help these enzymes to act on a wide variety of amide substrates with different side chains. Recently, Koch et al. (2014) have reported a acyl homoserine lactone (AHL) substrate switch from C_{12}-HSL to C_8-HSL in the case of AHL acylase PvdQ by the mutagenesis of two residues near the active site. Many Ntn hydrolases (including PVAs) have significant uses in the industry. These are thus prospective resources for protein engineering, to understand and tweak their substrate spectrum. In addition, further studies on Gram-negative CGHs will also help enhance our understanding of the roles they play in microbial physiology through knowledge of their substrates and binding mechanisms.

Chapter 5

Characterization of PVA from *Agrobacterium tumefaciens* (*At*PVA) and hydrolysis of acyl-homoserine lactones (AHLs) by PVAs

5.1. Introduction:

Penicillin acylases enjoy an immense importance in the pharmaceutical industry; but there is little concrete knowledge of their roles in natural microbial physiology and metabolism. The hydrolysis of Pen V by PVAs is not thought to confer any resistance to antibiotics, thus providing no evolutionary advantage (Cole 1969). Some studies on the roles of penicillin acylases in nature have been discussed in Chapter 1, like the probability that penicillin acylases could act as scavenger enzymes for alternative carbon sources (Valle et al. 1991). Recently, studies have indicated the involvement of penicillin acylases and close homologues in the Ntn hydrolase family in bacterial signaling and pathogenesis (Avinash et al. 2014).

Quorum sensing (Fuqua et al. 2001) refers to the phenomenon of bacterial signalling, which allows the bacteria to perceive its population density through the secretion of auto-inducer molecules. Once a critical level or "quorum" is reached, the auto-inducer signals act to modulate the level of expression of various genes to trigger certain metabolic pathways. Quorum sensing is known to be involved in modulating virulence, bioluminescence, swarming motility and many other physiological processes (Gera and Srivastava 2006). Although a variety of small molecules that function as signals in bacteria have been discovered (Henke and Bassler 2004; Takano 2006; Bogino et al. 2015), acyl-homoserine lactones (AHLs) are the most studied till date. AHLs are produced and utilized in quorum sensing mainly by Gram-negative proteobacteria. Structurally, they consist of a homoserine lactone ring linked via amide bond to an acyl side chain (C_4-C_{18}) which may be saturated or unsaturated, or with a hydroxy, oxo or no substituent on the carbon at 3-position of the N-linked acyl chain (Bassler 2002). They are synthesized by the luxI or luxM family of AHL synthetases from S-adenosyl methionine and charged acyl-acyl carrier protein (ACP), and are regulated by the luxI/luxR system (More et al. 1996; Miller and Bassler 2001). Synthesized AHLs accumulate outside the cell and diffuse into neighbouring cells, where they modulate gene expression through binding to the luxR family of regulators (Henke and Bassler 2004). While *Vibrio fischeri*, *Agrobacterium tumefaciens* and *Pectobacterium carotovorum* produce C_6-C_8HSLs (Fuqua et al. 2001), other bacteria like *Pseudomonas aeruginosa* utilize C_4 and 3-oxo-C12-HSLs as signals for auto-induction (Pearson et al. 1994, 1995).

Due to the significance of AHL-based quorum sensing mechanisms in regulating many bacterial physiological processes, the disruption of such mechanisms (termed "quorum quenching") has been observed to be useful in controlling bacterial pathogenesis and biofilm formation (Dong et al. 2007). Interference in QS can occur through AHL mimics or by enzymatic degradation of the AHL molecules (Uroz et al. 2009). AHL lactonases (that cleave the lactone ring) and AHL acylases (that cleave the amide bond) have been recently characterized from quite a few bacteria, including *Variovax paradous* (Leadbetter et al. 2000), *Bacillus* sp. (Dong et al. 2001), *P. aeruginosa* (Sio et al. 2006), *Ralstonia* sp. (Lin et al. 2003) and *Streptomyces* sp. (Park et al. 2005). AHL acylases have been observed to have variable substrate specificities. While the *Variovax* and *Ralstonia* acylases act on both long and short chain AHLs, *Pseudomonas* acylases show activity only on long chain AHLs (Krzeslak et al. 2007).

It is evident that the action of AHL acylases is very similar to that of penicillin acylases, with both classes of enzymes acting on structurally related substrates. AHL acylases also exhibit considerable sequence homology with penicillin G acylases. The three-dimensional structure of PvdQ (AHL acylase from *P. aeruginosa*) is homologous to the PGA from *E. coli*; both possess the αββα structural fold and catalytic mechanisms typical to the Ntn hydrolase protein family (Bokhove et al. 2010). In addition, certain AHL acylases and penicillin G acylases have been shown to cross-react on each other's substrates (Park et al. 2005; Mukherji et al. 2014). A new AHL acylase from *P. aeruginosa* (PA0305, Wahjudi et al. 2011) has been reported to cleave Pen V to a small extent; however, AHL degradation by PVA enzymes has rarely been explored so far.

We have cloned and characterized PVA enzymes from two related Gram-negative plant pathogenic bacteria, *Pectobacterium atrosepticum* (*Pa*PVA) and *Agrobacterium tumefaciens* (*At*PVA). This chapter details the structural and biochemical characteristics of *At*PVA. These PVAs share a 62% sequence identity, and exhibit similar characteristics with minor structural differences. Furthermore, this study also explores the activity of these PVA enzymes on AHLs as substrates, and its possible significance in the physiology of the bacteria that produce these enzymes.

5.2. Materials and methods:

5.2.1. Cloning, expression and purification of *At*PVA enzyme:

The *pva* gene from *A. tumefaciens* was cloned into a pET22b plasmid vector (Invitrogen) between NdeI and XhoI restriction sites using the primers, AtuF (gcttga*catatg*tgcacgcgtttcgtttatatag) and AtuR (ctgaat*ctcgag*aagcccgagaaacttgaaag). Recombinant plasmids were selected for ampicillin resistance. The PVA enzyme was expressed in *E. coli* BL21 star cells with a C-terminal His-tag, and was purified to homogeneity using a HIS Select Ni^{2+} affinity column and ENrich^{TM} 650 (BioRad) size exclusion column, using a similar procedure as described for *Pa*PVA in Chapter 2. The protein was dialyzed against 10mM Tris HCl buffer pH 7.4 containing 100mM NaCl and 1mM DTT and stored at 4°C.

5.2.2. PVA enzyme activity assay:

Pen V hydrolysis activity was estimated by studying the formation of Schiff's conjugate with the product 6-APA and p-dimethyl amino benzaldehyde (Shewale et al. 1987). One unit (IU) of enzyme activity was defined as the amount of enzyme producing 1 μmol 6-APA in 1 min.

5.2.3. AtPVA crystallization and structure determination:

Crystallization trials were set up with *At*PVA (concentrated to 15 mg/ml) using the sitting drop vapour diffusion technique. The protein crystallized in 0.1M HEPES pH 7.5 and 12% (w/v) PEG 3350 condition of the PEG Rx crystallization screen. The crystals were frozen in liquid nitrogen with 25% 2,5-hexanediol as cryoprotectant. Diffraction data were collected at 2.8 Å at the SSRL-BL12-2 beamline at the Stanford Synchrotron Linear Accelerator Center (SLAC, USA). Data was collected for 180° in 0.2° oscillation frames with exposure time of 0.3 s each. Investigation and scaling of the diffraction data was performed using XDS (Kabsch 2010) and SCALA (Evans 2006). The *At*PVA structural model was built using molecular replacement on Phaser ver. 2.5.6 (McCoy et al. 2007) and Autobuild (Phenix), with the refined structure of *Pa*PVA as the template. Further model building and refinement was done using Coot and Refmac5 (CCP4 software suite) respectively.

5.2.4. Biochemical characterization of *At*PVA:

The PVA activity was assayed (as detailed above) at different pH values from 4.0 – 9.0 and temperatures (20 – 70°C) to ascertain the optimum conditions for Pen V hydrolysis.

*At*PVA stability was studied by incubating the protein in 10 mM Tris HCl buffer pH 7.4 for 2 h at different temperatures from 30 to 90°C, and assaying for PVA activity at 45°C after different time intervals. Effect of pH on enzyme stability was studied by incubating the protein in 100 mM buffers of different pH (1-11) for 4 h at 25°C and assaying the residual activity. Buffers used were: HCl-KCl (pH 1-2), acetate (3-6), phosphate (7-8), Tris (8-9) and carbonate-bicarbonate (10-11). All buffers were freshly prepared with pH adjusted at room temperature and filtered before use.

Kinetic parameters were determined by assaying the enzyme activity with increasing concentrations (5-240mM) of Pen V (potassium salt, Sigma) as substrate, and fitting the curve to the Equation 2.1 (Chapter 2).

5.2.5. Bioluminescence assay for detection of AHL degradation:

The presence of AHLs in the reaction medium was examined using a bioassay which employs bioengineered biosensor strains that are able to detect the presence of AHLs. These strains exhibit bioluminescence properties modulated by the availability of specific AHLs. Quenching of bioluminescence levels can be used as an indication of AHL hydrolysis by the acylase enzymes (Steindler and Venturi 2007).

For the assay, 0.5 µL of 5 mM AHLs **(Fig. 5.1)** stock solution in DMSO was spotted to flat bottom µClear white microplate (Greiner Bio-One), and carefully dissolved in reaction mixture (100 µl) containing 5 µg enzyme in 100 mM NaCl, 1 mM DTT and 25 mM Tris HCl buffer pH 7.4 (for *At*PVA) or 20 mM sodium acetate buffer pH 5.2 (for *Pa*PVA). After 4 h incubation at 25°C, equal volume of modified PBS (137 mM NaCl, 2.7 mM KCl, 100 mM Na_2HPO_4, 1.8 mM KH_2PO_4) was added to each well, followed by 100 µl of 100-fold diluted overnight biosensor. Luminescence of the biosensor as a response to remaining AHLs was measured at 30°C during 12 h time-course using FLUOstar Omega (BMG Labtech) as described previously (Papioannou

et al. 2009). Control reactions were performed in the same manner using heat-inactivated enzyme (100°C for 15 min). *Escherichia coli* (pSB536) was used to analyse C_4-HSL degradation; *E. coli* (pSB401) was used to visualize C_6- till C_8-HSL (Swift et al. 1997), and *E. coli* (pSB1142) was used to analyze C_{10}- till (3-OH- and 3-oxo-) C_{12}-HSL degradation (Winson et al. 1998). The experiments were performed in duplicate in three independent experiments. To determine the enzyme activity on AHLs, ratio of luminescence unit to biosensor growth in OD_{600} from active enzymes was compared to those from inactive enzymes.

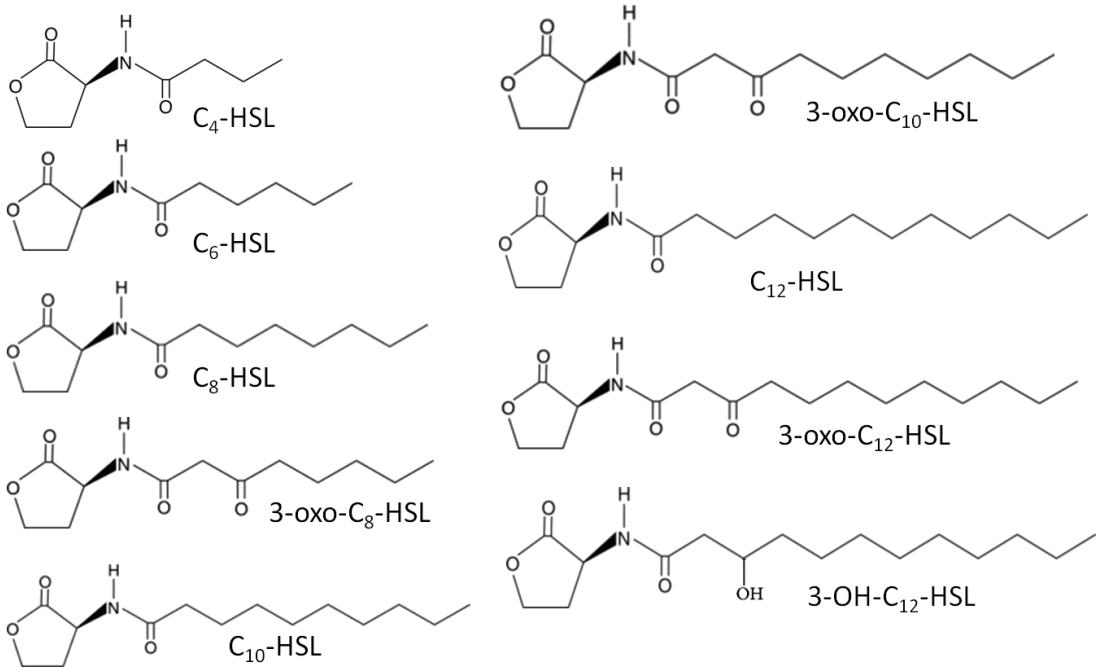

Fig. 5.1.Chemical structures of AHL substrates used for bioluminescence assay.

5.2.6. Analysis of C_{10}-HSL deacylase activity by HPLC:

To confirm the deacylase activity of PVA enzyme on long chain AHLs, the reaction with C_{10}-HSL was analyzed by HPLC as described by Uroz et al. (2008). The enzymes (25µg in the same reaction mixture as bioluminescence assay) were incubated with 0.4 mM C_{10}-HSL for 4 h at 25°C (heat-inactivated enzyme was used as a control). Samples of 750 µl from time 0 and 4 h were processed for detection of residual substrate C_{10}-HSL, HSL and decanoic acid (Wahjudi et al. 2011).

For detection of the substrate, residual C_{10}-HSL in the reaction mixture was extracted twice with equal volume of acidified ethyl acetate. The free HSL released

during the reaction was dansylated with equal volume of 2.5 mg/ml dansyl chloride (in acetone) and incubated overnight at 37°C (Lin et al. 2003). After speedvac evaporation, the sample was neutralized with 50 µl of 0.2M HCl and diluted with 250 µl acetonitrile. Decanoic acid in the sample was extracted thrice with equal volume of hexane followed by drying under nitrogen stream and derivatization with 4-bromomethoxy-7-methyl coumarin (BrMMC) reagent as described previously (Wolf and Korf 1990).

HPLC was carried out in Shimadzu LC-10AT VP system using Phenomenex Luna C18 reverse-phase column (250 x 4.60 mm, 5 µm) coupled with SPD-M10AVP PDA detector. The column was washed with 5% acetonitrile in water (solvent A), and sample was eluted in a linear gradient to 100% acetonitrile (solvent B). C10-HSL was detected at 219 nm, dansylated HSL at 267 nm, and BrMMC-derivatized decanoic acid at 328 nm (Uroz et al. 2008). Reaction control of reference substrate and products showed that the dansylation and BrMMC derivatization was specific to HSL and decanoic acid, respectively (data not shown).

5.2.7. Kinetics of AHL degradation by PVAs:

The activity of *At*PVA and *Pa*PVA on 3-oxo-C_{12}-HSL was determined by end-point assay using ortho-phthalaldehyde (OPA) derivatization of the HSL product. OPA reagent in conjunction with reduced sulfhydryl groups reacts with the free amine group of HSL to form fluorescence derivatives. 3-oxo-C_{12}-HSL stock in DMSO was prepared into 8 different concentrations at which the substrate was completely soluble (0.01-0.25 mM). The reaction mixture consisted of 100 mM NaCl, 1 mM DTT and 25 mM sodium phosphate buffer pH 7.4 (for *At*PVA) or 20 mM sodium acetate buffer pH 5.2 (for *Pa*PVA). DMSO concentration was kept at 0.8% for each reaction. Enzyme (2 µg *At*PVA or 0.5 µg *Pa*PVA) was added into 1 ml reaction mixture; 90 µL sample was taken immediately and thereafter regularly at 1 min intervals. The enzyme was inactivated with 10 µL of 1M NaOH. This step inactivated both enzymes, and did not interfere with the subsequent derivatization. The enzyme was removed by centrifugation, and 50 µL of the sample was transferred into black Fluotrac microplate (Greiner Bio-One) and mixed with 50 µL ortho-phthalaldehyde reagent, followed by 20 min incubation at 25°C. Fluorescence measurement was performed on FLUOstar Omega, BMG Labtech with excitation at

355 nm and emission at 460 nm. Standard curve using 0-0.25 mM HSL standard prepared in reaction mixture showed a straight line that can be fitted in the following equation: y = 77290x + 490.5 (R^2=0.9996). Initial velocity was limited in the range of 15% substrate conversion and calculated from the standard curve.

5.2.8. Docking of AHLs to *Pa*PVA and *At*PVA:

The 3D structures of C_6-HSL, C_{10}-HSL and 3-oxo-C_{12}-HSL used in the docking study were obtained from PubChem compound database (Bolton et al. 2008). Partial atomic charges of each ligand atom were determined from OPLS_2005 all-atom force field using LigPrep. Grid based ligand docking program Glide (Freisner et al. 2006) was used for docking these ligands in the binding site of *Pa*PVA and *At*PVA. The binding site was defined as a grid box of dimension 26x26x26 Å, centered on Cys1 residue. Receptor grid generation was followed by ligand docking where the ligands were docked flexibly using Glide's extra precision.

Free energy of binding is roughly estimated by using an empirical scoring function called GlideScore, which includes electrostatic, van der Waals interaction and other terms for rewarding or penalizing interactions that are known to influence ligand binding. All structural figures were prepared using PyMol or *CCP4MG*.

5.3. Results and Discussion

5.3.1. Biochemical characterization of *At*PVA:

The PVA enzyme from *Agrobacterium tumefaciens* (*At*PVA) shares a 62% sequence similarity with *Pa*PVA. *At*PVA was also observed to be highly specific for Pen V over bile salts and other β-lactam antiobiotics, showing a specific activity of 205 IU/mg at 50 mM Pen V. The enzyme showed maximum Pen V hydrolysing activity in optimum pH 6 - 7 and temperature 45°C **(Fig. 5.2)**. *At*PVA differed with *Pa*PVA in pH and temperature stability. The enzyme was stable in the pH range 5-8, while *Pa*PVA was more stable in the acidic pH range. *At*PVA also showed a drastic reduction in activity and loss of tertiary structure at 60°C **(Fig. 5.3).** This trait is also shared by PVAs from Gram-positive bacteria; however, *Pa*PVA was active at 60°C and registered a complete loss in activity only at 80°C (Chapter 2).

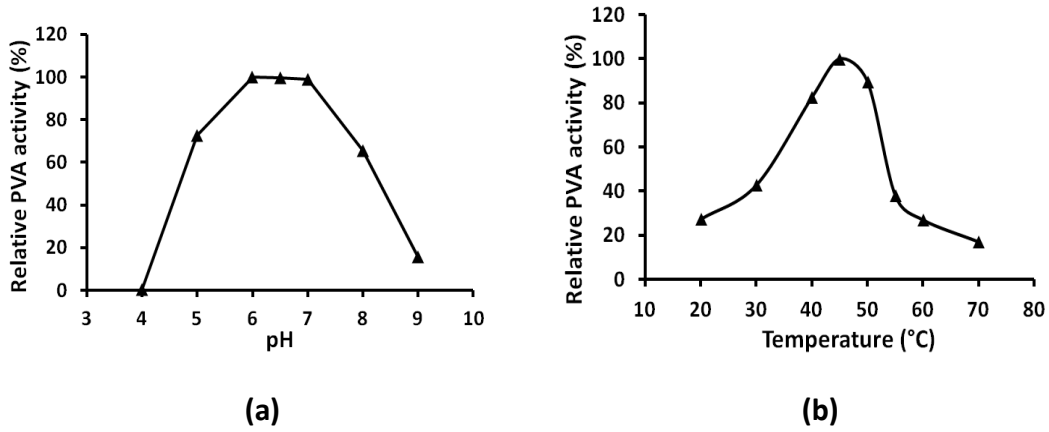

Fig. 5.2. Optimum pH (a) and temperature (b) for *Pa*PVA enzyme activity.

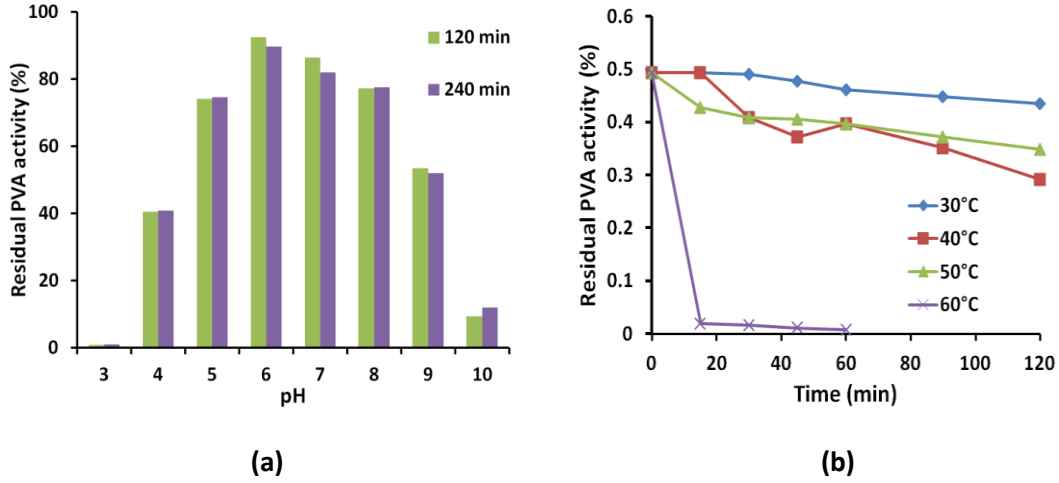

Fig. 5.3. Stability of *At*PVA at increasing (a) pH and (b) temperature.

Notwithstanding the difference in pH/temperature optima and stability, *At*PVA was observed to exhibit complex kinetic behaviour similar to *Pa*PVA. Cooperativity and substrate inhibition with Pen V and modulation of activity in the presence of bile salts were observed in *At*PVA, as was the case with *Pa*PVA. Although the standard error of estimation was high, it could be inferred that *At*PVA showed slightly less Vmax (641.9 µmol/min/mg) than *Pa*PVA (758.2 µmol/min/mg) **(Fig. 5.4)**. The major difference between *At*PVA and *Pa*PVA kinetics was in the extent of substrate inhibition; *At*PVA showed a Ki of 47.2 mM, compared to a much higher value of 163.1 mM for *Pa*PVA. Near complete reduction of *At*PVA activity was observed at a concentration of 240 mM Pen V, while *Pa*PVA still had considerable activity (20% of V_{max}) at the same concentration. Drastic reduction in Pen V hydrolysis was also observed in the presence of high GDCA concentrations over 5 mM **(Fig. 5.4)**.

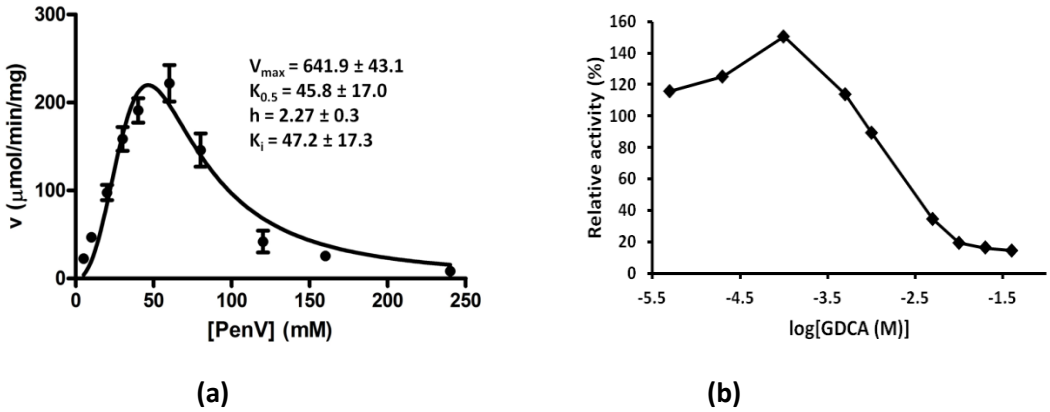

Fig. 5.4. (a) v/[S] plot of *At*PVA with Pen V as substrate. Kinetic parameters are given in inset. (b) Relative PVA activity in the presence of increasing concentrations of GDCA. Pen V concentration was kept constant at 50 mM.

5.3.2. *At*PVA structural analysis:

The structural features of *At*PVA closely resemble the *Pa*PVA structure. *At*PVA crystallized in the $P2_12_12_1$ space group with a single tetramer per asymmetric unit. The structure was solved using molecular replacement with the refined structure of *Pa*PVA monomer as the template. The data processing and refinement parameters are shown in **Table 5.1.** The final model (R_{work} = 0.2134, R_{free} = 0.2573) showed that 1.1% of the residues were Ramachandran outliers (recommended < 0.4%). However, all these residues were either prolines or belonged to a dynamic loop region (residues 137-148) that had very poor density (**Fig. 5.5**).

*At*PVA possesses a similar orientation and distance between subunits in the tetramer as *Pa*PVA; however, the angle between the opposite subunits was 169.6°, closer to the planar shape of *Bsp*PVA (171°) than *Pa*PVA (158°). Superposition of the two structures **(Fig. 5.5)** reveals the presence of a longer loop2 (residues 61-74) near the active site in *Pa*PVA. In the case of *At*PVA and other PVAs from Gram-negative genera, the 5-residue insertion (GRGKM in *Pa*PVA) is not observed. It is probable that the length of this loop might play a role in modulating the substrate inhibition in PVAs from Gram-negative bacteria. *At*PVA also possesses two Trp residues (W21, W80), separated by a centroid distance of 5.11 Å with a dihedral angle of 67.9°, that could interact with the Pen V molecule through aromatic interactions. The significance of these residues in PVA activity has been established (Chapter 4). Finally, in contrast to *At*PVA and *Bt*BSH, *Pa*PVA displays a longer loop covering

the region 228-239 that is exposed to the solvent; though the significance of the loop is not yet known.

Table 5.1. X-ray diffraction data collection and structure model refinement of *At*PVA. Values in parentheses represent outer shell.

X-ray diffraction and data collection	
X-ray source (wavelength)	INDUS –II (1.98 Å)
Space group	$P\ 2_12_12_1$
Resolution range	39.55-2.8 Å
Unit cell parameters (Å)	a=50.66, b= 134.77, c = 215.07
Molecules per asymmetric unit	1 tetramer
Matthews coefficient ($Å^3Da^{-1}$)	2.48
Solvent content (%)	50.44%
Total no. of reflections	259813 (37088)
No. of unique reflections	37299 (5327)
Multiplicity	7.0 (7.0)
Completeness (%)	99.9 (99.9)
Average I/σ(I)	11.9 (4.0)
R-merge (%)	0.136 (0.490)
Structure refinement:	
R-factor	0.2134
R-free	0.2573
Number of atoms:	
Protein	20148
Water	107
Average B-factors:	
Protein	42.71
Water	23.49
Ramachandran plot (%)	
Most favourable	95.0
Allowed	5.0
Disallowed	0.0

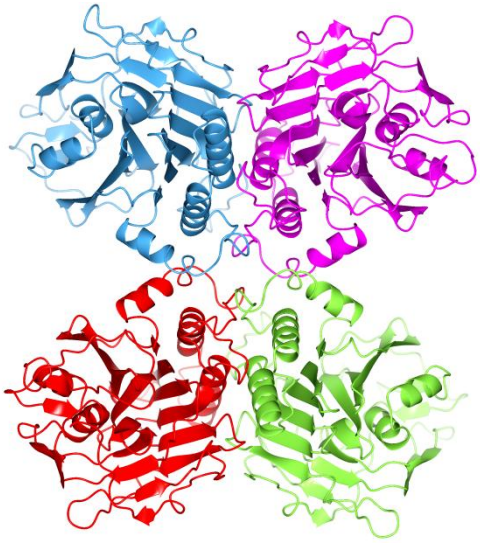

(a)

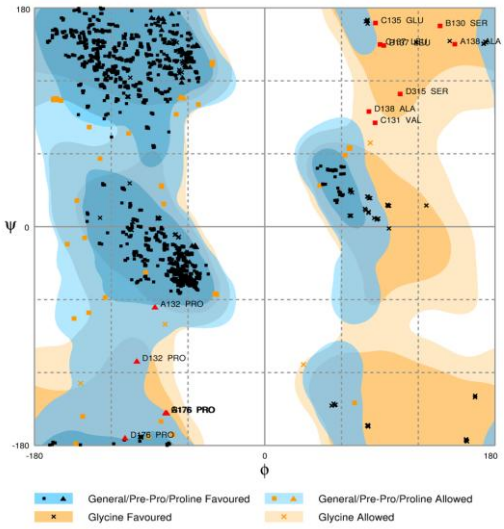

(b)

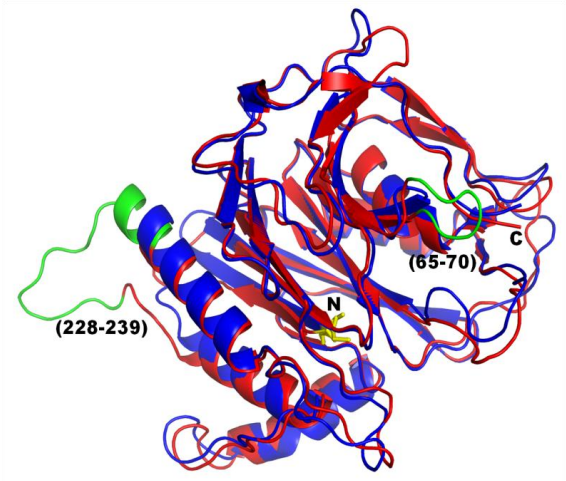

(c)

Fig. 5.5. (a) Tetramer structure of *At*PVA. Subunits are shown in different colours.

(b) Ramachandran plot of final refined model.

(c) Superposition of monomer structures of *At*PVA and *Pa*PVA. The loop extensions in *Pa*PVA are shown in green. N-terminal cysteine is shown in yellow (stick representation).

5.3.3. Analysis of AHL degradation by *Pa*PVA and *At*PVA:

The ability of PVAs (*Pa*PVA and *At*PVA) to hydrolyze AHL molecules (involved in bacterial signaling) was studied to throw some light on the roles of PVA enzymes in microbial physiology. After incubation with the PVAs for 4h, AHL degradation was checked through the quenching of bioluminescence by specific reporter strains. Both *Pa*PVA and *At*PVA failed to hydrolyze short-to-mid chain AHLs (C_4 till C_7 – HSL). However, incubation of long chain AHLs with pure PVA enzymes showed reduction in bioluminescence compared to heat-inactivated enzyme **(Table 5.2)**.

*At*PVA was observed to act on C_8 till C_{12}-HSL (25 μM), while *Pa*PVA showed activity on C_{10} and C_{12}-HSL. Although it appears that *Pa*PVA showed less reduction with C_8-HSL and substituted long chain AHLs, it is tricky to compare the results as the experimental conditions were different for the two enzymes. Nevertheless, it can be established that these PVAs exhibit the ability to act on long chain AHLs as substrates, with C_{10}-HSL and C_{12}-HSL probably being the most preferred subtrates for both enzymes **(Table 5.2)**. AHL acylases characterized from *P. aeruginosa* (Krzeslak et al. 2007) and AhlM from *Streptomyces* sp. (Park et al. 2005) have been observed to have a similar substrate spectrum, acting only on long chain (C_{10}-C_{14} HSLs) and not on short chain AHLs. The *Ralstonia* AHL acylase also showed activity on 3-oxo-C_8 till C_{12}-HSLs, and feeble activity on 3-oxo-C_6-HSL (Lin et al. 2003). On the other hand, certain acylases show better activity on short chain AHLs; porcine kidney acylase acts on C_4-HSL and C_8-HSL (Xu et al. 2003), while *Kc*PGA acts on C_6 and 3-oxo-C_6-HSL (Mukherji et al. 2014).

Table 5.2. Specificity of purified *At*PVA and *Pa*PVA for different AHL substrates. Remaining AHLs after degradation assay were detected by suitable lux-based biosensor at 30°C for 12h. Bioluminescence (%RLU) is expressed relative to heat-inactivated enzyme (taken as 100%).

AHL substrate	*At*PVA	*Pa*PVA
C_4-HSL	116.3 ± 12.3	119.6 ± 19.3
C_6-HSL	81.3 ± 17.9	116.3 ± 19.6
C_7-HSL	91.1 ± 25.7	128.0 ± 21.6
C_8-HSL	45.3 ± 15.1	116.7 ± 13.8
3-oxo-C_8-HSL	90.2 ± 15.3	119.1 ± 12.0
C_{10}-HSL	8.6 ± 1.1	10.0 ± 1.4
3-oxo-C_{10}-HSL	9.2 ± 5.0	102.6 ± 1.2
C_{12}-HSL	4.3 ± 1.3	10.4 ± 6.3
3-oxo-C_{12}-HSL	6.0 ± 2.2	61.2 ± 17.2
3-OH-C_{12}-HSL	39.5 ± 8.1	28.9 ± 7.8

To confirm the acylase activity of the PVA enzymes on AHLs, the degradation of C_{10}-HSL was monitored by HPLC analysis. C_{10}-HSL was detected as a specific peak with retention time 17.8 min. Both *At*PVA and *Pa*PVA caused a significant reduction in the C_{10}-HSL concentration after 4h incubation with the substrate. Detection of the reaction products was also performed, through dansylation of the free amine of released HSL and derivatization of decanoic acid by BrMMC. HPLC analysis showed the presence of dansylated HSL and specific peak for BrMMC-decanoic acid with retention times 16.4 min and 14.7 min, respectively. Appearance of these peaks in the 4h sample clearly indicates the acylase activity PVAs on C_{10}-HSL **(Fig. 5.6)**.

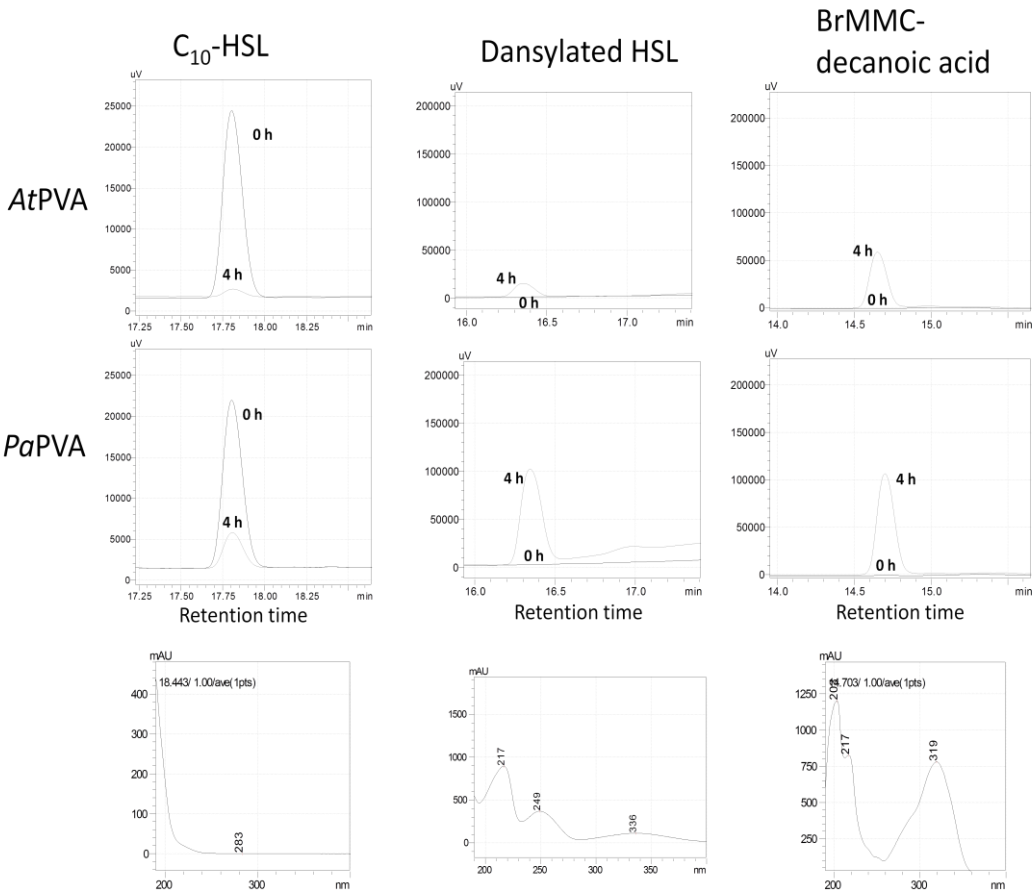

Fig. 5.6. HPLC analysis of residual C_{10}-HSL and released HSL and decanoic acid, for *At*PVA (upper panels) and *Pa*PVA (middle panels) after 4h incubation with C_{10}-HSL at 25 C. Reduction of C_{10}-HSL levels was corroborated with the occurence of free HSL and decanoic acid, confirming the acylase activity of PVAs on C_{10}-HSL. The lower panels show spectra of C_{10}-HSL, dansylated HSL and BrMMC-decanoic acid.

5.3.4. Kinetics of AHL degradation:

The extent of activity of PVAs on AHL substrates was studied using kinetic analysis with 3-oxo-C_{12}-HSL. This molecule was chosen as a representative substrate, as it is one of the well-studied signal molecules produced by *Pseudomonas aeruginosa* and has significant clinical relevance (Cooley et al. 2010; Mayiri et al. 2006). Besides, very few studies on kinetic data are available for acylases active on AHLs for comparison. Kinetic studies using the AHL acylase PA0305 from *P. aeruginosa* with C_8-HSL and 3-oxo-C_{12}-HSL as substrates showed that the enzyme is active on these AHLs with k_{cat}/K_mvalues of $0.14x10^4$ $M^{-1}s^{-1}$ and $7.8x10^4$ $M^{-1}s^{-1}$, respectively (Wahjudi et al. 2011). On the other hand, the penicillin G acylase from *Kluyvera citrophila* (*Kc*PGA) was active on C_6-HSL and 3-oxo-C_6-HSL with catalytic efficiency of $0.65x10^3$ $M^{-1}s^{-1}$ and $0.1x10^3$ $M^{-1}s^{-1}$, respectively (Mukherji et al. 2014).

In constrast with the bioluminescence method that uses biosensor strains to detect the degradation of AHLs, the fluorescence-based assay used for kinetic analysis estimates the amount of HSL released during the reaction. This is achieved by quantifying the fluorescent derivative formed by reacting the free amine of HSL with o-pthalaldehyde (OPA) reagent. HPLC and spectroscopic methods can thus be reasoned to be more precise and accurate due to the direct measurement of reaction product, while the biosensor approach is better suited for initial screening. *At*PVA showed better quenching of bioluminescence (94% reduction vs 39% for *Pa*PVA). However, during kinetic analysis, *Pa*PVA (18.9 μmol/min/mg) was observed to exhibit 6-fold higher activity over *At*PVA (4.0 μmol/min/mg) with 0.2 mM 3-oxo-C12-HSL as substrate. This result corroborates with the fact that *Pa*PVA also shows higher specific activity than *At*PVA with Pen V as substrate (Chapter 2).

*At*PVA and *Pa*PVA showed sigmoid v/[S] curves with increasing concentrations of 3-oxo-C_{12}HSL, indicating allosteric behaviour. This was also the case with Pen V as substrate, where both the enzymes show cooperativity and substrate inhibition. In the case of 3-oxo-C_{12}-HSL as substrate, saturation could not be achieved for both the enzymes as the low solubility of AHLs in aqueous buffer did not permit rate measurements at concentrations higher than 0.25 mM. A reasonable estimate of values for kinetic parameters could be calculated by applying initial values as

constraints to the allosteric sigmoidal equation. *Pa*PVA exhibited a slightly lower $K_{0.5}$, and a significantly higher Vmax compared to *At*PVA **(Fig. 5.7)**. The k_{cat}/K_m values for *Pa*PVA and *At*PVA were calculated to be $13.5x10^4$ and $2.7x10^4$ $M^{-1}s^{-1}$ respectively, which were comparable to the available value for PA0305 acylase ($7.8x10^4$ $M^{-1}s^{-1}$) with 3-oxo-C12-HSL as substrate (Wahjudi et al. 2011).

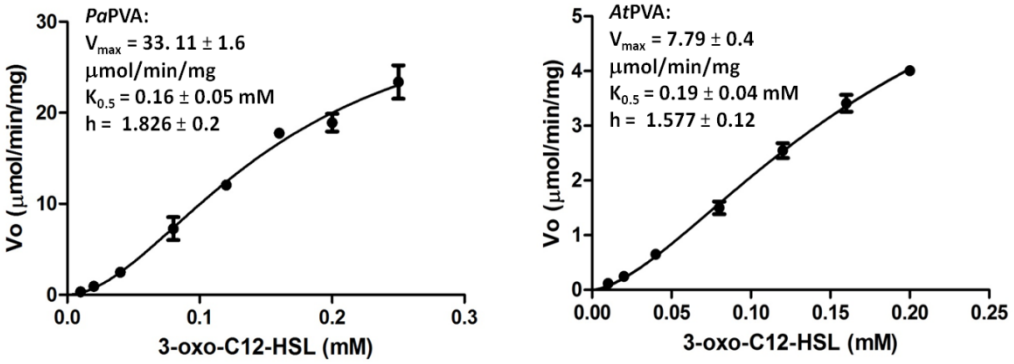

(a) **(b)**

Fig. 5.7. v/[S] curves for (a) *Pa*PVA and (b) *At*PVA showing allosteric (sigmoid) kinetic behaviour with 3-oxo-C_{12}-HSL as substrate.

5.3.5. Binding of long chain AHLs to PVAs:

Docking studies were performed to understand the structural interactions responsible for the selective activity of PVAs on long chain AHLs. The mode of binding was identical in both PVAs; the results for *Pa*PVA have been explained since it exhibited higher specific activity with 3-oxo-C_{12}-HSL (above). All the three AHLs analyzed (C_6-HSL, C_{10}-HSL and 3-oxo-C_{12}-HSL) were observed to bind to the active site in a similar orientation. However, the extent of interaction of active site residues with the substrate molecule and binding energy for favourable substrate binding seemed to increase with the increase in length of acyl chain of the AHL molecule.

The lactone ring was housed in the same pocket where the β-lactam moiety was bound in the case of Pen V, with N271 involved in hydrogen bonding with the NH group of the amide bond. The acyl chain fits into a hydrophobic pocket lined primarily by residues W23, W87, L88 and A147. Due to the longer nature of their acyl chain, C_{10}-HSL and 3-oxo-C_{12}-HSL were observed to be involved in more number of hydrophobic interactions **(Fig. 5.8)**, interacting with residues in the loop2

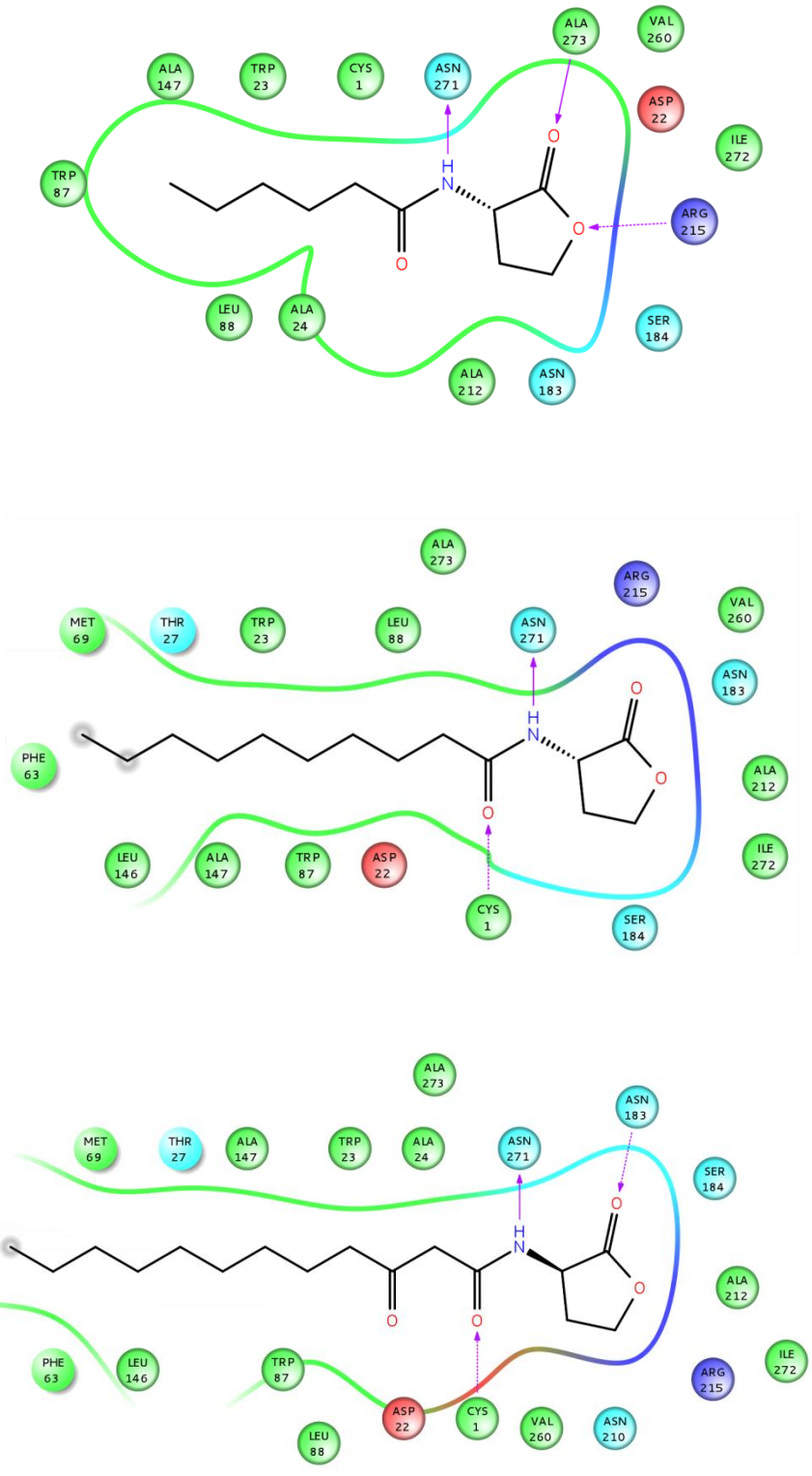

Fig. 5.8. Ligand interaction diagrams (4 Å cutoff) of (upper) C6-HSL, (middle) C10-HSL and (lower) 3-oxo-C12-HSL with *Pa*PVA. [Colour scheme: green – hydrophobic residues, red – acidic residues, blue – basic residues, cyan – polar residues, solid arrows – backbone hydrogen bonds, dotted arrows – side chain hydrogen bonds].

(61-74) and loop3 (137-148) regions in *Pa*PVA. The residues F68, M69 and L146 form additional interactions with the hydrophobic acyl chain of the substrate, probably enhancing the strength of binding and orienting the AHL molecule in the active site. The distance of the amide bond from the nucleophilic cys residue is also favourable for activity. Docking with C_6-HSL showed a lower Glidescore, and a farther distance of the carbonyl carbon of the amide bond from the N-terminal cysteine than in long chain AHLs **(Table 5.3)**. Bioluminescence assays and kinetic analyses have also shown that PVAs are more effective towards long chain AHLs. It can be inferred that the presence of extended acyl chain probably leads to increased and better interactions with the residues in the hydrophobic pocket, thus allowing for favourable binding and better AHL degradation activity (**Fig. 5.9)**.

Table 5.3. Properties of different AHL substrates and results of docking with *Pa*PVA structure (AlogP = hydrophobicity, SA = surface area, Nadist = Nucleophilic attack distance between SH group of cys1 and carbonyl carbon atom of AHL).

Ligand (AHL)	MW	AlogP	Polar SA	Rotatable bonds	H-bond donors	H-bond acceptors	Glidescore	Nadist (Å)
C_6	199.3	1.133	55.4	6	1	3	-6.46	5.19
C_{10}	255.4	2.958	55.4	10	1	3	-6.22	4.7
3-oxo-C_{12}	297.4	2.729	72.5	12	1	4	-7.213	4.76

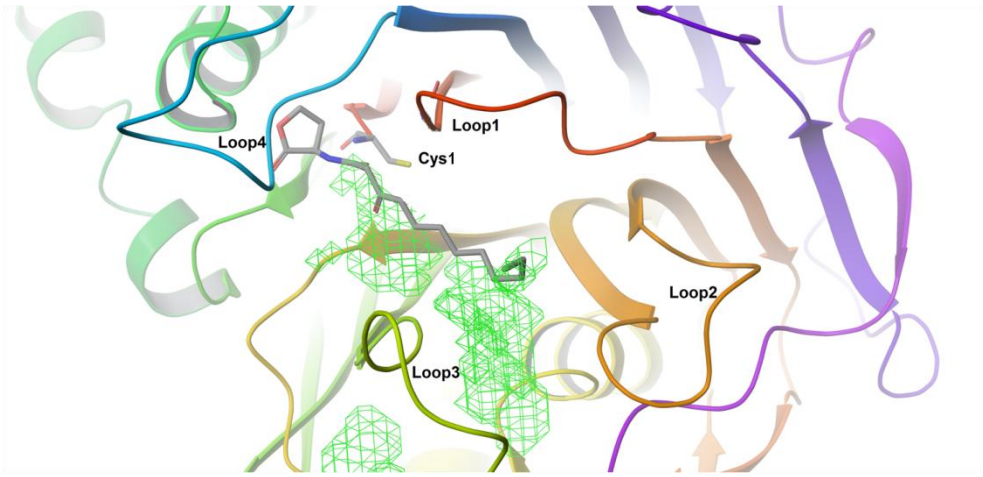

Fig. 5.9. Mode of binding of 3-oxo-C_{12}-HSL in the binding site pocket of *Pa*PVA. The hydrophobic pocket in which the alkyl side chain fits is shown as green mesh.

5.3.6. Significance of AHL degradation by PVAs:

The ability of enzymes to hydrolyze AHLs has gained traction in recent years as an efficient way of quorum quenching, which can be exploited to develop new antibacterials (Dong et al. 2007). Over the last decade, a growing number of acylases active on AHL signal molecules involved in quorum sensing have been characterized (Chen et al. 2013); these enzymes share significant sequence and structural homology with penicillin and cephalosporin acylases. Recently, these enzymes have also been observed to cross-react with each other's substrates. In this study, the activity of penicillin V acylases from Gram-negative bacteria on different AHL molecules has been demonstrated.

Torres-Bacete et al. (2015) have claimed that the acylase from *Streptomyces lavendulae*, which is active on Pen V, could hydrolyze AHLs. However, *Sl*PVA shows better activity and specificity towards penicillins with aliphatic side chains like octanoyl penicillin (Pen K). It has a heterodimeric subunit composition, similar to AHL acylases and PGAs and shares significant sequence similarity with these enzymes. Moreover, *Sl*PVA is thought to possess a long hydrophobic pocket capable of accommodating alkyl chains, similar to the AHL acylase PvdQ (Torres-Bacete et al. 2015; Bokhove et al. 2010). Another penicillin acylase that degrades AHLs, *Kc*PGA, has also been shown to possess a hydrophobic pocket where the fatty acid chain of C6-HSL is housed during binding and activity (Mukherji et al. 2014). In contrast, bacterial PVAs are usually homotetramers and share low sequence homology (<20%) with PGAs and AHL acylases. In this context, it is significant that these PVAs can also participate in AHL hydrolysis. Moreover, PVAs characterized in this study showed catalytic efficiency (k_{cat}/K_m) comparable to AHL acylase PA0305 from *P. aeruginosa.* Considering their structural similarity, it might be safe to assume that other cholylglycine hydrolases (PVAs from Gram-positive bacteria and BSHs) could also degrade AHLs to some degree.

AHL-dependent quorum sensing systems have now been studied in various Gram-negative bacteria (Gera and Srivastava 2006), and are known to play a major role in regulating virulence and many other metabolic processes. Although AHLs are related by structure, they can differ in the length of their acyl side chain. Different bacteria produce different individual AHLs; likewise, many bacterial species can

also produce more than one type of AHL. Enzymes able to degrade AHLs have been thought to be involved in AHL turnover in the environment, to either use them as carbon sources or recycle them to synthesize new AHLs (Roche et al. 2004). It has also been hypothesized that AHL-degrading enzymes could actively interfere with quorum sensing mechanisms of other bacteria in microbial communities and biofilms, thus giving a competitive edge to the bacteria producing these enzymes. Certain AHL-degrading enzymes have been characterized from AHL-producing bacteria themselves; the role of such enzymes in modulating the concentration of AHLs in the cell to control quorum sensing-dependent phenotypes cannot be discounted (Roche et al. 2004).

The knowledge of AHL-hydrolysis activity of PVAs adds a new facet to the fascinating interplay between quorum sensing and quorum quenching in bacteria. PVAs from Gram-negative bacteria show allosteric behaviour in degrading AHLs, which has not been reported so far in any acylase acting on AHLs. The phenonmenon of positive cooperativity has been perceived to amplify the sensitivity of the enzyme to small changes in substrate concentration, thereby providing a metabolic advantage (Koshland and Hamadani 2002). Although *in vitro* kinetic analyses may not reflect the titres of enzymes or AHLs in the natural environment, it could be speculated that the allosteric nature of PVAs from Gram-negative bacteria (coupled with the periplasmic location of these enzymes) indicates a prominent role in influencing AHL turnover in the environment. It is also possible that PVAs might also be involved in other functions beside AHL degradation. The AHL acylase PvdQ, for instance, is involved in pyoverdine biosynthesis in *P. aeruginosa* (Huang et al. 2003). Careful analyses of PVA knockout mutants through proteomics and metabolomics methods could provide interesting insights into the relevance of PVAs in quorum sensing and microbial physiology.

Chapter 6

Application of immobilized penicillin V acylase system for 6-APA production

6.1. Introduction:

Penicillin acylases have been used in the pharmaceutical industry since their discovery for the production of 6-APA and semi-synthetic antibiotics. Beta-lactam antibiotics (penicillins and cephalosporins) make up over 65% of the world market for antibiotics (Elander 2003). Significant advances have occurred in the last two decades, in the use of enzymes as a greener and inexpensive approach (Chandel et al. 2008) to meet the requirements for bulk antibiotic production. PGA produced by *E. coli* has been employed extensively to produce 6-APA (Maresova et al. 2014) and semi-synthetic antibiotics including ampicillin, amoxicillin, cephalothin and so on. Strain improvement, media optimization techniques and the use of thermostable PGAs (*Alcaligenes faecalis*, Verhaert et al. 1997) have helped enhance the efficiency of application of penicillin acylases in the pharmaceutical industry. In addition, PGAs have also been applied in peptide synthesis and resolution of racemic mixtures (Arroyo et al. 2003).

On the other hand the use of PVAs in the production of 6-APA has been very limited, probably owing to the slightly higher cost of Pen V substrate and the non-availability of highly active enzymes so far. Nevertheless, some authors have emphasized the advantages of using a Pen V-PVA system for 6-APA production (Shewale and Sudhakaran 1997). Pen V has greater stability in aqueous solutions, especially at lower pH required for extraction. PVAs also possess higher activity in acidic pH range and show better conversion efficiency at higher substrate concentrations. These characteristics emphasize the need for increased application of PVAs in the industry. Presently, most of the 6-APA is produced using PGAs, and the Pen V – PVA system only accounts for 10-15% of the total 6-APA production.

For industrial applications, free enzymes or whole cells are usually immobilized on various supports. Enzymes and cells can be immobilized through a variety of techniques (Matiasson 1983) including adsorption, encapsulation and covalent cross-linking. Different supports such as alginate, chitosan, polyvinyl alcohol, mesoporous silica, ion-exchange resins and so on, have been applied for immobilizing cells or enzymes. The alginate – $CaCl_2$ system has been one of the most widely used and mild, inexpensive technique for the immobilization of living cells and enzymes (Zhou et al. 2010). Immobilization protects the enzymes from changes in process

conditions such as pH, temperature and mechanical shear, and enhances their stability (Sheldon 2007). Immobilized enzymes and cells can also be reused a number of times with minimal damage to their conversion efficiency. Other techniques such as cell permeabilization and cross-linking with glutaraldehyde or polyethylene imine (PEI) serve to further enhance the activity and stability of the enzymes (Felix 1982, Prabhune et al. 1992).

While a plethora of immobilized PGA systems and better downstream processing steps have been developed over the years, not much advances have been associated with the application of PVA-Pen V system in the industry. This chapter details the attempts to immobilize the recombinant *E. coli* cells producing *Pa*PVA and develop this system for maximum conversion of Pen V to 6-APA.

6.2. Materials and methods:

6.2.1. Materials:

Sodium alginate and media components were procured from HiMedia, India. Penicillin V (potassium salt) was a gift from Sparsh Biotech, Ahmedabad (India). Cetyltrimethyl ammonium bromide (CTAB) was obtained from Qualigens, India and all other chemicals were of analytical or HPLC grade.

6.2.2. Cloning and expression of *Pa*PVA enzyme:

The *pva* gene from *P. atrosepticum* was cloned into a pET28b plasmid vector between NcoI and XhoI restriction sites. The PVA enzyme was expressed in *E. coli* BL21 star cells with a C-terminal His-tag as described in Chapter 2.

6.2.3. Cultivation of *E. coli* – *Pa*PVA cells:

For maximum production of biomass, the cells were cultivated in Studier's (2005) auto-induction medium ZYM-5052. After 4 h incubation at 37°C (OD_{600} ~ 1.0), the culture was transferred to 27°C for 18 h. The resultant biomass was harvested by centrifugation and washed with phosphate buffered saline (PBS) pH 7.2.

6.2.4. PVA activity assay and biotransformation:

Pen V hydrolysis activity was estimated by studying the formation of Schiff's conjugate with the product 6-APA and p-dimethyl amino benzaldehyde (Shewale et al. 1987). One unit (IU) of enzyme activity was defined as the amount of enzyme producing 1 μmol 6-APA in 1 min under standard conditions (pH 5, 45°C). The biotransformation was carried out in a lab-scale bioreactor, with a double-jacketed vessel connected to a water bath, with 20mg free cells or corresponding amount of beads in 50 ml of Pen V (2% w/v).

6.2.5. Permeabilization of *E. coli – Pa*PVA cells:

*E. coli – Pa*PVA cells were permeabilized using 0.1% (w/v) cetyl triethyl ammonium bromide (CTAB) detergent (20 mg wet cells/ml) with a treatment time of 15 min at 25°C. The cells were then washed twice with distilled water to remove excess CTAB.

6.2.6. Immobilization of *E. coli – Pa*PVA cells:

Freshly harvested cells from 50 ml overnight culture were permeabilized with CTAB, and added (550 mg wet weight) to appropriate volume of 2% (w/v) sodium alginate. The suspension was extruded dropwise through a thin needle into ice-cold solution of 0.2 M $CaCl_2.2H_2O$ while stirring gently. The calcium alginate beads formed (1.5-2 mm diameter) were allowed to harden in the same solution for 1h and stored in $CaCl_2$ solution at 4°C for 18h. The beads were washed with distilled water and treated with 0.2% (w/v) glutaraldehyde for 30 min, giving a cell loading of 10% w/w (wet cell mass/ weight of beads). They were then washed thoroughly with distilled water and stored in 50mM $CaCl_2$ at 4°C, for use in the biotransformation reaction.

6. 2.7. Optimization of reaction parameters:

In separate experiments, the biotransformation of penicillin V to 6-APA was carried out using different specified temperatures, pH values, biocatalyst concentration, and the initial substrate concentration to optimize the reaction parameters to achieve maximum conversion efficiency. Biotransformation was carried out using 5 g alginate beads (with a cell loading of 100 mg/g beads) in 50 ml of Pen V with

constant stirring at 200 rpm. Aliquots (0.5 ml) were withdrawn at regular time intervals and amount of 6-APA was determined.

6.2.8. Stability and Recyclability of the immobilized system:

The storage stability of alginate beads with immobilized cells was estimated by determining the conversion of Pen V to 6-APA after different time intervals. Beads (5g, with 0.5 g wet cell weight) were either stored wet in 50 mM $CaCl_2$ solution at 4°C or dried to constant weight at room temperature and stored dry. The reusability of the immobilized system was assessed by carrying out the hydrolysis of 4 % (w/v) Pen V (in 0.1 M acetate buffer pH 5) at 35°C. After each cycle of hydrolysis (1 h), the solution with the reaction products was removed; the beads were taken out and re-hardened in 0.2M $CaCl_2$ for 1 h. The next cycle was then started with fresh substrate. 6-APA yield was calculated for each cycle.

6.3. Results and Discussion:

6.3.1. Cultivation of *E. coli* – *Pa*PVA:

As described in Chapter 2, *Pa*PVA has been expressed in *E. coli* with high protein yields over 250 mg/l on LB supplemented with kanamycin. To further enhance the cell mass and enzyme productivity, *E. coli* – *Pa*PVA was grown in Studier's (2005) auto-induction media (AIM, ZYM-5052).

Table 6.1. Enzyme productivity of *E. coli* – *Pa*PVA on different media.

Medium	Kanamycin (μg/ml)	IPTG (mM)	Incubation time (h)	PVA Activity (IU/g)	Cell mass (g/L)	Productivity (IU/L)
LB	35	0.2	24	1959	9.2	18023
			48	1393	8.6	11910
Terrific broth	100	0.2	24	1879	17.0	31849
			48	2015	17.4	35061
AIM	100	-	24	2511	20.7	51852
			48	2697	19.2	51782

AIM provides a better supply of nutrients and microelements for the bacteria to grow, resulting in higher cell densities. In addition, the presence of lactose negates the need for use of IPTG to induce recombinant protein production. In the case of *Pa*PVA, growth in AIM provided a cell mass of 20.7 g/l with 51852 IU/L enzyme productivity within 24 h **(Table 6.1)**. This could be easily scaled up using a fermentor and high aeration rates for application of recombinant *Pa*PVA enzyme in the pharmaceutical industry.

6.3.2. Permeabilization of *E. coli* – *Pa*PVA cells:

The use of whole cells for biotransformation circumvents the problem of purification and provides a more favourable environment for the enzymes to function (Babu and Panda 1991). Additionally, immobilization of cells could facilitate product separation and also make the cells recyclable, thus simplifying the process and lowering the cost of production. However, it also suffers from the disadvantage of relatively lower activity compared to free enzymes, as a result of reduced diffusion of reactants or products through the cell membrane (Wang et al. 2012). Permeabilization involves the use of chemical agents to slightly weaken the membrane, thereby alleviating this problem (Felix 1982).

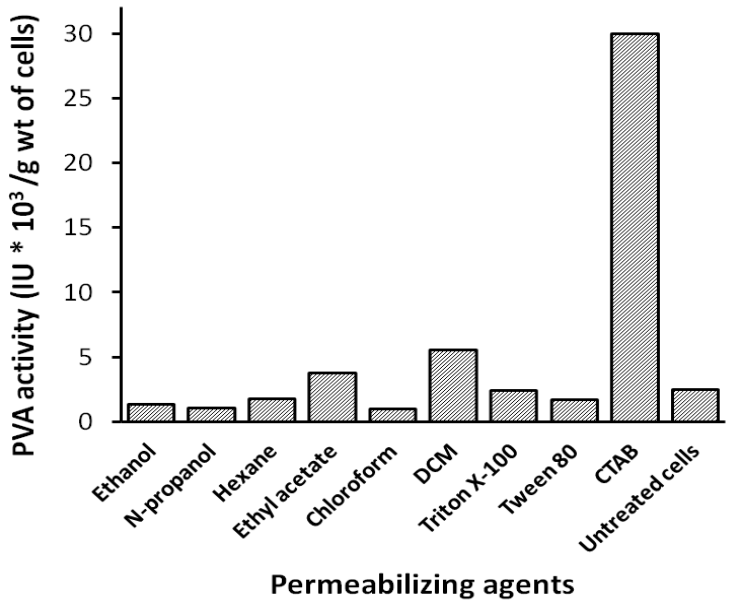

Fig. 6.1. Cell-bound PVA activity of *E. coli* – *Pa*PVA cells permeabilized with different detergents (0.1% w/v) or organic solvents (1ml/20 mg cells) for 15 min.

In this study, a variety of detergents and solvents were explored for the permeabilization of *E. coli* cells expressing *Pa*PVA. Cationic detergent CTAB significantly increased in the cell bound PVA activity by 14.4 fold, while certain solvents like dichloromethane and ethylacetate showed a moderate increase in PVA activity **(Fig. 6.1)**. Kumar et al. (2008) have reported the enhancement of cell-bound PVA activity in yeast *Rhodotorula aurantiaca* using CTAB. Many other studies (Prabhune et al. 1992, Nagalakshmi and Pai 1994, Norouzian et al. 2002, Cheng et al. 2006) have identified CTAB as a mild but potent permeabilizing agent for enhancing PGA activity in *E. coli*. The free permeabilized *E.coli – Pa*PVA cells exhibited 36,700 IU/g cell bound activity on treatment with 0.1% (w/v) CTAB for 15 min.

6.3.3. Encapsulation of *E. coli – Pa*PVA cells in alginate:

While there has been a perennial interest in the immobilization of PGA as pure enzyme or cells (Cheng et al. 2006), there are very few reports of PVA based immobilized enzyme systems. Initial commercial preparations that have been employed in the industry include Novozyme 217 (Gestrelius 1982, Karlsen and Villadsen 1984) and Semacylase (Mollgaard 1987, Mollgaard and Karlsen 1988) by Novo Industri, Denmark. Sudhakaran and Shewale (1993) have immobilized the partially purified PVA enzyme from *Fusarium* sp. SKF 235 on a cation exchange resin (Amberlite CG-50) with a specific activity of 250-280 IU/g beads. Another study (Torres-Bacete et al. 2000) details the covalent immobilization of PVA from *Streptomyces lavendulae* on Eupergit C epoxy-activated acrylic beads.

However, the application of immobilized PVA is scarce probably owing to the higher substrate costs and non-availabilty of high activity enzyme preparations. The development of a commercial PVA/Pen V based enzyme process for 6-APA production has been stagnant over the last decade. This study was an attempt to develop an immobilized system using *E. coli – Pa*PVA cells as a preliminary step for industrial application of this enzyme. The elevated specific activity of *Pa*PVA and high recombinant enzyme yields make it an attractive proposition for its industrial use. Initial trials were made to immobilize the extracted and purified enzyme by covalent cross-linking with glutaraldehyde to form cross-linked enzyme aggregates, or with epoxy polymer beads (DILbeads, Fermenta Biotech, Thane, India). Such

attempts suffered from low recovery of enzyme activity (<10%) and reduction in enzyme stability. Hence, the encapsulation of whole cells was preferred. *E. coli – Pa*PVA whole cells were permeabilized by treatment with CTAB and encapsulated in 2% calcium alginate hydrogel for biotransformation **(Fig. 6.2)**. Further, the cells were cross-linked with 0.2% (w/v) glutaraldehyde for 30 min. Glutaraldehye treatment has been reported to enhance the stability of the immobilized cell system by preventing enzyme leakage (Prabhune et al. 1992, Cheng et al. 2006).

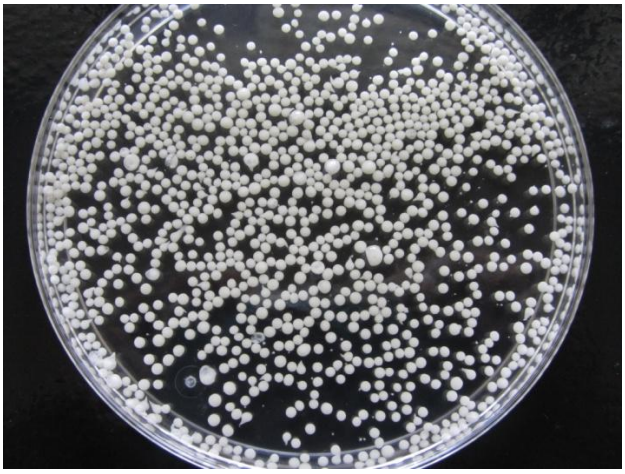

Fig. 6.2. Calcium alginate beads with encapsulated *E. coli – Pa*PVA cells.

Comparative biotransformation studies with 2% (w/v) Pen V showed that permeabilized free cells gave a faster initial reaction rate and consequently a higher yield of 6-APA after reaction for 40 min as against immobilized preparation **(Fig. 6.3)**. This might be attributed to (i) lower transfer rate of substrate and product inside and out of the immobilized cells through the alginate matrix, or (ii) hydrophilic nature of alginate leading to a lower concentration of hydrophobic Pen V surrounding the immobilized cells. However, both free and immobilized cells achieved full conversion at the end of 60 min. There was a gradual decline in 6-APA yield after 60 min in the case of free cells and 90 min with immobilized cells (data not shown), possibly due to decomposition of the product.

In spite of lower initial reaction rate and slightly longer reaction time, immobilized cells could also achieve maximum yield of 6-APA equal to that of free cells. In view of their potential for reuse and better stability, immobilized cells can be generally used efficiently for the biotransformation process (Prabhune et al. 1992; Cheng et al. 2006).

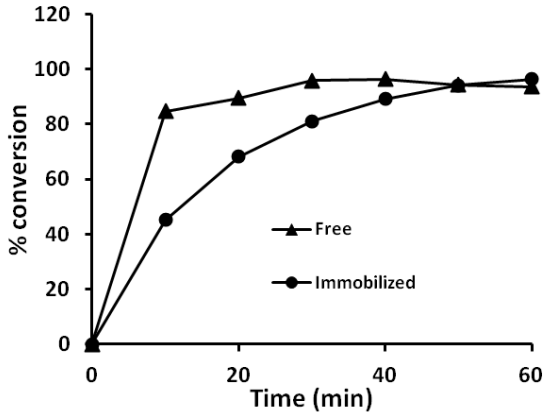

Fig. 6.3. Conversion of Pen V (2% w/v) to 6-APA by permeabilized free cells (*E. coli* – *Pa*PVA) and cells immobilized in alginate beads.

6.3.4. Effect of reaction parameters:

Both free and immobilized cells showed an optimum pH of 4 and optimum temperature of 45°C for maximum initial activity **(Fig. 6.4)**. Immobilized cells showed better activity over a wider pH and temperature range compared to free cells. However, biotransformation reaction for a longer period of time under the determined optimal conditions showed lower conversion and reduction in 6-APA yield, possibly as a result of weakening of beads or inactivation of cells. Therefore, milder conditions of pH 5 and temperature 35°C were selected for the biotransformation reaction.

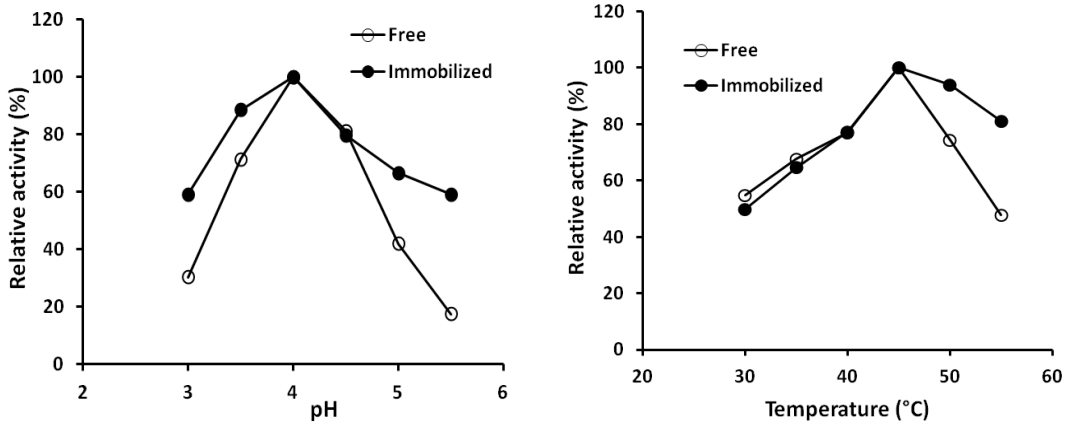

Fig. 6.4. Relative initial activity of free and immobilized *Pa*PVA – *E. coli* cells at increasing pH and temperature. Initial enzyme activity was measured after 5 min reaction.

The cell loading was optimum at 10% (w/w), with 5g of beads containing 0.5 g wet cell weight used for each reaction. Higher cell concentrations did not hasten the conversion, presumably due to mass transfer limitations.

The initial Pen V concentration was varied from 2-8% (w/v). The fresh weight concentration of the immobilized cells was set at 10% (w/w), and the reaction was carried out at 35°C and pH 5 for a period of 90 min. Substrate conversion profiles **(Fig. 6.5)** showed that almost complete conversion to 6-APA (97-100%) could be achieved till a concentration of 4% Pen V in 60 min. Further increase in initial substrate concentration progressively slowed the reaction, leading to a reduction in conversion. This could possibly be caused by the occurence of substrate inhibition in *Pa*PVA enzyme (explored in Chapter 2) or inhibition by the product 6-APA (Gestrelius et al. 1983). Substrate and product inhibition has been documented even in the case of immobilized penicillin G acylases (Prabhune et al. 2002; Cheng et al. 2006). Sudhakaran and Shewale (1993) have also reported an optimum concentration of 4% (w/v) Pen V for the production of 6-APA. Regardless of inhibition, it is significant that the immobilized cells were able to achieve full conversion of 4% (w/v) Pen V within 60 min, which was better than earlier reports on PVA (Sudhakaran and Shewale 1993; Gestrelius et al. 1983; Singh et al. 1988). In addition, the enhanced activity of *Pa*PVA and high expression yields could help reduce the amount of biocatalyst required to scale up the process.

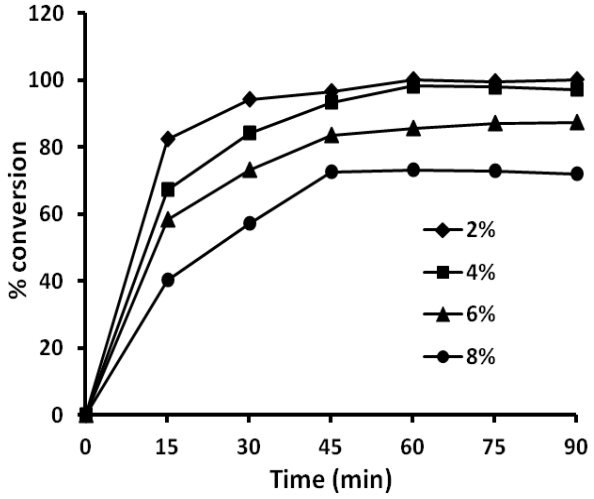

Fig. 6.5. Conversion of Pen V to 6-APA by immobilized *Pa*PVA – *E. coli* cells at increasing initial concentrations (% w/v) of Pen V.

6.3.5. Storage and recyclability of immobilized system:

The immobilized cells showed good storage stability when stored in 50 mM $CaCl_2$ at 4°C, effecting 80% conversion to 6-APA in 60 min even after 28 days **(Fig. 6.6)**. When the beads were dried, their weight decreased to 0.2g from 5g initial weight; however, they re-swelled to 2g in water. Although drying reduced the enzyme activity to 50% conversion in 60 min, the dried beads could be stored at room temperature for longer time periods without further loss of activity **(Fig. 6.6)**.

The recyclability of the immobilized cell system was rather low, as a set of beads could only be used for three cycles (1h each) before they became weak and started to disintegrate . This probably happens due to the action of the monovalent cations (Na, K) from the acetate buffer and Pen V (potassium salt), that are known to compete with calcium ions for guluronic acid binding sites and gradually weaken the alginate gel structure (LeRoux et al. 1999). Re-hardening of the beads in 0.2M $CaCl_2$ solution for 1h between cycles helped to an extent in retaining the activity and integrity of the immobilized cell system for at least 10 cycles (75% conversion to 6-APA).

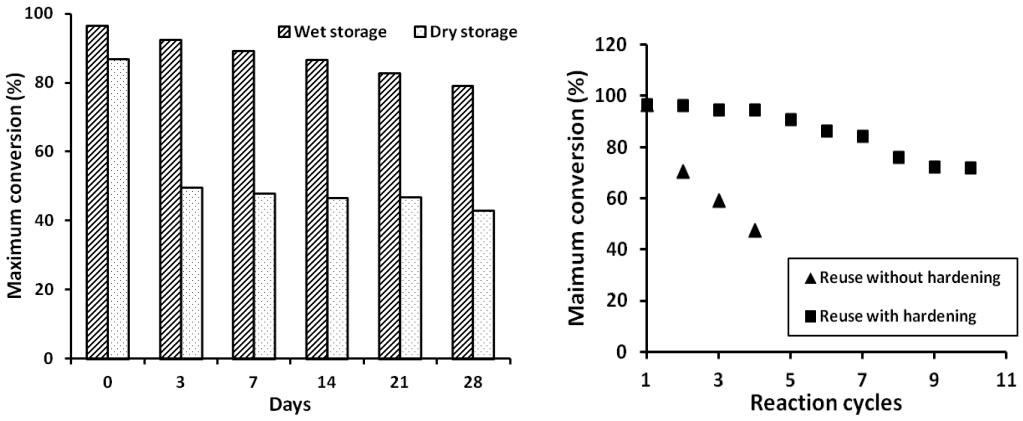

Fig. 6.6. (a) Storage stability of wet beads (4°C) and dry beads (room temperature, 25 °C) containing *Pa*PVA – *E. coli* cells. (b) Recyclability of immobilized PaPVA – *E. coli* cells without hardening, and hardening in 0.2M $CaCl_2$ for 1h after each cycle.

Torres-Bacete et al. (2000) have reported the use of immobilized *Sl*PVA for 50 consecutive batch reactions, while the immobilized PVA from *Fusarium* sp. could be used for 68 consecutive cycles with average 85% conversion (Sudhakaran and Shewale 1993). Although low recyclability of *E. coli* – *Pa*PVA immobilized on

alginate compared to other PVA-based systems is a concern, it is highly probable that the use of stronger supports based on synthetic polymers like the polyvinyl alcohol-based Lentikats® (Cardenas-Fernandez et al. 2012) could improve the potential for reuse. Nevertheless, it should be emphasized that *Pa*PVA boasts of the maximum specific activity among reported PVA enzymes, and the use of recombinant *E. coli* gives high enzyme productivity. Further, protein engineering strategies could pave a way to understand and circumvent the substrate and product inhibition mechanisms slowing down the reaction. These factors, along with the results presented in this study, make a convincing argument for the industrial applicability of the *Pa*PVA based immobilized system as a viable economical alternative for the production of the active pharmaceutical intermediate 6-APA from penicillin V.

Summary and future prospects

The family of Ntn hydrolases includes an assortment of structurally related enzymes that exhibit acylase/amidase activity on a wide range of substrates. Two penicillin V acylases belonging to this family have been studied in this thesis. Biochemical, structural and computational analyses were used to explore the activity and substrate specificity of these enzymes.

In addition their significant footprint in the pharmaceutical industry, penicillin acylases also possess intriguing catalytic and structural characteristics that make them appealing to study. The PVAs from Gram-negative bacteria (*Pa*PVA and *At*PVA) characterized in this work were observed to display considerably enhanced activity and specificity on Pen V over reported PVAs, with unique kinetic behaviour showing cooperativity and substrate inhibition. Expression of these enzymes in *E. coli* gave significant protein yields, making them very promising systems to develop for industrial applications. Immobilization and biotransformation trials were attempted in this direction with recombinant *E. coli – Pa*PVA. The structure of PVAs from Gram-negative bacteria also displayed unique differences in oligomer interactions and active site residues compared to their counterparts from Gram-positive bacteria. The crucial roles of two tryptophan residues in the active site involved in substrate binding were established in the study. Aromatic stacking interactions between these residues and the phenyl ring of Pen V play a significant part in orienting the Pen V molecule in the active site for maximum activity.

The role of penicillin acylases in the natural environment has remained largely unexplored till recent years. In this study, the ability of PVAs to hydrolyze acylhomoserine lactones (AHLs) involved in bacterial signaling has been established. The addition of PVA to the increasing number of enzymes involved in AHL degradation presents new avenues for use in quorum quenching applications.

The results from this study demonstrate the fascinating nature of PVAs from Gram-negative bacteria and provide new insights into their catalytic behaviour. Further exploration of these enzymes could provide a plethora of opportunities for protein engineering and development of better PVA-based systems for industrial 6-APA production. Moreover, a comprehensive proteomics and metabolomics-based approach would help further explore the place of penicillin acylases within the complex maze of microbial metabolic networks.

Bibliography

- Abuin, E., Lissi, E., Biasutti, M.A., Duarte, R. (2007) Kinetics of *p*-nitrophenyl acetate hydrolysis catalyzed by *Mucor javanicus* lipase in AOT reverse micellar solutions formulated in different organic solvents. *Protein J.* **26**, 475–9.
- Alkema, W.B.L., Dijkhuis, A.J., de Vries, E., Janssen, D.B. (2002) The role of hydrophobic active-site residues in substrate specificity and acyl transfer activity of penicillin acylase. *Eur. J. Biochem.* **269**, 2093-2100.
- Alkema, W.B.L., Hensgens, C.M.H., Kroezinga, E.H., de Vries, E., Floris, R., van der Laan, J.M., Dijkstra, B.W., Janssen, D.B. (2000) Characterization of the β-lactam binding site of penicillin acylase of *Escherichia coli* by structural and site-directed mutagenesis studies. *Prot. Eng.* **13**, 857-863.
- Allen, M.P. (2004) Introduction to molecular dynamics simulation. In Attig, N., Binder, K., Grubmüller, H., Kremer, K., (eds). Computational soft matter: from synthetic polymers to proteins, pp. 1–27, John von Neumann Institute for Computing, Jülich.
- Ambedkar, S.S., Deshpande, B.S., Sudhakaran, V.K., Shewale, J.G. (1991) *Beijerinckia indica* var penicillanicum penicillin V acylase - Enhanced enzyme production by catabolite repression-resistant mutant and effect of solvents on enzyme activity. *J. Ind. Microbiol.* **7**, 209-214.
- Arroyo, M., de la Mata, I., Acebal, C., Castillon, M.P. (2003) Biotechnological applications of penicillin acylases: state-of-the-art. *Appl. Microbiol. Biotechnol.* **60**, 507-514.
- Arroyo, M., Torres, R., de la Mata, I., Castillon, M.P., Acebal, C. Interaction of penicillin V acylase with organic solvents: catalytic activity modulation on the hydrolysis of penicillin V, *Enzyme Micro. Technol.* **25**,378-383.
- Arroyo, M., Torres-Guzman, R., de la Mata, I., Castillon, M.P., Acebal, C. (2000) Prediction of penicillin V acylase stability in water-organic co-solvent monophasic systems as a function of solvent composition. *Enzyme Micro Technol.* **27**, 122-126.
- Avinash, V.S., Ramasamy, S., Pundle, A.V., Suresh, C.G. (2015) Penicillin V acylase from Pectobacterium atrosepticum exhibits high specific activity and unique kinetics. *Int. J. Biol. Macromol.* **79,** 1-7.
- Babu, P.S.R., Panda, T. (1991) Studies on improved techniques for immobilizing and stabilizing penicillin amidase associated with *E. coli* cells. *Enzyme Microb. Technol.* **13**, 676–682.

- Bassler, B.L. (2002) Small talk. Cell-to-cell communication in bacteria. *Cell* **109**, 421-424.
- Batchelor, F.R., Doyle, F.P., Nayler, J.H.C., Rolinson, G.N. (1959) Synthesis of penicillin - 6-aminopenicillanic acid in penicillin fermentations. *Nature* **183**, 257-258.
- Becker, O.M., Watanabe, M., (2001). Dynamics methods. *In:* Becker, O.M., Mackarell, A.D., Jr., Roux, B., Watanabe, M., eds. Computational Biochemistry and Biophysics. Marcel Dekker, Inc., New York. pp 39-67.
- Bi, J., Fang, F., Lu, S., Du, G., Chen, J. (2013) New insight into the catalytic properties of bile salt hydrolase. *J Mol. Catal. B.* **96**, 46-51.
- Blow, D. (2002) Outline of Crystallography for Biologist. *Ed.*1. New York, Oxford University Press.
- Bogino, P.C., Nievas, F.L., Giordano, W. (2015) A review: Quorum sensing in *Bradyrhizobium. Appl. Soil Ecol.* **94**, 49-58.
- Bokhove, M., Jimenez, P.N., Quax, W.J., Dijkstra, B.W. (2010) The quorum-quenching N-acyl homoserine lactone acylase PvdQ is an Ntn-hydrolase with an unusual substrate-binding pocket. *Proc. Nat. Acad. Sci.* **107**, 686-691.
- Bokhove, M., Yoshida, H., Hensgens, C.M.H., van der Laan, J.M., Sutherland, J.D., Dijkstra, B.W. (2010) Structures of an Isopenicillin-N converting Ntn-Hydrolase reveal different catalytic roles for the active site residues of precursor and mature enzyme. *Structure* **18**, 301-308.
- Bompard-Gilles, C., Villeret, V., Davies, G.J., Fanuel, L., Joris, B., Frere, J.M., Van Beeumen, J. (2000) A new variant of the Ntn hydrolase fold revealed by the crystal structure of L-aminopeptidase D-Ala-esterase/amidase from Ochrobactrum anthropi. *Structure* **8**, 153-162.
- Bradford, M.M. (1976) A rapid and sensitive method for the quantification of microgram quantities of protein utilizing the principle of protein–dye binding. *Anal. Biochem*. **72**, 248-54.
- Brannigan, J.A., Dodson, G., Duggleby, H.J., Moody, P.C.E., Smith, J.L., Tomchick, D.R., Murzin, A.G. (1995) A protein catalytic framework with an N-terminal nucleophile is capable of self-activation. *Nature* **378**, 416-419.
- Brunger, A.T. **(**1992) Free R-value: a novel statistical quantity for assessing the accuracy of crystal-structures. *Nature* **355,** 472-475.
- Burley, S.K., Petsko, G.A. **(**1985) Aromatic-aromatic interaction: A mechanism of protein-structure stabilization. *Science* **229,** 23-28.
- Burley, S.K., Petsko, G.A. (1986) Amino-aromatic interactions in proteins. *FEBS* **203**, 139-143.

- Cai, G., Zhu, S.C., Yang, S., Zhao, G.P., Jiang, W.H. (2004) Cloning, overexpression, and characterization of a novel thermostable penicillin G acylase from *Achromobacter xylosoxidans*: Probing the molecular basis for its high thermostability. *Appl. Environ. Microbiol.* **70**, 2764-2770.
- Cao, L.Q., van Rantwijk, F., Sheldon, R.A. (2000) Cross-linked enzyme aggregates: A simple and effective method for the immobilization of penicillin acylase. *Org. Lett.* **2**, 1361-1364.
- Cardenas-Fernandez, M., Neto, W., Lopez, C., Alvaro, G., Tufvesson, P., Woodley, J.M. (2012) Immobilization of Escherichia coli containing ω-transaminase activity in LentiKats®. *Biotechnol. Prog.* **28**, 693‑698.
- Carlsen, F., Emborg, C. (1981) *Bacillus sphaericus* V-penicillin acylase. I. fermentation. *Biotechnol. Lett.* **3**, 375-378.
- Chandel, A.K., Rao, L.V., Narasu, M.L., Singh, O.V. (2008) The realm of penicillin acylase in β-lactam antibiotics. *Enzyme Microb. Technol.* **42**, 199-207.
- Chandra, P. M., Brannigan, J. A., Prabhune, A., Pundle, A., Turkenburg, J. P., Dodson, G.G., Suresh, C.G. (2005) Cloning, preparation and preliminary crystallographic studies of penicillin V acylase autoproteolytic processing mutants. *Acta Cryst. F* **61**, 124-127.
- Chen, J.A., Tanaka, T. (2011) Charged residues on a flap-loop structure of *Lactococcus lactis* prolidase play critical roles in allosteric behavior and substrate inhibition, *Biochim. Biophys. Acta.* **1814**, 1677–85.
- Chen,F., Gao, Y., Chen, X., Yu, Z., Li, X. (2013) Quorum quenching enzymes and their application in degrading signal molecules to block quorum sensing-dependent infection. *Int. J. Mol. Sci.* **14**, 17477-17500.
- Cheng, S., Wei, D., Song, Q., Zhao, X. (2006) Immobilization of whole cell permeabilized penicillin G acylase from *Alcaligenes faecalis* using pore matrix crosslinked with glutaraldehyde. *Biotechnol. Lett.* **28**, 1129-1133.
- Christiaens, H., Leer, R.J., Pouwels, P.H., Verstraete, W. (1992) Cloning and expression of a conjugated bile-acid hydrolase gene from *Lactobacillus plantarum* by using a direct plate assay. *Appl. Environ. Microbiol.* **58**, 3792-3798.
- Cole, M., Sutherland, R. (1966) Role of penicillin acylase in resistance of Gram negative bacteria to penicillins. *J. Gen. Microbiol.* **42**, 345-56.
- Cooley, M.A., Whittall, C., Rolph, M.S. (2010) *Pseudomonas* signal molecule 3-oxo-C12-homoserine lactone interferes with binding of rosiglitazone to human PPARgamma. *Microbes Infect.* **12**, 231-237.
- Cooper, A., Dryden, D.T.F. (1984). Allostery without conformational change - a plausible model. *Eur. Biophys. J.* **11**, 103-109.

- Corzo, G., Gilliland, S.E. (1999) Bile salt hydrolase activity of three strains of *Lactobacillus acidophilus*. *J. Dairy Sci.* **82**, 472-480.
- Damian, L., (2013). Isothermal titration calorimetry for studying protein-ligand interactions. *Methods Mol. Biol.* **1008**, 103-118.
- de Souza, V.R., Silva, A.C.G., Pinotti, L.M., Araujo, H.S.S., Giordano, R.D.C. (2005) Characterization of the penicillin G acylase from *Bacillus megaterium* ATCC 14945. *Braz. Arch. Biol. Technol.* **48**, 105-111.
- Delpino, M.V., Marchesini, M.I., Estein, S.M., Comerci, D.J., Cassataro, J., Fossati, C.A., Baldi, P.C. (2007) A bile salt hydrolase of *Brucella abortus* contributes to the establishment of a successful infection through the oral route in mice. *Infect.Immun.* **75**, 299-305.
- Demain, A.L., Elander, R.P. (1999) The β-lactam antibiotics: past, present, and future. *Antonie Van Leeuwenhoek.* **75**, 5-19.
- Deshpande, B.S., Ambedkar, S.S., Shewale, J.G. (1996) Cephalosporin C acylase and penicillin V acylase formation by Aeromonas sp ACY 95. *World J. Microbiol. Biotechnol.* **12**, 373-378.
- Deshpande, B.S., Ambedkar, S.S., Sudhakaran, V.K., Shewale, J.G. (1994) Molecular-biology of β-lactam acylases. *World J. Microbiol. Biotechnol.* **10**, 129-138.
- Dever, L.A., Dermody, T.S. (1991) Mechanisms of bacterial resistance to antibiotics. *Arch. Internal Med.* **151**, 886-895.
- Ditzel, L., Huber, R., Mann, K., Heinemeyer, W., Wolf, D.H., Groll, M. (1998) Conformational constraints for protein self-cleavage in the proteasome. *J. Mol. Biol.* **279**, 1187-1191.
- Dong, Y.H., Wang, L.H., Xu, J.L., Zhang, H.B., Zhang, X.F., Zhang, L.H. (2001) Quenching quorum-sensing-dependent bacterial infection by an N-acyl homoserine lactonase. *Nature* **411**, 813-817.
- Dong, Y.H., Wang, L.Y., Zhang, L.H. (2007) Quorum-quenching microbial infections: mech-anisms and implications. *Philos. Trans. R. Soc. Lond. B Biol. Sci.* **362**, 1201–1211.
- Duggleby, H.J., Tolley, S.P., Hill, C.P., Dodson, E.J., Dodson, G., Moody, P.C.E. (1995) Penicillin acylase has a single-amino-acid catalytic center. *Nature* **373**, 264-268.
- Dussurget, O., Cabanes, D., Dehoux, P., Lecuit, M., Buchrieser, C., Glaser, P., Cossart, P. (2002) *Listeria monocytogenes* bile salt hydrolase is a PrfA-regulated virulence factor involved in the intestinal and hepatic phases of listeriosis. *Mol. Microbiol.* **45**, 1095-1106.
- Elander, R.P. (2003) Industrial production of β-lactam antibiotics. *Appl. Microbiol. Biotechnol.* **61**, 385-392.

- Elkins, J.M., Kershaw, N.J., Schofield, C.J. (2005) X-ray crystal structure of ornithine acetyltransferase from the clavulanic acid biosynthesis gene cluster. *Biochem. J.* **385**, 565-573.
- Engh, R.A., Huber, R. **(**1991) Accurate bond and angle parameters for X-ray protein-structure refinement. *Acta Crystallogr.*A **47,** 392-400.
- Erickson, R.C., Bennett, R.E. (1965) Penicillin acylase activity of *Penicillium chrysogenum*. *Appl. Microbiol.* **13**, 738-742.
- Fadnavis, N.W., Devi, A.V., Jasti, L.S. (2008) Resolution of racemic 2-chlorophenyl glycine with immobilized penicillin G acylase. *Tetrahedron Asymm.***19**, 2363-2366.
- Fadnavis, N.W., Radhika, K.R., Devi, A.V. (2006) Preparation of enantiomerically pure (R)- and (S)-3-amino-3-phenyl-1-propanol via resolution with immobilized penicillin G acylase. *Tetrahedron Asymm.* **17**, 240-244.
- Fan, Y.X., Ju, M., Zhou, J.M., Tsou, C.L. (1996) Activation of chicken liver dihydrofolate reductase by urea and guanidine hydrochloride is accompanied by conformational change at the active site, *Biochem. J.* **315**, 97–102.
- Felix, H. (1982) Permeabilized cells. *Anal Biochem.* **120**, 211-234.
- Friesner, R.A., Murphy, R.B., Repasky, M.P., Frye, L.L., Greenwood, J.R., Halgren, T.A., Sanschagrin, P.C., Mainz, D.T., (2006). Extra Precision Glide: Docking and Scoring Incorporating a Model of Hydrophobic Enclosure for Protein-Ligand Complexes. *J. Med. Chem.* **49**, 6177–6196.
- Fuganti, C., Grasselli, P., Seneci, P.F., Servi, S., Casati, P. (1986) Immobilized benzylpenicillin acylase - Application to the synthesis of optically-active forms of carnitin and propranalol. *Tetrahedron Lett.* **27**, 2061-2062.
- Fuqua, C., Parsek, M.R., Greenberg, E.P. (2001) Regulation of gene expression by cell-to-cell communication: Acyl-homoserine lactone quorum sensing. *Ann. Rev.Genetics* **35**, 439-468.
- Gabor, E.M., de Vries, E.J., Janssen, D.B. (2005) A novel penicillin acylase from the environmental gene pool with improved synthetic properties. *Enzym.Microb. Technol.* **36**, 182-190.
- Galan, B., Garcia, J.L., Prieto, M.A. (2004) The PaaX repressor, a link between penicillin G acylase and the phenylacetyl-coenzyme A catabolon of *Escherichia coli* W. *J. Bacteriol.* **186**, 2215-2220.
- Garman, E.F., Schneider, T.R. **(**1997) Macromolecular cryocrystallography. *J. Appl. Crystallogr.* **30,** 211-237.
- Gera, C., Srivastava, S. (2006) Quorum sensing: The phenomenon of microbial communication. *Curr. Sci.* **90**, 666-677

- Gervasio, F.L., Chelli, R., Procacci, P., Schettino, V. (2002) The nature of intermolecular interactions between aromatic amino acid residues. *Prot.* **48**, 117-125.
- Gestrelius, S. (1982) Immobilized penicillin V acylase – Development of an industrial catalyst. *Appl. Biochem. Biotechnol.* **7**, 19-21.
- Gestrelius, S., Nielsen B.H., Mollgaard, H. (1983) Continuous 6-APA production and 7-ADCA production using Semacylase™ (Immobilized PEN-V acylase). *Ann. N. Y. Acad. Sci.* **413**, 554-556.
- Glide, version 5.8, Schrodinger, LLC, New York, NY, 2012.
- Gopalsrivastava, R., Hylemon, P.B. (1988) Purification and characterization of bile salt hydrolase from *Clostridium perfringens*. *J. Lipid Res.* **29**, 1079-1085.
- Groll, M., Ditzel, L., Lowe, J., Stock, D., Bochtler, M., Bartunik, H.D., Huber, R. (1997) Structure of 20S proteasome from yeast at 2.4 angstrom resolution. *Nature* **386**, 463-471.
- Guncheva, M., Ivanov, I., Galunsky, B., Stambolieva, N., Kaneti, J. (2004) Kinetic studies and molecular modelling attribute a crucial role in the specificity and stereoselectivity of penicillin acylase to the pair ArgA145-ArgB263. *Eur. J. Biochem.* **271**, 2272-2279.
- Harding, S.E., Chowdry, B.Z. (2001) Protein-ligand interactions: A practical approach. Volume 1: hydrodynamics and calorimetry. Oxford University Press.
- Helman, Y., Chernin, L. Silencing the mob: disrupting quorum sensing as a means to fight plant disease. *Mol. Plant. Pathol.* **16**, 316-329.
- Henke, J.M., Bassler, B.M. (2004). Bacterial social engagements. *Trends Cell Biol.* **14**, 648-656.
- Hevehan, D., De Bernardez Clark, E. (1997) Oxidative renaturation of lysozyme at high concentrations. *Biotechnol. Bioeng.* **54**, 221-30.
- Hewitt, L., Kasche, V., Lummer, K., Lewis, R.J., Murshudov, G.N., Verma, C.S., Dodson, G.G., Wilson, K.S. (2000) Structure of a slow processing precursor penicillin acylase from *Escherichia coli* reveals the linker peptide blocking the active-site cleft. *J. Mol. Biol.* **302**, 887-898.
- Huang, J.J., Han, J.I., Zhang, L.H., Leadbetter, J.R. (2003) Utilization of acyl-homoserine lactone quorum signals for growth by a soil pseudomonad and *Pseudomonas aeruginosa* PAO1. *Appl. Environ. Microbiol.* **69**, 5941–5949.
- Ignatova, Z., Hornle, C., Nurk, A., Kasche, V. (2002) Unusual signal peptide directs penicillin amidase from *Escherichia coli* to the tat translocation machinery. *Biochem. Biophys. Res. Comm.* **291**, 146-149.
- Ignatova, Z., Wischnewski, F., Notbohm, H., Kasche, V. (2005) Pro-sequence and Ca2+-binding: Implications for folding and maturation of Ntn-hydrolase penicillin amidase

from *E. coli*. *J. Mol. Biol.* **348**, 999-1014.

- Ines Marchesini, M., Connolly, J., Victoria Delpino, M., Baldi, P.C., Mujer, C.V., DelVecchio, V.G., Comerci, D.J. (2011) *Brucella abortus* choloylglycine hydrolase Affects Cell Envelope Composition and Host Cell Internalization. *Plos One* **6,** e28480. doi:10.1371/journal.pone.0028480.
- Ismail, H., Lau, R. M., van Langen, L.M., van Rantwijk, F., Svedas, V.K., Sheldon, R.A. (2008) A green, fully enzymatic procedure for amine resolution, using a lipase and a penicillin G acylase. *Green Chem.* **10**, 415-418.
- Jager, S.A.W., Jekel, P.A., Janssen, D.B. (2007) Hybrid penicillin acylases with improved properties for synthesis of β-lactam antibiotics. *Enzym.Microb.Technol.* **40**, 1335-1344.
- Karlsen, L. G., Villadsen, J. (1984) Optimization of a reactor assembly for the production of 6-APA from penicillin V. *Biotechnol. Bioeng.***26,** 1485-1491.
- Kasche, V., Galunsky, B., Ignatova, Z. (2003) Fragments of pro-peptide activate mature penicillin amidase of *Alcaligenes faecalis*. *Eur. J. Biochem.* **270**, 4721-4728.
- Kasche, V., Ignatova, Z., Markl, H., Plate, W., Punckt, N., Schmidt, D., Wiegandt, K., Ernst, B. (2005) Ca2+ is a cofactor required for membrane transport and maturation and is a yield-determining factor in high cell density penicillin amidase production. *Biotechnol. Prog.* **21**, 432-438.
- Katre, U.V., Suresh, C.G. **(**2009) Features of homotetrameric molecular association in protein crystals. *Acta Crystallogr. D* **65,** 1-10.
- Kelly, S.M., Jess, T.J., Price, N.C. (2005) How to study proteins by circular dichroism. *Biochim. Biophys. Acta* **1751,** 119-139.
- Kern, D., Zuiderweg, E.R.P. (2003). The role of dynamics in allosteric regulation. *Curr. Opin. Struct. Biol.* **13**, 748-757.
- Kerr, D.E. (1997) A colorimetric assay for penicillin V amidase. *Anal. Biochem.* **209,** 332‑334.
- Kim, D.W., Kang, S.M., Yoon, K.H. (2001) Characterization of glutaryl 7-ACA acylase from *Pseudomonas diminuta* KAC-1. *J.Microbiol. Biotechnol.* **11**, 452-457.
- Kim, H.S., Kang, T.S., Hyun, J.S., and Kang, H.S. (2004) Regulation of penicillin G acylase gene expression in *Escherichia coli* by repressor PaaX and the cAMP-cAMP receptor protein complex. *J.Biol. Chem.***279**, 33253-33262.
- Kim, J.H., Krahn, J.M., Tomchick, D.R., Smith, J.L., Zalkin, H. (1996) Structure and function of the glutamine phosphoribosylpyrophosphate amidotransferase glutamine site and communication with the phosphoribosylpyrophosphate site. *J. Biol. Chem.* **271**, 15549-15557.

- Kim, Y., Yoon, K.H., Khang, Y., Turley, S., Hol, W.G.J. (2000) The 2.0 angstrom crystal structure of cephalosporin acylase. *Structure* **8**, 1059-1068.
- Kim, Y., Bigelow, L., Buck, K., Joachimiak, A.(2007) Crystal Structure of Choloylglycine Hydrolase from Bacteroides thetaiotaomicron VPI. (PDB ID: 3HBC, www.rcsb.org)
- Klaver, F.A.M., Vandermeer, R. (1993) The assumed assimilation of cholesterol by lactobacilli and *Bifidobacterium bifidum* is due to their bile salt-deconjugating activity. *Appl.Environ. Microbiol.* **59**, 1120-1124.
- Klei, H.E., Daumy, G.O., Kelly, J.A. (1995) Purification and preliminary crystallographic studies of penicillin G acylase from *Providencia rettgeri*. *Prot. Sci.* **4**, 433-441.
- Koch, G., Nadal-Jimenez, P., Reis, C.R., Muntendam, R., Bokhove, M., Melillo, E., Dijkstra, B.W., Cool, R.H., Quax, W.J., 2014. Reducing virulence of the human pathogen *Burkholderia* by altering the substrate specificity of the quorum-quenching acylase PvdQ. *Proc. Nat. Acad. Sci.* **111**, 1568-1573.
- Kondo, M.D., Adachi, K. (1972). The nature of the inhibition and activation of epidermal phosphofructokinase: An allosteric enzyme, *J. Invest. Dermatol.* **59**, 397–401.
- Koreishi, M., Zhang, D.M., Imanaka, H., Imamura, K., Adachi, S., Matsuno, R., Nakanishi, K. (2006) A novel acylase from *Streptomyces mobaraensis* that efficiently catalyzes hydrolysis/synthesis of capsaicins as well as N-Acyl-L-amino acids and N-acyl-peptides. *J. Agri. Food Chem.* **54**, 72-78.
- Koshland, D.E., Hamadani, K. (2002) Proteomics and models for enzyme cooperativity. *J. Biol. Chem.* **277**, 46841-6844.
- Kovacikova, G., Lin, W., Skorupski, K. (2003) The virulence activator AphA links quorum sensing to pathogenesis and physiology in *Vibrio cholerae* by repressing the expression of a penicillin amidase gene on the small chromosome. *J.Bacteriol.***185**, 4825-4836.
- Krzeslak, J., Wahjudi, M., Quax, W.J. (2007) Quorum quenching acylases in *Pseudomonas aeruginosa.* In: Ramos, J.L., Filloux, A. (eds.) *Pseudomonas*, pp. 429-449. Springer, New York.
- Kumar, A., Singh, S., Poddar, P., Prabhune, A., Pundle, A. (2008). Effect of cultural conditions and media constituents on production of penicillin V acylase and CTAB treatment to enhance whole-cell enzyme activity of *Rhodotorula aurantiaca* (NCIM 34425). *Appl. Biochem. Biotechnol.* **157**, 463-472.
- Kumar, A., Prabhune, A., Suresh, C.G., Pundle, A. (2008) Characterization of smallest active monomeric penicillin V acylase from new source: A yeast, *Rhodotorula aurantiaca* (NCIM 3425). *Process Biochem.* **43**, 961-967.

- Kumar, R.S., Brannigan, J.A., Prabhune, A.A., Pundle, A.V., Dodson, G.G., Dodson, E.J., Suresh, C.G. (2006) Structural and functional analysis of a conjugated bile salt hydrolase from *Bifidobacterium longum* reveals an evolutionary relationship with penicillin V acylase. *J. Biol.Chem.* **281**, 32516-32525.
- Laemmli, U.K. (1970) Cleavage of structural proteins during the assembly of the bacteriophage T4, *Nature* **227**, 680‑685.
- Lakomek, K., Dickmanns, A., Kettwig, M., Urlaub, H., Ficner, R., Luebke, T. (2009) Initial insight into the function of the lysosomal 66.3 kDa protein from mouse by means of X-ray crystallography. *Bmc Struct. Biol.* **9**:56 doi:10.1186/1472-6807-9-56.
- Lambert, J. M., Siezen, R.J., de Vos, W.M., Kleerebezem, M. (2008) Improved annotation of conjugated bile acid hydrolase superfamily members in Gram-positive bacteria. *Microbiol. Sgm* **154**, 2492-2500.
- Landis, B.H., Mullins, P.B., Mullins, K.E., Wang, P.T. (2002) Kinetic resolution of β-amino esters by acylation using immobilized penicillin amidohydrolase. *Org. Proc. Res. Dev.* **6**, 539-546.
- Lanzarotti, E., Biekofsky, R.R., Estrin, D.A., Marti, M.A., Turjanski, A.G. (2011) Aromatic-aromatic interactions in proteins: Beyond the dimer. *J. Chem. Inform. Mod.* **51,** 1623-1633.
- Leadbetter, J.R., Greenberg, E.P. (2000) Metabolism of acyl-homoserine lactone quorum-sensing signals by *Variovorax paradoxus*. *J. Bacteriol.* **182**, 6921-6926.
- LeRoux, M.A., Guilak, F., Setton L.A. (1999) Compressive and shear properties of alginate gel: effects of sodium ions and alginate concentration. *J. Biomed. Mater. Res.* **47**, 46-53.
- LigPrep, version 2.5, Schrodinger, LLC, New York, NY, 2012.
- Lin, Y.H., Xu, J.L., Hu, J.Y., Wang, L.H., Ong, S.L., Leadbetter, J.R., Zhang, L.H. (2003) Acyl-homoserine lactone acylase from *Ralstonia* strain XJ12B represents a novel and potent class of quorum-quenching enzymes. *Mol. Microbiol.* **47**, 849-860.
- Littlechild, J.A. **(**1991) Protein crystallization - magical or logical - can we establish some general rules. *J. Phys. D* **24,** 111-118.
- Liu, S.L., Song, Q.X., Wei, D.Z., Zhang, Y.W., Wang, X.D. (2006) Preparation of optically pure tert-leucine by penicillin G acylase-catalyzed resolution. *Prep. Biochem. Biotechnol.* **36**, 235-241.
- Lodola, A., Branduardi, D., De Vivo, M., Capoferri, L., Mor, M., Piomelli, D., Cavalli, A. (2012) A Catalytic Mechanism for Cysteine N-Terminal Nucleophile Hydrolases, as Revealed by Free Energy Simulations. *Plos One* **7**, e32397.
- Lowe, D.A., Romancik, G., Elander, R.P. (1986) Enzymatic hydrolysis of penicillin V to

6-aminopenicillanic acid by *Fusarium oxysporum*. *Biotechnol. Lett.* **8**, 151-156.

- Lowe, J., Stock, D., Jap, R., Zwickl, P., Baumeister, W., Huber, R. (1995) Crystal structure of the 20s proteasome from the archaeon *Thermoplasma acidophilum* at 3.4-angstrom resolution. *Science* **268**, 533-539.
- Lundeen, S.G., Savage, D.C. (1992) Multiple forms of bile salt hydrolase from *Lactobacillus* sp. strain 100-100. *J. Bacteriol.* **174**, 7217-7220.
- Luque, I., Leavitt, S.A., Freire, E. (2002). The linkage between protein folding and functional cooperativity: Two sides of the same coin? *Ann. Rev. Biophys. Biomol. Struct.* **31**, 235-256.
- Ma, B.Y., Elkayam, T., Wolfson, H., Nussinov, R. **(**2003) Protein-protein interactions: Structurally conserved residues distinguish between binding sites and exposed protein surfaces. *Proc. Nat. Acad. Sci.* **100,** 5772-5777.
- Maresova, H., Plackova, M., Grulich, M., and Kyslik, P. (2014) Current state and perspectives of penicillin G acylase-based biocatalyses. *Appl. Microbiol. Biotechnol.* **98**, 2867-2879.
- Margolin, A.L. (1996) Novel crystalline catalysts. *Trends Biotechnol.* **14**, 223-230.
- Margolin, A.L., Svedas, V.K., Berezin, I.V. (1980) Substrate specificity of penicillin amidase from *Escherichia coli*. *Biochim. Biophys. Acta* **616**, 283-289.
- Matsumoto, K. (1993) Production of 6-APA, 7-ACA, and 7-ADCA by immobilized penicillin and cephalosporin amidases. *Bioprocess Tech.* **16**, 67-88.
- Matthews, B.W. (1968) Solvent content of protein crystals. *J. Mol. Biol.* 33:491-497.
- Matthews, B.W. **(**1985) Determination of protein molecular-weight, hydration, and packing from crystal density. *Methods Enzymol.* **114,** 176-187.
- Mattiasson, B. (1983) Immobilized cells and organelles, vols. 1 and 2. Boca Raton: CRC Press.
- McGaughey, G.A., Gagne, M., Rappe, A. (1998) π-stacking interactions: Alive and well in proteins. *J. Biol. Chem.* **273**, 15458-15463.
- McPherson, A. (1982) Preparation and analysis of protein crystals. John Wiley & Sons.
- McRee, Duncan E. (1993). *Practical Protein Crystallography*. San Diego: Academic Press, pp. 1-23.
- McVey, C.E., Walsh, M.A., Dodson, G.G., Wilson, K.S., Brannigan, J.A. (2001) Crystal structures of penicillin acylase enzyme-substrate complexes: Structural insights into the catalytic mechanism. *J. Mol. Biol.* **313**, 139-150.
- Merino, E., Balbas, P., Recillas, F., Becerril, B., Valle, F., Bolivar, F. (1992) Carbon regulation and the role in nature of the *Escherichia coli* penicillin acylase (pac) gene. *Mol. Microbiol.* **6**, 2175-2182.

- Michalska, K., Bujacz, G., Jaskolski, M. (2006) Crystal structure of plant asparaginase. *J. Mol. Biol.* **360**, 105-116.
- Miller, M.B., Bassler, B.L. (2001) Quorum sensing in bacteria. *Ann. Rev. Microbiol.* **55**, 165-199.
- Miller, M.T., Gerratana, B., Stapon, A., Townsend, C.A., Rosenzweig, A.C. (2003) Crystal structure of carbapenam synthetase (CarA). *J. Biol. Chem.* **278**, 40996-41002.
- Miyari, S., Tateda, K., Fuse, E.T., Ueda, C., Saito, H., Takabatake, T., Ishii, Y., Horikawa, M., Ishiguro, M. Standiford, T.J., Yamaguchi, K. (2006) Immunization with 3-oxododecanoyl-L-homoserine lactone-protein conjugate protects mice from lethal *Pseudomonas aeruginosa* lung infection. *J. Med. Microbiol.* **55**, 1381-1387.
- Mocz, G., Ross, J.A., (2013). Fluorescence techniques in analysis of protein-ligand interactions. *Methods Mol. Biol.* **1008**, 169-210.
- Mollgaard, H. (1987) Choice of reactor for Semacylase^{TM}: An industrial penicillin V acylase. *Ann. N. Y. Acad. Sci.* **501**, 473-476.
- Mollgaard, H. and Karlsen, L. G. (1988) 6-APA production in a pilot plant with an immobilized penicillin V acylase. *Enzyme Eng.* **9**,360-365.
- Monera, O.D., Kay, C.M., Hodges, R.S. (1994) Protein denaturation with guanidine hydrochloride or urea provides a different estimate of stability depending on the contributions of electrostatic interactions. *Protein Sci.* **3**, 1984–91.
- More, M.I., Finger, L.D., Stryker, J.L., Fuqua, C., Eberhard, A.,Winans, S.C. (1996) Enzymatic synthesis of a quorum-sensing autoinducer through use of defined substrates. *Science* **272**, 1655–1658.
- Mukherji, R., Varshney, N. K., Panigrahi, P., Suresh, C. G., Prabhune, A. (2014) A new role for penicillin acylases: Degradation of acyl homoserine lactone quorum sensing signals by *Kluyvera citrophila* penicillin G acylase. *Enzyme Microb. Technol.* **56**, 1-7.
- Murao, S. (1955). Penicillin-amidase. III. Mechanism of penicillin-amidase on sodium penicillin G. *J. Agric. Chem. Soc. (Japan)* **29**, 404-407.
- Murshudov, G.N., Vagin, A.A., Dodson, E.J. (1997) Refinement of macromolecular structures by the maximum-likelihood method. *Acta Crystallogr. D* **53,** 240-255.
- Nagalakshmi, V. and Pai, J.S. (1994) Permebilization of *Escherichia coli* cells for enhanced penicillin acylase activity. *Biotechnol. Tech.* **8**, 431-434.
- Nakai, T., Hasegawa, T., Yamashita, E., Yamamoto, M., Kumasaka, T., Ueki, T., Nanba, H., Ikenaka, Y., Takahashi, S., Sato, M., Tsukihara, T. (2000) Crystal structure of N-carbamyl-D-amino acid amidohydrolase with a novel catalytic framework common to amidohydrolases. *Structure* **8**, 729-737

- Neugebauer, J. A guide to the properties and uses of detergents in biology and biochemistry. Calbiochem-Novabiochem. Corp, LaJolla, California, 2000
- Ng, J.S., Wang, P.T., Landis, B.H., Yonan, E.E., Topgi, R.S. (2001) Method and apparatus for preparation of chiral β-amino acids using penicillin G acylase. International Patent Application US 6214609.
- Norouzian, D., Javadpour, S., Moazami, N., Akbarzadeh, A. (2002) Immobilization of whole cell penicillin G acylase in open pore gelatin matrix. *Enzyme Microb. Technol.* **30**, 26‑29.
- Novikov, F.N., Stroganov, O.V., Khaliullin, I.G., Panin, N.V., Shapovalova, I.V., Chilov, G.G., Svedas, V.K. (2013) Molecular modeling of different substrate-binding modes and their role in penicillin acylase catalysis. *FEBS J.* **280**, 115-26.
- Ohashi, H., Katsuta, Y., Hashizume, T., Abe, S.N., Kajiura, H., Hattori, H., Kamei, T., Yano, M. (1988) Molecular cloning of the penicillin G acylase gene from *Arthrobacter viscosus*. *Appl. Environ. Microbiol.* **54**, 2603-2607.
- Oinonen, C., Rouvinen, J. (2000) Structural comparison of Ntn-hydrolases. *Prot. Sci.* **9**, 2329-2337.
- Oinonen, C., Tikkanen, R., Rouvinen, J., Peltonen, L. (1995) Three-dimensional structure of human lysosomal aspartylglucosaminidase. *Nat. Struct. Biol.* **2**, 1102-1108.
- Okada, T., Suzuki, H., Wada, K., Kumagai, H., Fukuyama, K. (2006) Crystal structures of γ-glutamyltranspeptidase from *Escherichia coli*, a key enzyme in glutathione metabolism, and its reaction intermediate. *Proc. Nat. Acad. Sci.* **103**, 6471-6476.
- Olsson, A., Hagstrom, T., Nilsson, B., Uhlen, M., Gatenbeck, S. (1985) Molecular-cloning of *Bacillus sphaericus* penicillin V amidase gene and its expression in *Escherichia coli* and *Bacillus subtilis*. *Appl. Environ. Microbiol.* **49**, 1084-1089.
- Panigrahi, P., Sule, M., Sharma, R., Ramasamy, S., Suresh, C.G. (2014) An improved method for specificity annotation shows a distinct evolutionary divergence among the microbial enzymes of the cholylglycine hydrolase family. *Microbiol. Sgm* **160**, 1162-1174.
- Papaioannou, E., Wahjudi, M., Nadal-Jimenez, P., Koch, G., Setroikromo, R., Quax, W.J. (2009) Quorum-quenching acylase reduces the virulence of *Pseudomonas aeruginosa* in a *Caenorhabditis elegans* infection model. *Antimicrob. Agents Chemother.* **53**, 4891-4897.
- Park, S.Y., Kang, H.O., Jang, H.S., Lee, J.K., Koo, B.T., Yum, D.Y. (2005) Identification of extracellular N-acylhomoserine lactone acylase from a *Streptomyces* sp and its application to quorum quenching. *Appl. Environ. Microbiol.* **71**, 2632-2641.
- Parkin, S., Hope, H. **(**1998) Macromolecular cryocrystallography: Cooling, mounting,

storage and transportation of crystals. *J. Appl. Crystallogr.* **31,** 945-953.

- Parmar, A., Kumar, H., Marwaha, S., Kennedy, J.F. (2000) Advances in enzymatic transformation of penicillins to 6-aminopenicillanic acid (6-APA). *Biotechnol. Adv.* **18**, 289-301.
- Pastra-Landis, S.C., Evans, D.R., Lipscomb, W.L. (1978) The effect of pH on the cooperative behaviour of aspartate trans-carbamoylase from *Escherichia coli. J. Biol. Chem.* **253**, 4624-30.
- Pearson, J.P., Gray, K.M., Passador, L., Tucker, K.D., Eberhard, A., Iglewski, B.H., Greenberg, E.P. (1994) Structure of the autoinducer required for expression of *Pseudomonas aeruginosa* virulence genes. *Proc. Natl.Acad. Sci. USA* **91**, 197–201.
- Pearson, J.P., Passador, L., Iglewski, B.H., Greenberg, E.P. (1995) A second N-acylhomoserine lactone signal produced by *Pseudomonas aeruginosa*. *Proc. Natl. Acad. Sci. USA* **92**, 1490–1494.
- Petit, C.M., Zhang, J., Sapienza, P.J., Fuentes, E.J., Lee, A.L. (2009). Hidden dynamic allostery in a PDZ domain. *Proc. Nat. Acad. Sci.* **106**, 18249-18254.
- Plapp, B.V. (1995) Site-directed mutagenesis: a tool for studying enzyme catalysis. *Methods Enzymol.* **249**, 91-119.
- Polderman-Tijmes, J.J., Jekel, P.A., de Vries, E.J., van Merode, A.E.J., Floris, R., van der Laan, J.M., Sonke, T., Janssen, D.B. (2002) Cloning, sequence analysis, and expression in *Escherichia coli* of the gene encoding an α-amino acid ester hydrolase from *Acetobacter turbidans*. *Appl. Environ. Microbiol.* **68**, 211-218.
- Prabhune, A. A., Rao, B. S., Pundle, A. V., Sivaraman H. (1992) Immobilization of permeabilized *Escherichia coli* cells with penicillin acylase activity. *Enzyme Microb. Technol.* **14**, 161-163.
- Prieto, M.A., Diaz, E., Garcia, J.L. (1996) Molecular characterization of the 4-hydroxyphenylacetate catabolic pathway of *Escherichia coli* W: Engineering a mobile aromatic degradative cluster. *J. Bacteriol.* **178**, 111-120.
- Pronk, S., Pall, S., Schulz, R., Larsson, P., Bjelkmar, P., Apostolov, R., Shirts, M.R., Smith, J.C., Kasson, P.M., van der Spoel, D., Hess, B., Lindahl, E., (2013). GROMACS 4.5: a high-throughput and highly parallel open source molecular simulation toolkit. *Bioinform.* **29**, 845-854.
- Pundle, A., SivaRaman, H. (1997) *Bacillus sphaericus* penicillin V acylase: Purification, substrate specificity, and active-site characterization. *Current Microbiol.* **34**, 144-148.
- Rajendhran, J., Gunasekaran, P. (2004) Recent biotechnological interventions for developing improved penicillin G acylases. *J. Biosci. Bioeng.* **97**, 1-13.
- Rajendhran, J., Gunasekaran, P. (2007) Molecular cloning and characterization of

thermostable β-lactam acylase with broad substrate specificity from *Bacillus badius*. *J. Biosci. Bioeng.* **103**, 457-463.

- Rajendhran, J., Krishnakumar, V., Gunasekaran, P. (2002) Optimization of a fermentation medium for the production of penicillin G acylase from *Bacillus* sp. *Lett. Appl. Microbiol.* **35**, 523-527.
- Ramachandran, G.N., Sasisekharan, V. **(**1968) Conformation of polypeptides and proteins. *Adv. Protein. Chem.* **23,** 283-438.
- Rathinaswamy, P., Gaikwad, S.M., Suresh, C.G., Prabhune, A.A., Brannigan, J.A., Dodson, G.G., and Pundle, A.V. (2012) Purification and characterization of YxeI, a penicillin acylase from *Bacillus subtilis*. *Int. J. Biol. Macromol.* **50**, 25-30.
- Rathinaswamy, P., Gaikwad, S.M., Suresh, C.G., Prabhune, A.A., Brannigan, J.A., Dodson, G.G., Pundle, A.V. (2012) Purification and characterization of YxeI, a penicillin acylase from *Bacillus subtilis*. *Int. J. Biol. Macromol.* **50**, 25-30.
- Rathinaswamy, P., Pundle, A.V., Prabhune, A.A., SivaRaman, H., Brannigan, J.A., Dodson, G.G., Suresh, C.G. (2005) Cloning, purification, crystallization and preliminary structural studies of penicillin V acylase from *Bacillus subtilis*. *Acta Cryst. F* **61**, 680-683.
- Ren, J., Sun, K., Wu, Z., Yao, J., Guo, B. (2011) All 4 Bile Salt Hydrolase Proteins Are Responsible for the Hydrolysis Activity in *Lactobacillus plantarum* ST-III. *J. Food Sci.* **76**, M622-M628.
- Rhodes, G. (2000) Crystallography Made Crystal Clear. Academic Press.
- Roa, A., Castillon, M.P., Goble, M.L., Virden, R., Garcia, J.L. (1995) New insights on the specificity of penicillin acylase. *Biochem. Biophys. Res. Comm.* **206**, 629-636
- Roche, D.M., Byers, J.T., Smith, D.S., Glansdorp, F.G., Spring, D.R., Welch, M. (2004) Communications blackout? Do N-acylhomoserinelactone-degrading enzymes have any role in quorum sensing? *Microbiol.* **150**, 2023-2028.
- Rosano, G.L., Cecarelli, E.A. (2014) Recombinant protein expression in *E. coli*: advances and challenges, *Front. Microbiol.* **5**, 172.
- Rossmann, M. (2008) Structural analysis of proteins of human sphingolipid metabolism. Berlin Freie Univ., Berlin.
- Rossmann, M.G., Blow, D.M. **(**1962) Detection of sub-units within crystallographic asymmetric unit. *Acta Crystallogr*. *A* **15,** 24-31.
- Rossocha, M., Schultz-Heienbrok, R., von Moeller, H., Coleman, J. P., Saenger, W. (2005) Conjugated bile acid hydrolase is a tetrameric N-terminal thiol hydrolase with specific recognition of its cholyl but not of its tauryl product. *Biochemistry* **44**, 5739-5748.

- Sabonmatsu, K.Y., Tung C.S., (2007). High performance computing in biology: multimillion atom simulations of nanoscale systems. *J. Struct. Biol.* **157**, 479-480.
- Sakaguchi, K., Murao, S. (1950). A preliminary report on a new enzyme, penicillinamidase. *J. Agric. Chem. Soc.(Japan)* **23**, 411.
- Sakoda, M., Hiromi, K. (1976) Determination of the best-fit values of kinetic parameters of the Michaelis–Menten equation by the method of least squares with the Taylor expansion, *J. Biochem.* **80**, 547–55.
- Samanta, U., Pal, D., Chakrabarti, P. **(**1999) Packing of aromatic rings against tryptophan residues in proteins. *Acta Crystallogr.D* **55,** 1421-1427.
- Sambrook, J., Fritsch, E.F., Maniatis, T., Molecular Cloning: A Laboratory Manual, 2nd ed., Cold Spring Harbor Laboratory Press, New York, 1989.
- Seemuller, E., Lupas, A., Baumeister, W. (1996) Autocatalytic processing of the 20S proteasome. *Nature* **382**, 468-470.
- Sevo, M., Degrassi, G., Skoko, N., Venturi, V., Ljubijankic, G. (2002) Production of glycosylated thermostable *Providencia rettgeri* penicillin G amidase in *Pichia pastoris*. *FEMS Yeast Res.* **1**, 271-277.
- Sheldon, R. A. (2007) Enzyme immobilization: the quest for optimum performance. *Adv. Synth. Catal.* **349**, 1289-1307.
- Shewale, G.J., Kumar, K.K., Ambekar, G.R. (1987) Evaluation of determination of 6-aminopenicillanic acid by p-dimethyl aminobenzaldehyde. *Biotechnol. Tech.* **1**, 69–72.
- Shewale, J.G., Sivaraman, H. (1989) Penicillin acylase – Enzyme production and its application in the manufacture of 6-APA. *Process Biochem.* **24**, 146-154.
- Shewale, J.G., Sudhakaran, V.K. (1997) Penicillin V acylase: Its potential in the production of 6-aminopenicillanic acid. *Enzyme Microb. Technol.* **20**, 402-410.
- Singh, D., Goel, R., Johri, B.N. (1988) Deacylation of penicillins by the immobilized mycelia of the thermophilic *Malbranchea*. *J. Gen.Appl. Microbiol.* **34**, 333–339.
- Sio, C.F., Otten, L.G., Cool, R.H., Diggle, S.P., Braun, P.G., Bos, R., Daykin, M., Camara, M., Williams, P., Quax, W.J. (2006) Quorum quenching by an N-acyl homoserine lactone acylase from *Pseudomonas aeruginosa* PAO1. *Infect. Immun.* **74**, 1673-1682.
- Sio, C.F., Quax, W.J. (2004) Improved β-lactam acylases and their use as industrial biocatalysts. *Curr. Opin. Biotechnol.* **15**, 349-355.
- SiteMap, version 2.5, Schrodinger, LLC, New York, NY, 2011.
- Skrob, F., Becka, S., Plhackova, K., Fotopulosova, V., Kyslik, P. (2003) Novel penicillin G acylase from *Achromobacter* sp. CCM 4824. *Enzyme Microb. Technol.* **32**, 738-744.
- Smith, J.L., Zaluzec, E.J., Wery, J.P., Niu, L.W., Switzer, R.L., Zalkin, H., Satow, Y.

(1994) Structure of the allosteric regulatory enzyme of purine biosynthesis. *Science* **264**, 1427-1433.

- Sousa da Silva, A.W., Vranken, W.F., (2012). ACPYPE - AnteChamber PYthon Parser interfacE. *BMC Res. Notes* **5**, 367-367.
- Steindler, L., Venturi, V. (2007) Detection of quorum sensing N-acyl homoserine lactone signal molecules with bacterial biosensors. *FEMS Microbiol. Lett.***266**,1-9.
- Stellwag, E.J., Hylemon, P.B. (1976) Purification and characterization of bile-salt hydrolase from *Bacteroides fragilis* subsp fragilis. *Biochim.Biophys. Acta* **452**, 165-176.
- Studier, F. W. (2005) Protein production by auto-induction in high density shaking cultures. *Prot. Exp. Pur.* **41**, 207-234.
- Sudhakaran, V. K., Shewale, J. G. Enzymatic splitting of penicillin V for the production of 6-APA using immobilized penicillin V acylase. *World J. Microbial. Biotechnol.*, **9,** 631-634.
- Sudhakaran, V.K., Borkar, P.S. (1985) Phenoxymethyl penicillin acylase: sources and study--a sum up. *Hind. Ant. Bull.* **27**, 44-62
- Suresh, C.G., Pundle, A.V., SivaRaman, H., Rao, K.N., Brannigan, J.A., McVey, C.E., Verma, C.S., Dauter, Z., Dodson, E.J., and Dodson, G.G. (1999) Penicillin V acylase crystal structure reveals new Ntn-hydrolase family members. *Nat. Struct. Biol.* **6**, 414-416.
- Svedas, V., Guranda, D., vanLangen, L., vanRantwijk, F., Sheldon, R. (1997) Kinetic study of penicillin acylase from *Alcaligenes faecalis*. *FEBS Lett.* **417**, 414-418.
- Takahash.T, Yamazaki, Y., Kato, K. (1974) Substrate specificity of an α-amino acid ester hydrolase produced by *Acetobacter turbidans* ATCC 9325. *Biochem. J.* **137**, 497-503.
- Takano, E. (2006) γ-butyrolactones: *Streptomyces* signaling molecules regulating antibiotic production and differentiation. *Curr. Opin. Microbiol.* **9**, 287-294.
- Tanaka, H., Hashiba, H., Kok, J., Mierau, I. (2000) Bile salt hydrolase of *Bifidobacterium longum* - Biochemical and genetic characterization. *Appl. Environ. Microbiol.* **66**, 2502-2512.
- Taranto, M.P., Sesma, F., Holgado, A.P.D., deValdez, G.F. (1997) Bile salts hydrolase plays a key role on cholesterol removal by *Lactobacillus reuteri*. *Biotechnol. Lett.* **19**, 845-847.
- The PyMOL Molecular Graphics System, Version 1.7.4 Schrödinger, LLC.
- Thomas, A., Meurisse, R., Charloteaux, B., Brasseur, R. **(**2002) Aromatic side-chain interactions in proteins. I. Main structural features. *Prot. Str. Func. Genetics.* **48,** 628-634.

- Torres, L.L., Ferreras, E.R., Cantero, A., Hidalgo, A., Berenguer, J. (2012) Functional expression of a penicillin acylase from the extreme thermophile *Thermus thermophilus* HB27 in *Escherichia coli*. *Microb. Cell Fact.* **11**, 105. doi:10.1186/1475-2859-11-105.
- Torres, R., de la Mata, I., Castillon, M.P., Arroyo, M., Torres, J., Acebal, C. Purification and characterization of penicillin V acylase from *Streptomyces lavendulae*, in: A. Ballesteros, F.J. Plou, J.L. Iborra, P.J. Halling (Eds.), Stability and Stabilization of Biocatalysts, Elsevier Science, New York,, pp. 719–724.
- Torres-Bacete, J. Arroyo, M. Torres-Guzman R., de la Mata, Castilon, M.P., Acebal C. (2000) Covalent immobilization of penicillin V acylase from *Streptomyces lavendulae*. *Biotechnol., Lett.* **22**, 1011-1014.
- Torres-Bacete, J., Arroyo, M., Torres-Guzman, R., de la Mata, I., Castillon, M.P., Acebal, C. (2000) Covalent immobilization of penicillin acylase from *Streptomyces lavendulae*. *Biotechnol. Lett.* **22**, 1011-1014.
- Torres-Bacete, J., Arroyo, M., Torres-Guzman, R., de la Mata, I., Castillon, M.P., and Acebal, C. (2000) Optimization of 6-aminopenicillanic acid (6-APA) production by using a new immobilized penicillin acylase. *Biotechnol. Applied Biochem.* **32**, 173-177.
- Torres-Bacete, J., Arroyo, M., Torres-Guzman, R., de la Mata, I., Castillon, M.P., and Acebal, C. (2001) Stabilization of penicillin V acylase from *Streptomyces lavendulae* by covalent immobilization. *J. Chem. Technol. Biotechnol.* **76**, 525-528.
- Torres-Bacete, J., Hormigo, D., Stuart, M., Arroyo, M., Torres, P., Castillon, M. P., Acebal, C., Garcia, J.L., de la Mata, I. (2007) Newly discovered penicillin acylase activity of Aculeacin A acylase from *Actinoplanes utahensis*. *Appl. Environ. Microbiol.* **73**, 5378-5381.
- Torres-Bacete, J., Hormigo, D., Torres-Guzman, R., Arroyo, M., Pilar Castillon, M.P., Luis Garcia, J., Acebal, C., de la Mata, I. (2015) Overexpression of Penicillin V Acylase from *Streptomyces lavendulae* and Elucidation of Its Catalytic Residues. *Appl. Environ. Microbiol.* **81**, 1225-1233.
- Torres-Guzman, R., de la Mata, I., Torres-Bacete, J., Arroyo, M., Castillon, M.P., Acebal, C. (2002) Substrate specificity of penicillin acylase from *Streptomyces lavendulae*. *Biochem.Biophys. Res. Comm.* **291**, 593-597.
- Torres-Guzman, R., de la Mata, I., Torres-Bacete, J., Arroyo, M., Castillon, M. P., and Acebal, C. (2002) Substrate specificity of penicillin acylase from *Streptomyces lavendulae*. *Biochem.Biophys. Res. Comm.* **291**, 593-597.
- Uroz, S., Dessaux, Y., Oger, P. (2009) Quorum sensing and quorum quenching: the yin and yang of bacterial communication. *Chembiochem* **10**, 205–216.
- Valle, F., Balbas, P., Merino, E., Bolivar, F. (1991) The role of penicillin amidases in

nature and in industry. *Trends Biochemical Sci.* **16**, 36-40.

- Valle, F., Gosset, G., Tenorio, B., Oliver, G., Bolivar, F. (1986) Characterization of the regulatory region of the *Escherichia coli* penicillin acylase structural gene. *Gene* **50**, 119-122.
- Van de Sandt, E., De Vroom, E. (2000) Innovations in cephalosporin and penicillin production: Painting the antibiotics industry green. *Chimica Oggi/Chemistry Today* **18**, 72-75.
- van Langen, L.M., Oosthoek, N.H.P., Guranda, D.T., van Rantwijk, F., Svedas, V. K., Sheldon, R.A. (2000) Penicillin acylase-catalyzed resolution of amines in aqueous organic solvents. *Tetrahedron Asymm.* **11**, 4593-4600.
- Vandamme, E.J. (1988). Immobilized biocatalyst and antibiotic production. Biochemical, genetic, and biotechnical aspects. In: Moo-Young, M. (ed.) *Bioreactor, Immobilized Enzymes and Cells: Fundamentals and Applications*. Marcel Dekker, New York, p261-286.
- Vandamme, E.J., Voets, J.P. (1973) Some aspects of penicillin V acylase produced by *Rhodotorula glutinis* var glutinis. *Zeitschrift Fur Allgemeine Mikrobiologie* **13**, 701-710.
- Vandamme, E.J., Voets, J.P. (1974) Microbial penicillin acylases. *Adv. Appl. Microbiol.* **17**, 311-369.
- Vandamme, E.J., Voets, J.P. (1975) Properties of purified penicillin V acylase of *Erwinia aroideae*. *Experientia* **31**, 140-143.
- Varshney, N.K., Kumar, R.S., Ignatova, Z., Prabhune, A., Pundle, A., Dodson, E., Suresh, C.G. (2012) Crystallization and X-ray structure analysis of a thermostable penicillin G acylase from *Alcaligenes faecalis*. *Acta Cryst. F* **68**, 273-277.
- Varshney, N.K., Ramasamy, S., Brannigan, J.A., Wilkinson, A.J., Suresh, C.G. (2013) Cloning, overexpression, crystallization and preliminary X-ray crystallographic analysis of a slow-processing mutant of penicillin G acylase from *Kluyvera citrophila*. *Acta Cryst. F* **69**, 925-929.
- Verhaert, R.M.D., Riemens, A.M., vanderLaan, J.M., vanDuin, J., Quax, W.J. (1997) Molecular cloning and analysis of the gene encoding the thermostable penicillin G acylase from *Alcaligenes faecalis*. *Appl. Environ. Microbiol.* **63**, 3412-3418.
- Wahjudi, M., Papaioannou, E., Hendrawati, O., van Assen, A.H.G., van Merkerk, R., Cool, R.H., Poelarends, G.J., Ouax, W.J. (2011) PA0305 of *Pseudomonas aeruginosa* is a quorum quenching acylhomoserine lactone acylase belonging to the Ntn hydrolase superfamily. *Microbiol. Sgm* **157**, 2042-2055.
- Wang, X.T., Chen, X.H., Xu, Y., Lou, W.H.,Wu, H., Zong, M.H. (2013) Biocatalytic anti-Prelog stereoselective reduction of ethylacetoacetate catalyzed by whole cells of

Acetobacter sp. CCTCC M209061. *J. Biotechnol.* **163**, 292-300.

- Waters, C.M., Bassler, B.L. (2005) Quorum sensing: Cell-to-cell communication in bacteria. *Ann. Rev. Cell. Dev. Biol.* **21**, 319-346.
- Wolf, J.H., Korf, J. (1990) Improved automated precolumn derivatization reaction of fatty acids with bromomethylmethoxycoumarin as label. *J. Chromatogr. A* **502**, 423–430.
- Xu, F., Byun, T., Dussen, H-J., Duke, K.R. (2003) Degradation of N-acylhomoserine lactones, the bacterial quorum sensing molecules, by acylase. *J. Biotechnol.***101**, 89-96.
- Xu, Q.A., Buckley, D., Guan, C.D., Guo, H.C. (1999) Structural insights into the mechanism of intramolecular proteolysis. *Cell* **98**, 651-661.
- Xuan, J.C., Tarentino, A.L., Grimwood, B.G., Plummer, T.H., Cui, T., Guan, C.D., Van Roey, P. (1998) Crystal structure of glycosylasparaginase from *Flavobacterium meningosepticum*. *Prot. Sci.* **7**, 774-781.
- Zhang, D., Koreishi, M., Imanaka, H., Imamura, K., Nakanishi, K. (2007) Cloning and characterization of penicillin V acylase from *Streptomyces mobaraensis*. *J. Biotechnol.* **128**, 788-800.
- Zhiryakova, D., Ivanov, I., Ilieva, S., Guncheva, M., Galunsky, B., Stambolieva, N. (2009) Do N-terminal nucleophile hydrolases indeed have a single amino acid catalytic center? *FEBS J.* **276**, 2589-2598.
- Zhou, Z., Li, G., Li, Y. (2010) Immobilization of *Saccharomyces cerevisiae* alcohol dehydrogenase on hybrid alginate-chitosan beads. *Int. J. Biol. Macromol.* **3**, 21–26.

List of Publications and Patents

- **Avinash, V.S.***, Panigrahi, P.*, Suresh, C.G., Pundle, A.V. and Ramasamy, S. Structural modelling of substrate binding and inhibition in penicillin V acylase from *Pectobacterium atrosepticum*, Biochem. Biophys. Res. Commun. 437, 538-543 (2013). *Equal contribution.

- **Avinash, V.S.**, Pundle, A.V., Suresh, C.G. and Ramasamy, S. Penicillin acylases revisited: Importance beyond their industrial utility. Crit. Rev. Biotechnol. (2014) doi: 10.3109/07388551.2014.960359.

- **Avinash, V.S.**, Ramasamy, S., Suresh, C.G. and Pundle, A.V. Penicillin V acylase from *Petcobacterium atrosepticum* shows high specific activity and unique kinetics. Int. J. Biol. Macromol. 79, 1-7 (2015).

- **Avinash, V.S.**, Panigrahi, P., Chand, D., Pundle, A.V., Suresh, C.G. and Ramasamy, S. Structural analysis of a penicillin V acylase from *Pectobacterium atrosepticum* confirms the importance of two Trp residues for activity and specificity. J. Struct. Biol. (2015) ***Under review.***

- **Avinash, V.S.**, Utari, P.D., Ramasamy, S., Quax, W.J. and Pundle, A.V. Degradation of long chain acyl homoserine lactones by penicillin V acylases from Gram-negative bacteria. (2015) ***Manuscript under preparation.***

- **Avinash, V.S.,** Chauhan, P., Gaikwad, S. and Pundle, A.V. Biotransformation of penicillin V to 6-APA using immobilized recombinant *E. coli* producing a highly active penicillin V acylase. (2015) ***Submitted to J. Bioproc. Biosyst. Eng.***

- **Avinash, V.S.**, Naik, N., Kumar, A. and Pundle, A.V. Characterization of a new *Bacillus cereus* ATUAVP1846 strain producing penicillin V acylase, and optimization of fermentation parameters. Ann. Microbiol. 62, 1287-93 (2012).

Patent

- **Avinash, V.S.**, Pundle, A.V., Ramasamy, S. A recombinant penicillin V acylase and the process for preparation thereof. Patent application **WO/2015/151118**